TOWARDS UNDERSTANDING THE TRAFFICKING AND FUNCTION OF IRON AND TITANIUM IONS IN ORGANISMS

A Dissertation
Submitted to
the Temple University Graduate Board

In Partial Fulfillment
of the Requirements for the Degree
DOCTOR OF PHILOSOPHY

---

by
Mark R. Zierden
December 2016

Examining Committee Members:

Ann M. Valentine, Advisory Chair, TU Department of Chemistry
Graham E. Dobereiner, TU Department of Chemistry
Michael J. Zdilla, TU Department of Chemistry
Ivan Dmochowski, External Member, U. of Pennsylvania Dept. of Chemistry

ABSTRACT

It is estimated that up to one third of all proteins are metalloproteins. These proteins have evolved to use the metals that are, or at least were at the time of their initial evolution, the most accessible. Some active centers of metalloenzymes resemble the structures of minerals presumed to be present in precipitates from hydrothermal solutions in the ocean billions of years ago. The metals in these proteins serve myriad purposes from structure to transport to catalysis. For these purposes organisms must find a way to incorporate, transport and possibly store the metal ions from the environment. Iron, among other metals, is used for all the before mentioned purposes but in oxic aqueous conditions is hydrolysis prone. Depending on its oxidation state iron is either insoluble or reacts to form reactive oxygen species and is dangerous to organisms. Organisms have thus evolved complex mechanisms to overcome the challenges of trafficking hydrolysis prone metals. This dissertation will focus on the study of the trafficking of hydrolysis prone iron and titanium by organisms, from metal selection to their use and storage. An examination of why metals are chosen, sequestration and transport of these metals, and use of the metals is presented. This research, as a whole, explores the cellular life cycle of hydrolysis prone metals.

It is thought that the first uses of metals before their incorporation by organisms were at mineral surfaces. To this end it would be useful for the organism to be able to attach to the mineral surface. *Rhodococcus ruber* GIN-1 was isolated for its ability to selectively bind to TiO_2 over other metal oxides. Biologically it could be advantageous to selectively bind to one mineral surface over another. The isolation and identification of

these proteins are examined within. *Rhodococcus ruber* GIN-1 has also been found to produce a novel siderophore. The siderophore is not yet completely identified but falls into the class of catecholates.

Once organisms begin to incorporate and use metals in proteins it would be useful to sequester and concentrate necessary metal ions that exist in low concentration in their environment. There are multiple organisms that are known to sequester high levels of titanium. One relatively unexplored family is that of *Sabellidae* or the feather duster worm. Organisms like this have been proposed as sentinel organisms to detect metal pollution in waters. In a model *Sabellidae* organism we have detected elevated levels of titanium, among other metals.

After metal sequestration from the environment, intraorganism transport of the ions to where they are necessary becomes important. Higher organisms use the transferrin family of proteins to traffic iron. While the transferrin cycle has been studied in depth, the reduction mechanism has not been elucidated in detail. We use a monolobal transferrin, nicatransferrin, from the model organism *Ciona intestinalis* to explore this iron reduction mechanism of the transferrin cycle and find that nicatransferrin can reduce iron with no external reductant. This reduction occurs on the timescale expected for the transferrin cycle and occurs without an iron (II) chelator. The source of the reducing equivalent is unknown but nicatransferrin was measured to have reduced up to 2.5 equivalents of iron.

Once transported to cells the metal ions can be put to use and incorporated into proteins or other structures. We examine the possible intentional use of titanium as a pigment in *Eudistoma purpuropuntatum*. The most abundant titanium sequesterer known

is *Eudistoma ritteri*, who concentrates titanium up to 1500 ppm (dry weight). *Eudistoma purpuropunctatum*, a close relative of *Eudistoma ritteri*, displays an interesting purple color due to small granules in its tunic. We investigate the source of the purple color in these granules and the ability of the organism to sequester titanium, finding that it has titanium concentrations on par with *Eudistoma ritteri*.

The metal ions that are not put to immediate use can be stored. Some metals exist in labile pools but due to iron's reactivity it is necessary to store it where it cannot cause cellular damage. The iron storage protein ferritin is a cage-like polymer made up of 24 ferritin monomers. The monomers exist as either H-chain or L-chain and the 24-mer can be comprised of just one type of these monomers or a mixture thereof. The covalent dimerization of the human L-chain 24-mer has been observed and the cause of this dimerization explored. We do not find direct evidence of the covalent linkage but do identify regions of the protein most likely to participate in the dimerization.

DEDICATION

For My Family

ACKNOWLEDGMENTS

First and foremost, I would like to thank Ann Valentine. I have had the privilege of working with her as both a research assistant and a teaching assistant. She has been a phenomenal advisor and mentor, leading by example in both research and teaching. With her guidance I have grown not only as a researcher and educator, but also as a person. I have been extremely fortunate to have learned from, and worked with Ann as my mentor.

I would like to thank Professors Graham Dobereiner and Michael Zdilla for being my committee members. Their support and ideas over the years have been very helpful and much appreciated. I need to specifically thank Professor Graham Dobereiner for his guidance throughout the last few years. I also appreciate Professor Ivan Dmochowski for his help and support. I would also like to thank Professors Bradford Wayland and Robert Stanley for their support and encouragement.

I would like to thank all the members of the Valentine Lab, past and present, for a wonderful environment to work in every day. I especially thank Katherine Buettner for not only being a great labmate but a great mentor and friend. I'd like to thank all the members of the group during my time: Corey Herbst-Gervasoni for our stimulating scientific and philosophical discussions, Kayleigh Jones for all the help in analyzing many of my samples on multiple instruments, Anna Gallo for being a magnificent friend and sounding board, Lauren Profitt for her enthusiasm and support, as well as Melanie Jalloh, Celia Zaouk, Laura Villareal, Jay Veras, Melissa Serrao, Darius Vrubliauskas, Nigam Padhair, and Olivia Stepanic. I would also like to thank the Stanley, Zdilla , and Schafmeister labs who were always willing to provide me with advice and loan me equipment whenever they could.

My time in graduate school would not have been possible without the help of numerous people. I have had wonderful support from Regina Shapiro, Sharon Kass, Shelah Cox, and Donald Deigh-Kai. The Chemistry Department has been fantastic in supporting and embracing the Student Distinguished Lectureship Program. I would to specifically thank Roger Cutitta for his support of my disaster relief training.

In my time at Temple I found myself part of a wonderful group of people. Graduate school would have been lacking without nights playing Bocce with Steve Peterson, Jesse Thornburg, Tim Davis, Jae Eun Cheong, Anna Gallo and Kate Buettner. I will forever be grateful to all of you for wonderful Fridays at the Diamond Club, enthusing over the latest research, commiserating, and generally goofing around.

I would not have made it here without the support of my family. They have encouraged me in everything I have done. The love my entire family, especially my parents and my sister, has been a source of strength throughout my entire time in graduate school. I cannot express how thankful I am for the love and encouragement of my parents throughout everything, especially times they questioned why they had kids.

TABLE OF CONTENTS

Page

LIST OF TABLES

LIST OF FIGURES

CHAPTER 1. BIOLOGICAL ROLE OF HYDROLYSIS PRONE METALS

1.1. Introduction

Many of the transition metals essential to biology are required in protein cofactors but can also cause cytotoxic reactions. Over the course of eons organisms have selected these metals for use in biological functions and must now traffic them safely from their environment to the desired internal locations. The metal requirements demand organisms to develop methods for both acquisition of the necessary metals and metal storage or efflux in times of abundance. Organisms have developed complex mechanisms for handling these metals, which exemplify biological control over inorganic coordination chemistry. These techniques include transmembrane transporters, metalloregulatory sensors, and cytoplasmic chaperones.

In these organisms each metal serves particular structural, transportation, or catalytic purposes and is needed in specified quantities. Some of the metal ions are also susceptible to hydrolysis and to hydrolytic precipitation in the oxic aqueous environments that most organisms inhabit. Studying how organisms select and traffic metals, particularly hydrolysis prone metals, like iron and titanium, is fundamental to our understanding of how they manage the potentially damaging effects of these metals, the uses of these metals, and of the co-evolution of Earth and organisms.

Understanding the aqueous chemistry of hydrolysis products of metal ions is of as much importance as understanding the biological chemistry.[1] Hydrolysis most often refers to solutions of salts and their reactions with water, by which they are converted to new ionic species, hydroxides, oxides, or precipitates. The hydrolysis chemistry of a

given metal complex can be complicated. General hydrolysis reactions and a detailed discussion of the thermodynamics of these reactions have been extensively reviewed.[2-4]

The metals chosen for the previously mentioned applications must be both relatively abundant and bioavailable. The metals abundance and bioavailability may have only been sufficient at the time when the specified metalloprotein requirement evolved and may have changed due to the chemical evolution of Earth over a geologic timescale. Organisms have had to adapt to the chemical evolution of the Earth as they concurrently evolved through time. The abundance of metals on Earth has remained fairly static, but the bioavailability of transition metals has changed.[5] Elements of high abundance in the crust may be available for cells through cellular uptake mechanisms. The elemental composition of the crust has been established showing that iron and titanium are the fifth and ninth most abundant elements in the crust, respectively.[6, 7]

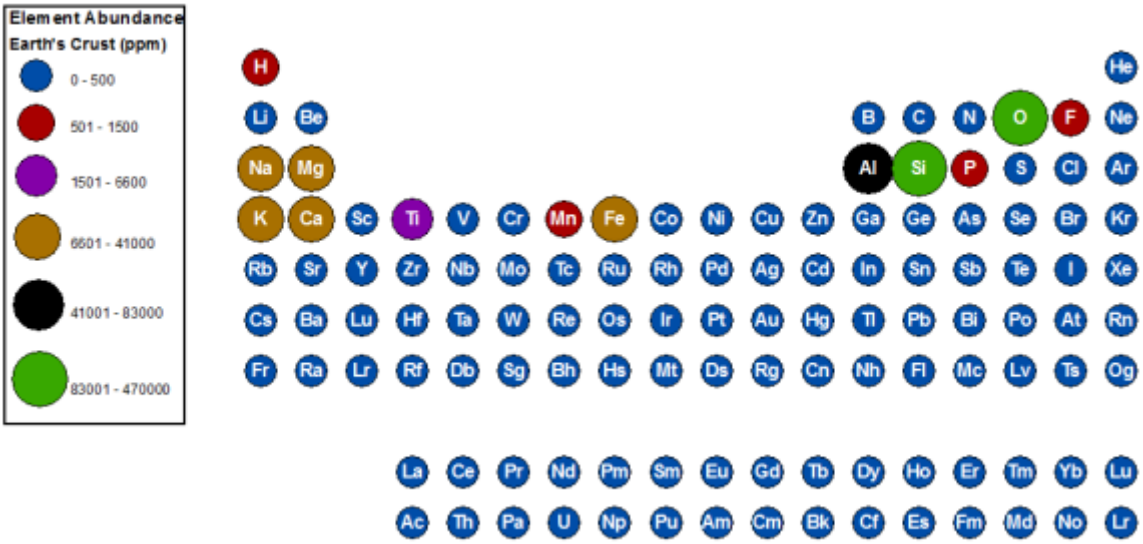

Figure 1.1 Periodic table of element abundance in the earth's crust by weight.

The more abundant the element the larger it appears on the periodic table. Made using data from reference 6.

The most well studied bioinorganic element is iron. Iron is abundant in the Earth's crust, but due to its tendency to hydrolyze in aqueous environments it is relatively insoluble. In aqueous environments it is present in the 2+ and 3+ oxidation states. This redox couple along with its high abundance are likely the cause of its vast use in organisms. Protein active sites can tune their steric and electronic configurations to access more oxidized, Fe(IV) and Fe(V), and reduced Fe(I) states.[8, 9] The solubility of Fe(III) in water at neutral pH is often cited to be 10^{-18} M,[10, 11] but an alternative soluble Fe(III) concentration of 1.4 nM has been proposed on theoretical grounds,[12, 13] and measured to be 0.3 nM.[4, 14]

Iron is necessary for all but a few organisms on the planet and is used in enzymes for photosynthesis, respiration, nitrogen fixation, ammonia assimilation, nitrate assimilation, and oxygen transportation but it also participates in highly damaging Fenton chemistry.[13, 15, 16] The biological uses of iron have been comprehensively studied in humans,[17, 18] and bacteria.[19-22] While the biological use of iron has been studied extensively, there are still iron metalloproteins that have not yet been identified.[23] In this work we explore the different stages of biological trafficking of hydrolysis prone iron and titanium.

REFERENCES CITED

1. J. P. Gaffney and A. M. Valentine, The challenges of trafficking hydrolysis prone metals and ascidians as an archetype, *Dalton Transactions*, 2011, **40**, 5827-5835.
2. C. F. Baes and R. E. Mesmer, *The Hydrolysis of Cations*, Wiley, New York, 1976.
3. C. F. Baes and R. E. Mesmer, The Thermodynamics of Cation Hydrolysis, *American Journal of Science*, 1981, **281**, 935-962.
4. P. L. Brown and C. Ekberg, *Hydrolysis of Metal Ions*, Wiley-VCH Verlag GmbH & Co. KGaA, Weinheim, Germany, 2016.
5. L. J. Robbins, S. V. Lalonde, M. A. Saito, N. J. Planavsky, A. M. Mloszewska, E. Pecoits, C. Scott, C. L. Dupont, A. Kappler and K. O. Konhauser, Authigenic iron oxide proxies for marine zinc over geological time and implications for eukaryotic metallome evolution, *Geobiology*, 2013, **11**, 295-306.
6. J. Emsley, *The Elements*, Clarendon Press, Oxford, U.K., 3rd edn., 1998.
7. M. J. Winter, Diffusion Cartograms for the Display of Periodic Table Data, *Journal of Chemical Education*, 2011, **88**, 1507-1510.
8. C. E. Tinberg and S. J. Lippard, Dioxygen Activation in Soluble Methane Monooxygenase, *Accounts of Chemical Research*, 2011, **44**, 280-288.
9. M. Y. Darensbourg, E. J. Lyon, X. Zhao and I. P. Georgakaki, The organometallic active site of Fe hydrogenase: Models and entatic states, *Proceedings of the National Academy of Sciences of the United States of America*, 2003, **100**, 3683-3688.

10. S. C. Andrews, A. K. Robinson and F. Rodriguez-Quinones, Bacterial iron homeostasis, *Fems Microbiology Reviews*, 2003, **27**, 215-237.
11. K. N. Raymond, E. A. Dertz and S. S. Kim, Enterobactin: An archetype for microbial iron transport, *Proceedings of the National Academy of Sciences of the United States of America*, 2003, **100**, 3584-3588.
12. J. R. Chipperfield and C. Ratledge, Salicylic acid is not a bacterial siderophore: a theoretical study, *Biometals*, 2000, **13**, 165-168.
13. C. Ratledge and L. G. Dover, Iron metabolism in pathogenic bacteria, *Annual Review of Microbiology*, 2000, **54**, 881-941.
14. A. Stefansson, Iron(III) hydrolysis and solubility at 25 degrees C, *Environmental Science & Technology*, 2007, **41**, 6117-6123.
15. J. F. Briat, Iron Assimilation and Storage in Prokaryotes, *Journal of General Microbiology*, 1992, **138**, 2475-2483.
16. M. Imbert and R. Blondeau, On the iron requirement of lactobacilli grown in chemically defined medium, *Current Microbiology*, 1998, **37**, 64-66.
17. M. D. Garrick and L. M. Garrick, Cellular iron transport, *Biochimica Et Biophysica Acta-General Subjects*, 2009, **1790**, 309-325.
18. M. D. Garrick, Human iron transporters, *Genes and Nutrition*, 2011, **6**, 45-54.
19. S. Dhungana and A. L. Crumbliss, Coordination chemistry and redox processes in siderophore-mediated iron transport, *Geomicrobiology Journal*, 2005, **22**, 87-98.

20. A. L. Crumbliss and J. M. Harrington, in *Advances in Inorganic Chemistry, Vol 61: Metal Ion Controlled Reactivity*, eds. R. VanEldik and C. D. Hubbard, 2009, vol. 61, pp. 179-250.

21. C. J. P. Siburt, T. A. Mietzner and A. L. Crumbliss, FbpA - A bacterial transferrin with more to offer, *Biochimica Et Biophysica Acta-General Subjects*, 2012, **1820**, 379-392.

22. C. K. Y. Lau, K. D. Krewulak and H. J. Vogel, Bacterial ferrous iron transport: the Feo system, *Fems Microbiology Reviews*, 2016, **40**, 273-298.

23. A. Cvetkovic, A. L. Menon, M. P. Thorgersen, J. W. Scott, F. L. Poole, II, F. E. Jenney, Jr., W. A. Lancaster, J. L. Praissman, S. Shanmukh, B. J. Vaccaro, S. A. Trauger, E. Kalisiak, J. V. Apon, G. Siuzdak, S. M. Yannone, J. A. Tainer and M. W. W. Adams, Microbial metalloproteomes are largely uncharacterized, *Nature*, 2010, **466**, 779-U718.

CHAPTER 2. CONTEMPLATING A ROLE FOR TITANIUM IN ORGANISMS[1]

2.1. Introduction

There is no known essential role for titanium in the biology of any organism. However, there are studies across many fields that suggest Ti is at least biologically active.[2] Most titanium on Earth is locked up in insoluble minerals, such that one might wonder how titanium could participate in biorelevant chemistry. Titanium is the ninth most abundant element in the crust at 0.6%,[3] so even a small percentage of solubilized material presents a large amount of metal.[4] Most of the titanium present in the environment exists as rutile, a crystal form of TiO_2, or as ilmenite, $FeTiO_3$.[4, 5] Geologically, titanium is often considered immobile although recent evidence suggests it may be mobile in rocks under weathering conditions[6, 7] and in soils.[8] Soluble titanium ranges from 4 pM in surface ocean waters,[9-11] where it is far under-saturated, to 100 μM in hot spring waters.[12] In both fresh water and seawater, thermodynamic models assume the predominance of $TiO(OH)_2$.[13] Complexation by organic ligands is important in at least some natural environments.[2] TiO_2 nanoparticles in both fresh water and marine systems agglomerate, forming micrometer size particles, or are incorporated into marine snow where particle feeders may ingest them.[14] Taken together, these various environments present the opportunity for organisms to use titanium in the form of soluble hydroxide species, as organically complexed species, or in mineral form.

Proteins have evolved to use the metals that are, or least were at the time of those proteins' evolution, the most accessible.[15-17] Some active centers of metalloenzymes

resemble the structures of minerals presumed to be present in precipitates from hydrothermal solutions in the ocean billions of years ago.[18, 19] Considering this use of available material and the vast abundance of titanium on the planet, it is conceivable that nature might have made use of this element, for example during evolution of the earliest prokaryotes. It is clear that some extant organisms do use and contain titanium in certain structures.

Titanium is capable of biologically interesting chemistry but has inherent characteristics that make it difficult to identify in biological systems. Modern experimental methods offer the possibility of identifying new roles for metals like titanium in bioinorganic chemistry. The metal and its ions bring a set of complications for common separation and -omic techniques. Choice of experimental system will be crucial, whether a well-studied and familiar model system or a lesser-known organism known to be associated with high titanium concentrations.

2.2. Historical Identification of Essential Elements

Many bioessential elements were identified because humans experienced symptoms from an accidental dietary deficiency, as for iron or cobalt, or exhibited diseases of metal mismanagement, like Wilson's disease for copper. Some metals, like chromium, were rigorously excluded from the diet to look for signs that the excluded metal was essential. Some metal ions in biology have conspicuous properties that make them easy to identify, like the color of blue copper proteins or the multiline EPR spectra of some manganese proteins.

Even in recent years, the list of metals having a native biological role continues to grow. In the oceans where zinc is scarce, a diatom species has a carbonic anhydrase that

utilizes cadmium in its active site instead of zinc.[20] Some methanotrophs natively feature the usually toxic lanthanides lanthanum and cerium instead of calcium in the active site of their methanol dehydrogenase.[21] Each of these discoveries was foreshadowed by the novel metals' binding in the active sites of the class of enzymes in question, cadmium to zinc enzymes and lanthanides to calcium enzymes. But a form with a unique requirement for cadmium and for lanthanide, respectively, was a significant development.

2.3. Characteristics of Titanium Relevant to Biology

The most stable oxidation state of titanium in an aqueous oxic environment is Ti(IV), which shares characteristics such as ionic radius with Al(III) and Fe(III).[2] These metals also share a thermodynamic preference for similar binding sites, though Ti(IV) is more strongly Lewis acidic (Figure 2.1).[22]

Ti(IV) can associate with some Fe(III) proteins. In vitro Ti(IV) binds more tightly than Fe(III) to the iron transport protein human serum transferrin.[23] The iron storage protein ferritin can also biomineralize titanium.[24, 25] Like those other ions, Ti(IV) is prone to hydrolysis and hydrolytic precipitation, though its insolubility is not as extreme as is often assumed.[2] Binding to small or large biomolecules increases the solubility of Ti(IV).

Turning to kinetics, Ti(IV) complexes exhibit a wide range of ligand exchange rates. Hydroxyl and water ligands are very labile and exchange with rate constants on the order of thousands per second.[26] But essentially no exchange is observed when the Ti ligand is the hexadentate siderophore enterobactin.[27] Falling somewhere in the middle of these extremes, over minutes to hours, are the rates for exchange with small bioligands like ascorbate or citrate, or with proteins like transferrin.[23, 28]

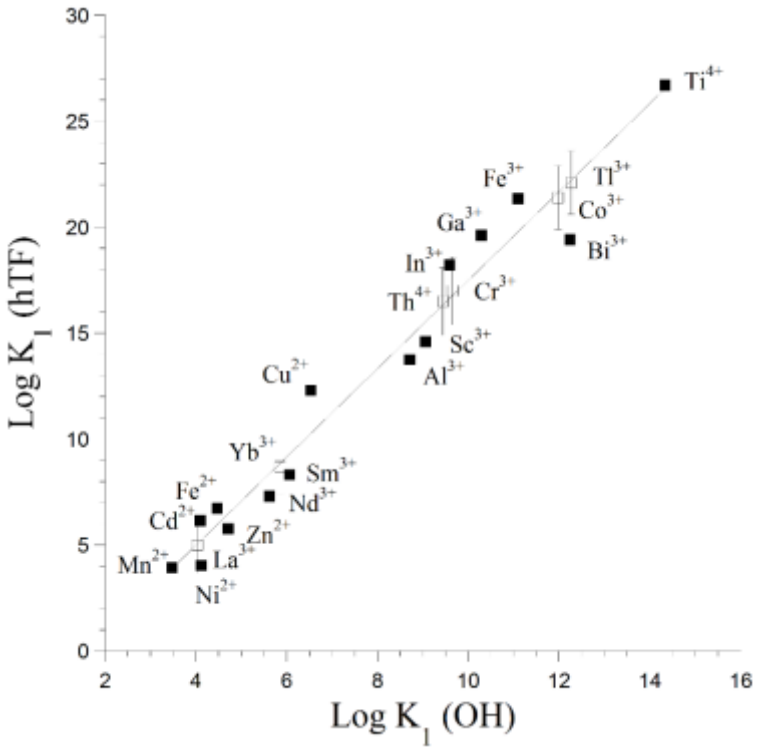

Figure 2.1 Correlation of binding constants for metal binding to human serum transferrin (hsTF) with metal Lewis acidity, as quantified by K_1 (OH).

Filled squares represent experimental values, while open squares represent estimated ones. Adapted from data in references 22 and 23.

Just considering the thermodynamic stability and kinetic lability of metal-ligand complexes ignores the powerful compartmentalization control that living cells exhibit over different metal species in vivo.[29, 30] Some cells use physical compartmentalization to overcome the inherent thermodynamic preferences of a protein binding site. Once a complex is removed from the compartmentalized environment, though, it is important to appreciate the fundamental thermodynamics and kinetics of the metal ion binding to its ligand(s).

2.4. The Possible Roles of Titanium

Against the backdrop of this fundamental chemistry, Nature would sequester Ti if it were useful to the organism. Some biochemical processes for which titanium might be suitable (or even uniquely excellent) are suggested by the many ways humans and human chemists use this element.

The powerful Lewis acidity of Ti(IV) could be deployed to deprotonate difficult-to-deprotonate substrates in a metalloenzyme active site. As a benchmark to illustrate its power, water molecules coordinated to Ti(IV) are deprotonated below pH 0.[2, 31] In chemical catalysis outside biology, titanium plays this role often and well, for example as a catalyst for aldol reactions.[32]

Depending on the ligand environment, a Ti(IV)/Ti(III) couple would be suitable for low-potential redox, for example in an electron transfer chain or redox metalloenzyme. The potential of the Ti(IV)/Ti(III) couple in acid is close to 0 V vs. NHE,[33] but ligands that tightly bind the oxidized form and stabilize it with respect to hydrolytic precipitation can tune the potential over a range down to at least -1 V.[2, 34, 35]

Titanium might assume a role in the construction or repair of soft biomaterials, for example in the acsidians that are avid accumulators of the element. Ascidians are also called tunicates because of their protective covering, the tunic.[36] The tunic varies between species but is composed of fibrous cellulose components linked with proteins.[37] Metals and polyphenolic secondary metabolites called tunichromes may be involved in tunic formation or wound repair.[38] Possible metal ligands in the tunic include the tunichromes, proteins or modified proteins (including those containing DOPA side chains) and carbohydrates. The tunic also contains free wandering blood cells from the ascidian's

open circulatory system. Some of these cells have high metal concentrations. Some are high in polyphenol content, and probably contain high concentrations of tunichromes, either with or without associated metals. During wound healing, these cells coagulate and lyse, and electron dense fibers form.[39] The metal may have a regulating effect by acting as a stabilizer of the component monomers for polymer formation, as a catalyst for polymerization, or as a regulator of the process.

Titanium minerals are widespread and stable. Titanium dioxide is a widely used pigment, and the oxide forms as a passivating coating when titanium metal and its alloys are used in medical implants.[2] Mineralized or biomineralized titanium could provide a protective coating or defense for organisms. One place titanium dioxide has found promising use is in dye-sensitized solar cells.[40] It is exciting to think that Nature has had the raw materials to take advantage of this chemistry for billions of years, though no natural TiO_2 solar cell is yet known.

Titanium might serve an antimicrobial function for an organism,[2] either in the presence or absence of light. UV irradiation of Ti compounds, especially in aqueous environments, generates singlet oxygen and superoxide anion. Both species are damaging cellular oxidants.

Finally, titanium may afford ultraviolet protection for organisms, in effect forming a sunscreen. TiO_2 is used as a commercial sunscreen because of its light-scattering properties. Depending on the identity of the ligand or the size of the particle, light absorption or scattering by a Ti compound or mineral may provide a similar protective effect. The tunic of the ascidian *Lissoclinum patella* absorbs UV-B (290 – 320 nm) but not visible light, providing a protective environment for a symbiotic

photosynthetic prokaryote.[41, 42] The symbiont provides oxygen to the ascidian, and cannot survive the UV exposure outside of the tunic. This particular ascidian species has not been associated with elevated Ti levels, though other ascidians are avid accumulators.

2.5. Detecting Titanium

Detecting Ti(IV) can be difficult; it is d^0, diamagnetic, and exhibits no EPR signal. Most titanium complexes are colorless or have indistinct ligand-to-metal charge transfer bands in the ultraviolet region. There are no practically useful NMR or radioisotopes,[2] and use of X-ray absorption spectroscopy (XAS) has been limited. Older elemental analysis methods such as flame atomic absorption (AA) were relatively insensitive to titanium. Importantly, in such single-element techniques, researchers had to be specifically looking for titanium to find it.

Techniques like Inductively Coupled Plasma – Mass Spectrometry (ICP-MS) are more sensitive than AA and are multi-element. But other kinds of considerations sometimes interfere with the detection of Ti. The excellent international GEOTRACES project[43] strives to characterize biogeochemical cycles of many trace elements. A few of the associated studies have focused on titanium,[11, 44-46] but much of the collection apparatus was constructed from titanium, presumably because it is quite inert and because there was relatively less interest in focusing on Ti as an experimental element.

Finally and in general, the inherent difficulty in characterizing metalloproteomes is well known.[47-52] In one important study,[47] although no Ti was detected in the growth medium, a relatively high Ti concentration (1.6 μM) was detected in the cytoplasmic extract of Pyrococcus furiosus. This cytoplasmic Ti concentration was fourth among trace metals after Fe, Zn, and W, and was higher than Ni, Co, or Mn. But Ti was no longer detected

after a relatively mild anion exchange separation; the fate of the Ti is not clear. Possibly it was not ever bound to protein, or it was very labile. This result led us to consider how the bioinorganic behaviour and properties of titanium might manifest during the application of emerging -omic methods to identify novel metalloproteins.

In a plausible experimental plan, an experimental organism would be chosen, driven by the desire for a well-studied model system or for a system already known to be associated with Ti. The biomolecules would be subjected to a separation method like liquid chromatography or gel electrophoresis. A downstream elemental analysis such as ICP-MS or a metal-specific sensor would identify which biomolecule(s) were associated with titanium. Minimal disruption of binding sites would be necessary. Finally, the biomolecules would be identified by some means. Each of these steps deserves special consideration in light of the properties and aqueous behavior of titanium.

2.6. Model Organisms

There are two options when deciding on where to search for putative titanium metalloproteins: well-studied generic model organisms or established sequesterers of titanium such as diatoms and ascidians. Each of these routes offers distinct advantages.

2.6.1. Well-Studied Model Organisms

The large body of work on organisms like *E. coli* and yeast allows for a better chance at identifying proteins using a shotgun style of proteomics.[47] Studying the metalloproteomes of *P. furiosus*, *E. coli* and *S. solfataricus* allowed for high throughput and quick identification of isolated proteins. There is some work on the effect of titanium compounds on the growth of yeast.[53] But as the cost of genome sequencing continues to

decrease, the availability of the organism's full genome ceases to be an impediment to the use of a more unusual system.

2.6.2. Avid Marine Sequesterers of Titanium

2.6.2.1. Diatoms

Diatoms cultured in the laboratory sequester Ti from the growth media up to 940 ppm in the whole organism from a media containing 60 ppm titanium[54] and given a TiO_2 rich diet can have local concentrations of up to 80 wt% in their frustules.[55] In native samples Ti has been observed at up to 1254 ppm in the diatom frustule.[56] The titanium uptake and incorporation into the frustules happens at the same rate as silicon uptake.[57] This incorporation of Ti may explain why dissolved Ti is depleted along with silicon during a spring diatom bloom[58] and may contribute to the surface depleted profile of Ti in the ocean.[9] This appearance of titanium could simply be due to titanium precipitation onto the frustule, but Ti could be actively incorporated by biomolecules in the organism. The enzymes that direct the biomineralization of silica in diatoms are called silaffins;[59] synthetic peptides derived from silaffins,[60] and recombinant silaffins[61, 62] direct TiO_2 mineralization given an otherwise soluble source of titanium (Figure 2.2).[63] Incorporation of titanium into the diatom frustule has bactericidal effects.[64]

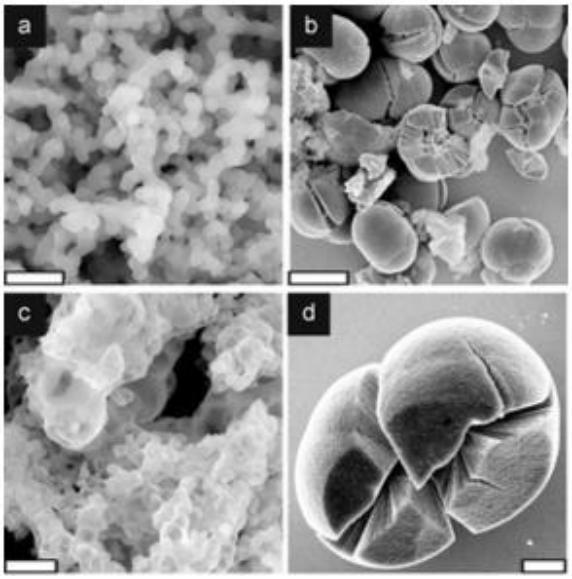

Figure 2.2 Titania formation by recombinant silafins, rSil1L and rSilC.

SEM images of precipitates formed by a) 53 μM rSil1L b-d) 32 μM rSilC in sodium phosphate/citrate buffer solution (50 mM, pH 7). In a) the particles fuse together forming an interconnected network. b) rSilC-titania contains two different structures; c) smaller hollow particles and d) larger particles with frequent cracks. Scale bars: 1 μm (a,c) 20 μm (b) and 5 μm (d). Adapted from reference 62.

2.6.2.2. Ascidians

Many ascidian species sequester high concentrations of metal ions, most famously vanadium.[65, 66] Several species accumulate titanium selectively.[67] *Eudistoma ritteri* has exhibited the highest concentration at up to 1500 ppm dry weight.[68] In other species, such as *Pyura chilensis* and *Ascidia dispar*, somewhat lower amounts of titanium have been detected, but for both species the highest concentration of titanium was detected in their blood cells.[69] There is also an equal distribution of titanium in these species' blood cells between the cell wall and the cytoplasm, whereas iron is amassed almost completely in the cytoplasm. Beyond this sequestration ascidians are noted for their production of secondary metabolites called tunichromes,[70] and proteins like ferreascidin[71] that feature

DOPA catechol moieties that would make them excellent binders of Lewis acidic metal ions such as Ti(IV). Another mechanism of transport for metals in ascidians is a transferrin-like pathway.[66] This mechanism has implications for titanium transport as titanium interactions with transferrins have been demonstrated.[23]

2.6.2.3. Sabellidae

Like ascidians, sabellidae or feather duster worms have been suggested as useful organisms for monitoring water pollution.[72] Members of the sabellidae family build tubes around themselves out of parchment-like material, sand and/or bits of shell.[73] The species *Eudistylia vancouveri* sequesters titanium. It secretes a parchment-like shell but its shell was not examined for metal content.[72] Other studies of sabellidae metal content have ignored examination of titanium content.[74]

2.6.3. Organisms Associated with Titanium Minerals

Many organisms exploit inorganic minerals for structural support, or as sensors or instruments.[75, 76] Although titanium minerals are abundant, examples of organisms associating with them are rare. In one classic text on biomineralization, titanium appears on a list of biomineralized elements with a reference to unpublished work by the author on ilmenite found in a prokaryote.[75] The identity of the prokaryote is unknown (S. Mann, personal communication).

Organisms produce biominerals with varying degrees of control or collect them as detrital materials from the environment. Mineralization of titanium would require a mechanism for sequestration from the environment and then active direction of mineralization. Collection from the environment would require a specific interaction between molecules on the cell-surface of the organism with the titanium mineral surface.

There are a few possibilities about how the latter molecular recognition process might work. Peptides might have evolved to bind specifically to TiO_2 mineral surfaces.[77, 78] Glycopeptides, phosphopeptides and phosphoproteins demonstrate a particularly high affinity for TiO_2,[79, 80] and nucleosides for TiO_2/ZrO_2.[81] The specifics of these biomolecule-surface interactions are being explored.[82-84]

2.6.3.1. Insects

Vespa orientalis, a type of hornet, attaches grains of a titanium-containing mineral in each cell of its honeycomb-shaped nest using its saliva (Figure 2.3).[85-87] The adhered minerals appear to be ilmenite, but titanium was not detected in a random sampling of the soil around the nest.[87] It is thought that the mineral may act as a gravity sensor[86] or may in fact act as an infrared reflector, as the titanium faces of the minerals appear to be intentionally placed facing into open space.[87]

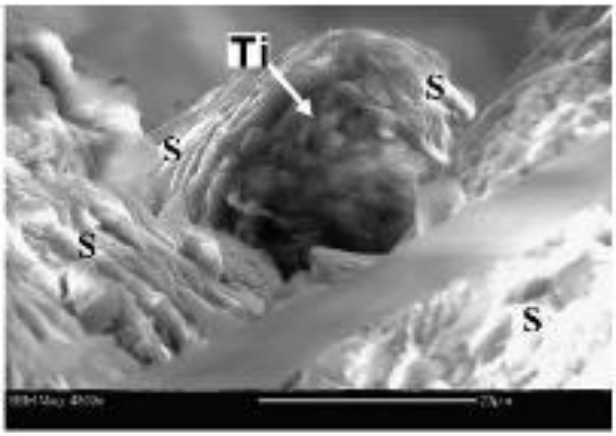

Figure 2.3 ESEM image of a titanium particle (arrow) from the roof of a hornet's comb cell.

"S" marks the saliva fibers. Scale bar = 20 μm. Adapted from reference 87.

2.6.3.2. TiO_2-Adhesive Bacteria

Nanoparticulate TiO_2 biosorption has been observed with *E. coli* and *P. aeruginosa* and is postulated to occur more broadly.[88-92] Adsorption of the bacteria to the surface has been observed as well as agglomeration of particles on the bacteria. These interactions are facilitated by both siderophores and polysaccharides on the cell surface.

Bacteria from the Mediterranean Sea were isolated by exploiting their ability to adhere to TiO_2 very strongly.[93] A Gram positive species was isolated, *Rhodococcus ruber* GIN-1, which adhered to TiO_2 selectively over other metal oxides in under 1 min, at pH values between 1 and 9, and at temperatures between 4 and 80 °C.[93] Cell adhesion to the mineral was not disrupted by dilute acids, alcohols, and cationic or nonionic detergents. A cell surface homolog of the normally cytosolic protein dihydrolipoamide dehydrogenase was among the proteins implicated in adhesion.[94]

2.7. Separations and Detection

Biomolecules are often subjected to a separation step and characterized by one of several techniques. Putative titanium biomolecules might fare better or worse than other metallobiomolecules in some of these procedures.

2.7.1. Separations Effect on Ion Occupancy

2.7.1.1. Gel Electrophoresis

The denaturation process involved with many gel electrophoresis techniques has been shown to lead to partial or even total loss of metal.[95, 96] Even the use of non-denaturing methods can be problematic as certain buffers can form metal complexes leading to metal loss,[95] although recent studies show improvements for certain metals.[97]

A biomolecule might offer a coordination environment (such as several catechol moieties) that would be much more stable than that offered by a buffer. But many functionalities present in buffers, like phosphates, would bind Ti(IV) and might remove it from a less stable coordination site.

2.7.1.2. Size exclusion chromatography

This technique may maintain even metalloproteins that are not very stable, because these separations do not involve strong physical interactions between the analyte and the stationary phase. As above, the choice of buffer is key. Phosphate buffers complex several metal ions so Good's buffers have often been preferred. However, typical buffers used in size exclusion chromatography can interact with metals,[98] and both HEPES and MOPS can cause zinc and iron release from plasma metalloproteins, which was accredited to their complexation properties.[99]

2.7.1.3. Ion exchange chromatography

Ion exchange chromatography is a highly efficient separation method. This technique however introduces the risk of metal displacement by competition with not only the mobile phase but also with the stationary phase.[100] Ti-transferrin complex recovery via a strong anion exchange column was significantly lower than that recovered from size exclusion chromatography, which itself was much less than 100%.[101]

During any of these separation techniques, it would be important to monitor the titanium inventory. If the metal did dissociate from an associated biomolecule, it might bind very tightly to a column or, alternatively, not bind at all, depending on speciation.

2.7.2. Methods of Identification

A variety of techniques can identify new metalloproteins. Simple searches of genomic or proteomic data require prior knowledge of a predicted metal binding sequence, and thus are not suitable for the identification of new motifs.[102] Accurate prediction of metalloproteins is limited to closely homologous well-characterized proteins. A recent metallomic study demonstrated that some metal binding motifs have not yet been recognized, even for common biologically relevant metals like iron.[47] Phage display identifies sequences with high affinity,[103] and phage display has identified TiO_2 binding sequences,[77, 104] but those specific sequences are not apparent in the proteomic databases. There are affinity proteomic methods that allow for detection of proteins in their natural environment,[105] but an appropriate affinity material must be chosen. Identifying a metal binding site deep within a folded protein remains a challenge. There are imaging techniques that can be useful in identifying metalloproteins.[106, 107] Recently, promising metal-specific sensors capable of in vivo detection were developed.[108] While each of these methods has its advantages, some of the most versatile methods for identifying and characterizing metalloproteins involve mass spectrometry after protein separations, which we will focus on. The immense growth of available genome sequences has led to a rapid rise in the power of bioinformatics. The combination of this vast knowledge with chromatography and mass spectrometry is a powerful tool in determination of metalloproteins.

2.7.2.1. Bottom-up Identification

The bottom-up mass spectrometric approach is the most commonly used for protein identification and has the distinct advantage of high-throughput methodology. In

this method, proteins, either purified or in crude extracts, are proteolytically digested and analysed by mass spectrometry. Tandem mass spectrometry can be used to sequence and characterize the peptides further. This method has also generated the large databases that are searched to identify proteins. But only 50-70% of the peptides of a particular protein are usually identified.[109] The method can lead to loss of information about post-translational modifications, particularly phosphates,[110] because they can be lost during collision induced dissociation. Phosphorylated proteins may be some of the most important for investigation of titanium mineral binding. Using this method to identify a titanium metalloprotein would require multiple digestions with different enzymes to generate complementary sets of data and a full sequence.

2.7.2.2. Top-down Identification

Top-down methods involve analysis of whole protein molecules by mass spectrometry, usually involving a Fourier transform-ion cyclotron resonance (FT-ICR) instrument.[111] This method provides complete sequence coverage. There are no issues with peptide generation and separation, and the MS/MS process can be modified so that post-translational modifications can be preserved, helping with observation of isoforms.[112] This method does however require large quantities of purified protein and the data are highly complex due to the multiply charged ions and the possibility of overlapping peptide ion envelopes. The main concern with top-down proteomics regarding titanium is the lack of high-throughput discovery.

2.8. Conclusion

Much data suggests that titanium is biologically relevant but it has not been demonstrated to be essential for any organism. Evolution has directed proteins to use

accessible metals and the abundance of titanium mineral and dissolved titanium argues for the existence of a titanium metalloprotein. The high concentrations of titanium in organisms and the chemical processes it is known to participate in support this idea. The identification of a true titanium metalloprotein is not an easy task. Titanium is normally a difficult metal to handle in an aqueous oxic environment. Attempting to manipulate a putative titanium metalloprotein without disturbing its protein environment complicates matters. The considerations outlined here for titanium apply more generally to many metal ions, especially those that are Lewis acidic and hydrolysis prone. This group includes established biometals like iron, which despite decades of study still occurs in coordination environments not yet recognized.[47] By understanding both how titanium is known to interact with organisms and how it interacts with local protein environments, it may be possible to address the essentiality of this quite abundant element.

REFERENCES CITED

1. M. R. Zierden and A. M. Valentine, Contemplating a role for titanium in organisms, *Metallomics : integrated biometal science*, 2016, **8**, 9-16.
2. K. M. Buettner and A. M. Valentine, Bioinorganic Chemistry of Titanium, *Chemical Reviews*, 2012, **112**, 1863-1881.
3. J. Emsley, *The Elements*, Clarendon Press, Oxford, U.K., 3rd ed. edn., 1998.
4. A. KabataPendias and A. B. Mukherjee, Trace Elements from Soil to Human, *Trace Elements from Soil to Human*, 2007.
5. C. W. Correns, in *Handbook of Geochemistry*, ed. K. H. Wedepohl, Springer, Berlin, 1969-1978, vol. 2.
6. X. Du, A. W. Rate and M. A. M. Gee, Redistribution and mobilization of titanium, zirconium and thorium in an intensely weathered lateritic profile in Western Australia, *Chemical Geology*, 2012, **330**, 101-115.
7. T. Taboada, A. M. Cortizas, C. Garcia and E. Garcia-Rodeja, Particle-size fractionation of titanium and zirconium during weathering and pedogenesis of granitic rocks in NW Spain, *Geoderma*, 2006, **131**, 218-236.
8. S. Cornu, Y. Lucas, E. Lebon, J. P. Ambrosi, F. Luizao, J. Rouiller, M. Bonnay and C. Neal, Evidence of titanium mobility in soil profiles, Manaus, central Amazonia, *Geoderma*, 1999, **91**, 281-295.
9. K. J. Orians, E. A. Boyle and K. W. Bruland, DISSOLVED TITANIUM IN THE OPEN OCEAN, *Nature*, 1990, **348**, 322-325.
10. K. W. Bruland and M. C. Lohan, in *The Oceans and Marine Geochemistry*, ed. H. Elderfield, Elsevier-Pergamon, Oxford, 2003, pp. 23-47.

11. A. Dammshaeuser, T. Wagener, D. Garbe-Schoenberg and P. Croot, Particulate and dissolved aluminum and titanium in the upper water column of the Atlantic Ocean, *Deep-Sea Research Part I-Oceanographic Research Papers*, 2013, **73**, 127-139.

12. M. R. Van Baalen, Titanium Mobility in Metamorphic Systems: A Review, *Chemical Geology*, 1993, **110**, 233-249.

13. D. R. Turner, M. Whitfield and A. G. Dickson, THE EQUILIBRIUM SPECIATION OF DISSOLVED COMPONENTS IN FRESH-WATER AND SEAWATER AT 25-DEGREES-C AND 1 ATM PRESSURE, *Geochimica Et Cosmochimica Acta*, 1981, **45**, 855-881.

14. J. J. Doyle, V. Palumbo, B. D. Huey and J. E. Ward, Behavior of Titanium Dioxide Nanoparticles in Three Aqueous Media Samples: Agglomeration and Implications for Benthic Deposition, *Water Air and Soil Pollution*, 2014, **225**.

15. C. L. Dupont, S. Yang, B. Palenik and P. E. Bourne, Modern proteomes contain putative imprints of ancient shifts in trace metal geochemistry, *Proceedings of the National Academy of Sciences of the United States of America*, 2006, **103**, 17822-17827.

16. R. E. M. Rickaby, Goldilocks and the three inorganic equilibria: how Earth's chemistry and life coevolve to be nearly in tune, *Philosophical transactions. Series A, Mathematical, physical, and engineering sciences*, 2015, **373**.

17. K. J. Waldron, J. C. Rutherford, D. Ford and N. J. Robinson, Metalloproteins and metal sensing, *Nature*, 2009, **460**, 823-830.

18. B. Herschy, A. Whicher, E. Camprubi, C. Watson, L. Dartnell, J. Ward, J. R. G. Evans and N. Lane, An Origin-of-Life Reactor to Simulate Alkaline Hydrothermal Vents, *Journal of Molecular Evolution*, 2014, **79**, 213-227.

19. W. Martin, J. Baross, D. Kelley and M. J. Russell, Hydrothermal vents and the origin of life, *Nature Reviews Microbiology*, 2008, **6**, 805-814.

20. T. W. Lane, M. A. Saito, G. N. George, I. J. Pickering, R. C. Prince and F. M. M. Morel, A cadmium enzyme from a marine diatom, *Nature*, 2005, **435**, 42-42.

21. A. Pol, T. R. M. Barends, A. Dietl, A. F. Khadem, J. Eygensteyn, M. S. M. Jetten and H. J. M. Op den Camp, Rare earth metals are essential for methanotrophic life in volcanic mudpots, *Environmental Microbiology*, 2014, **16**, 255-264.

22. H. Y. Li, P. J. Sadler and H. Z. Sun, Rationalization of the strength of metal binding to human serum transferrin, *European Journal of Biochemistry*, 1996, **242**, 387-393.

23. A. D. Tinoco and A. M. Valentine, Ti(IV) binds to human serum transferrin more tightly than does Fe(III), *Journal of the American Chemical Society*, 2005, **127**, 11218-11219.

24. M. T. Klem, J. Mosolf, M. Young and T. Douglas, Photochemical mineralization of europium, titanium, and iron oxyhydroxide nanoparticles in the ferritin protein cage, *Inorganic Chemistry*, 2008, **47**, 2237-2239.

25. F. F. Amos, K. E. Cole, R. L. Meserole, J. P. Gaffney and A. M. Valentine, Titanium mineralization in ferritin: a room temperature nonphotochemical preparation and biophysical characterization, *Journal of Biological Inorganic Chemistry*, 2013, **18**, 145-152.

26. P. Comba and A. Merbach, THE TITANYL QUESTION REVISITED, *Inorganic Chemistry*, 1987, **26**, 1315-1323.

27. T. Baramov, K. Keijzer, E. Irran, E. Moesker, M.-H. Baik and R. Suessmuth, Synthesis and Structural Characterization of Hexacoordinate Silicon, Germanium, and Titanium Complexes of the E-coli Siderophore Enterobactin, *Chemistry-a European Journal*, 2013, **19**, 10536-10542.

28. K. M. Buettner, J. M. Collins and A. M. Valentine, Titanium(IV) and Vitamin C: Aqueous Complexes of a Bioactive Form of Ti(IV), *Inorganic Chemistry*, 2012, **51**, 11030-11039.

29. S. Tottey, K. J. Waldron, S. J. Firbank, B. Reale, C. Bessant, K. Sato, T. R. Cheek, J. Gray, M. J. Banfield, C. Dennison and N. J. Robinson, Protein-folding location can regulate manganese-binding versus copper- or zinc-binding, *Nature*, 2008, **455**, 1138-U1117.

30. R. Kudva, K. Denks, P. Kuhn, A. Vogt, M. Mueller and H.-G. Koch, Protein translocation across the inner membrane of Gram-negative bacteria: the Sec and Tat dependent protein transport pathways, *Research in Microbiology*, 2013, **164**, 505-534.

31. L. Ciavatta, D. Ferri and G. Riccio, ON THE HYDROLYSIS OF THE TITANIUM(IV) ION IN CHLORIDE MEDIA, *Polyhedron*, 1985, **4**, 15-22.

32. R. Mahrwald, in *Aldol Reactions*, Springer Netherlands, Dordrecht, 2009, p. 73.

33. J. Schmets, J. Van Muylder and M. Pourbaix, in *Atlas of Electrochemical Equilibria in Aqueous Solutions*, ed. M. Pourbaix, Pergamon Press, Oxford, 1966, p. 213.

34. R. Uppal, C. D. Incarvito, K. V. Lakshmi and A. M. Valentine, Aqueous spectroscopy and redox properties of carboxylate-bound titanium, *Inorganic Chemistry*, 2006, **45**, 1795-1804.

35. B. A. Borgias, S. R. Cooper, Y. B. Koh and K. N. Raymond, SYNTHETIC, STRUCTURAL, AND PHYSICAL STUDIES OF TITANIUM COMPLEXES OF CATECHOL AND 3,5-DI-TERT-BUTYLCATECHOL, *Inorganic Chemistry*, 1984, **23**, 1009-1016.

36. I. Goodbody, in *Advances in Marine Biology*, Academic Press, New York, 1974, vol. 12, p. 2.

37. U. Welsch, in *Biology of the Integument 1: Invertebrates*, eds. J. Bereiter-Hahn, K. Matolsky and S. Richards, Springer-Verlag, New York, 1984, p. 800.

38. S. W. Taylor, B. Kammerer and E. Bayer, New perspectives in the chemistry and biochemistry of the tunichromes and related compounds, *Chemical Reviews*, 1997, **97**, 333-346.

39. E. Hirose, Y. Taneda and T. Ishii, Two modes of tunic cuticle formation in a colonial ascidian Aplidium yamazii, responding to wounding, *Developmental and Comparative Immunology*, 1997, **21**, 25-34.

40. B. Oregan and M. Gratzel, A LOW-COST, HIGH-EFFICIENCY SOLAR-CELL BASED ON DYE-SENSITIZED COLLOIDAL TIO2 FILMS, *Nature*, 1991, **353**, 737-740.

41. M. L. DionisioSese, M. Ishikura, T. Maruyama and S. Miyachi, UV-absorbing substances in the tunic of a colonial ascidian protect its symbiont, Prochloron sp., from damage by UV-B radiation, *Marine Biology*, 1997, **128**, 455-461.

42. M. L. Dionisio-Sese, T. Maruyama and S. Miyachi, Photosynthesis of Prochloron as affected by environmental factors, *Marine Biotechnology*, 2001, **3**, 74-79.

43. GEOTRACES, http://www.geotraces.org, 2015).

44. A. Dammshaeuser, T. Wagener and P. L. Croot, Surface water dissolved aluminum and titanium: Tracers for specific time scales of dust deposition to the Atlantic?, *Geophysical Research Letters*, 2011, **38**.

45. P. L. Croot, Rapid Determination of Picomolar Titanium in Seawater with Catalytic Cathodic Stripping Voltammetry, *Analytical Chemistry*, 2011, **83**, 6395-6400.

46. S. Poehle, K. Schmidt and A. Koschinsky, Determination of Ti, Zr, Nb, V, W and Mo in seawater by a new online-preconcentration method and subsequent ICP-MS analysis, *Deep-Sea Research Part I-Oceanographic Research Papers*, 2015, **98**, 83-93.

47. A. Cvetkovic, A. L. Menon, M. P. Thorgersen, J. W. Scott, F. L. Poole, II, F. E. Jenney, Jr., W. A. Lancaster, J. L. Praissman, S. Shanmukh, B. J. Vaccaro, S. A. Trauger, E. Kalisiak, J. V. Apon, G. Siuzdak, S. M. Yannone, J. A. Tainer and M. W. W. Adams, Microbial metalloproteomes are largely uncharacterized, *Nature*, 2010, **466**, 779-U718.

48. J. Estellon, S. O. de Choudens, M. Smadja, M. Fontecave and Y. Vandenbrouck, An integrative computational model for large-scale identification of metalloproteins in microbial genomes: a focus on iron-sulfur cluster proteins, *Metallomics*, 2014, **6**, 1913-1930.

49. D. Fu and L. Finney, Metalloproteomics: challenges and prospective for clinical research applications, *Expert Review of Proteomics*, 2014, **11**, 13-19.

50. A. Lothian, D. J. Hare, R. Grimm, T. M. Ryan, C. L. Masters and B. R. Roberts, Metalloproteomics: principles, challenges, and applications to neurodegeneration, *Frontiers in Aging Neuroscience*, 2013, **5**.

51. E. A. Roberts and B. Sarkar, Metalloproteomics: focus on metabolic issues relating to metals, *Current Opinion in Clinical Nutrition and Metabolic Care*, 2014, **17**, 425-430.

52. W. Shi, M. Punta, J. Bohon, J. M. Sauder, R. D'Mello, M. Sullivan, J. Toomey, D. Abel, M. Lippi, A. Passerini, P. Frasconi, S. K. Burley, B. Rost and M. R. Chance, Characterization of metalloproteins by high-throughput X-ray absorption spectroscopy, *Genome Research*, 2011, **21**, 898-907.

53. J. Hegoczki, B. Janzso and A. Suhajda, PREPARATION OF TITANIUM ENRICHED SACCHAROMYCES-CEREVISIAE, *Acta Alimentaria*, 1995, **24**, 181-190.

54. J. P. Riley and I. Roth, DISTRIBUTION OF TRACE ELEMENTS IN SOME SPECIES OF PHYTOPLANKTON GROWN IN CULTURE, *Journal of the Marine Biological Association of the United Kingdom*, 1971, **51**, 63-&.

55. C. Jeffryes, T. Gutu, J. Jiao and G. L. Rorrer, Metabolic Insertion of Nanostructured TiO2 into the Patterned Biosilica of the Diatom Pinnularia sp by a Two-Stage Bioreactor Cultivation Process, *Acs Nano*, 2008, **2**, 2103-2112.

56. J. H. Martin and G. A. Knauer, ELEMENTAL COMPOSITION OF PLANKTON, *Geochimica Et Cosmochimica Acta*, 1973, **37**, 1639-1653.

57. M. S. Chauton, L. M. B. Skolem, L. M. Olsen, P. E. Vullum, J. Walmsley and O. Vadstein, Titanium uptake and incorporation into silica nanostructures by the diatom Pinnularia sp (Bacillariophyceae), *Journal of Applied Phycology*, 2015, **27**, 777-786.

58. S. A. Skrabal, W. J. Ullman and G. W. Luther, ESTUARINE DISTRIBUTIONS OF DISSOLVED TITANIUM, *Marine Chemistry*, 1992, **37**, 83-103.

59. A. Scheffel, N. Poulsen, S. Shian and N. Kroeger, Nanopatterned protein microrings from a diatom that direct silica morphogenesis, *Proceedings of the National Academy of Sciences of the United States of America*, 2011, **108**, 3175-3180.

60. Y. Yan, D. Wang and P. Schaaf, Fabrication of N-doped TiO2 coatings on nanoporous Si nanopillar arrays through biomimetic layer by layer mineralization, *Dalton Transactions*, 2014, **43**, 8480-8485.

61. G. J. Bedwell, Z. Zhou, M. Uchida, T. Douglas, A. Gupta and P. E. Prevelige, Selective Biotemplated Synthesis of TiO2 Inside a Protein Cage, *Biomacromolecules*, 2015, **16**, 214-218.

62. N. Kroger, M. B. Dickerson, G. Ahmad, Y. Cai, M. S. Haluska, K. H. Sandhage, N. Poulsen and V. C. Sheppard, Bioenabled synthesis of rutile (TiO2) at ambient temperature and neutral pH, *Angewandte Chemie-International Edition*, 2006, **45**, 7239-7243.

63. M. Cargnello, T. R. Gordon and C. B. Murray, Solution-Phase Synthesis of Titanium Dioxide Nanoparticles and Nanocrystals, *Chemical Reviews*, 2014, **114**, 9319-9345.

64. Y. Lang, F. del Monte, B. J. Rodriguez, P. Dockery, D. P. Finn and A. Pandit, Integration of TiO2 into the diatom Thalassiosira weissflogii during frustule synthesis, *Scientific Reports*, 2013, **3**.

65. T. Ueki and H. Michibata, Molecular mechanism of the transport and reduction pathway of vanadium in ascidians, *Coordination Chemistry Reviews*, 2011, **255**, 2249-2257.

66. J. P. Gaffney and A. M. Valentine, The challenges of trafficking hydrolysis prone metals and ascidians as an archetype, *Dalton Transactions*, 2011, **40**, 5827-5835.

67. Swinehar.Jh, W. R. Biggs, D. J. Halko and Schroede.Nc, VANADIUM AND SELECTED METAL CONTENTS OF SOME ASCIDIANS, *Biological Bulletin*, 1974, **146**, 302-312.

68. E. P. Levine, OCCURRENCE OF TITANIUM, VANADIUM, CHROMIUM, AND SULFURIC ACID IN ASCIDIAN EUDISTOMA RITTERI, *Science*, 1961, **133**, 1352-&.

69. D. A. Roman, J. Molina and L. Rivera, INORGANIC ASPECTS OF THE BLOOD-CHEMISTRY OF ASCIDIANS - IONIC COMPOSITION, AND TI, V, AND FE IN THE BLOOD-PLASMA OF PYURA-CHILENSIS AND ASCIDIA-DISPAR, *Biological Bulletin*, 1988, **175**, 154-166.

70. M. Sugumaran and W. E. Robinson, Structure, biosynthesis and possible function of tunichromes and related compounds, *Comparative Biochemistry and Physiology B-Biochemistry & Molecular Biology*, 2012, **163**, 1-25.

71. L. C. Dorsett, C. J. Hawkins, J. A. Grice, M. F. Lavin, P. M. Merefield, D. L. Parry and I. L. Ross, FERREASCIDIN - A HIGHLY AROMATIC PROTEIN

CONTAINING 3,4-DIHYDROXYPHENYLALANINE FROM THE BLOOD-CELLS OF A STOLIDOBRANCH ASCIDIAN, *Biochemistry*, 1987, **26**, 8078-8082.

72. J. D. Popham and J. M. Dauria, A NEW SENTINEL ORGANISM FOR VANADIUM AND TITANIUM, *Marine Pollution Bulletin*, 1982, **13**, 25-27.

73. A. Arias, A. Giangrande, M. C. Gambi and N. Anadon, Biology and new records of the invasive species Branchiomma bairdi (Annelida: Sabellidae) in the Mediterranean Sea, *Mediterranean Marine Science*, 2013, **14**, 162-171.

74. D. Fattorini, A. Notti, M. Nigro and F. Regoli, Hyperaccumulation of vanadium in the Antarctic polychaete Perkinsiana littoralis as a natural chemical defense against predation, *Environmental Science and Pollution Research*, 2010, **17**, 220-228.

75. H. A. Lowenstam and S. Weiner, *On Biomineralization*, Oxford University Press, New York, 1989.

76. S. Weiner and L. Addadi, Crystallization Pathways in Biomineralization, *Annual Review of Materials Research, Vol 41*, 2011, **41**, 21-40.

77. K. I. Sano and K. Shiba, A hexapeptide motif that electrostatically binds to the surface of titanium, *Journal of the American Chemical Society*, 2003, **125**, 14234-14235.

78. L. Agosta, G. Zollo, C. Arcangeli, F. Buonocore, F. Gala and M. Celino, Water driven adsorption of amino acids on the (101) anatase TiO2 surface: an ab initio study, *Physical Chemistry Chemical Physics*, 2015, **17**, 1556-1561.

79. Q. Sheng, X. Li, W. Yin, L. Yu, Y. Ke and X. Liang, Retention mechanism and enrichment of glycopeptides on titanium dioxide, *Analytical Methods*, 2013, **5**, 7072-7080.

80. X. Zhao, Q. Wang, S. Wang, X. Zou, M. An, X. Zhang and J. Ji, Citric Acid-Assisted Two-Step Enrichment with TiO2 Enhances the Separation of Multi- and Monophosphorylated Peptides and Increases Phosphoprotein Profiling, *Journal of Proteome Research*, 2013, **12**, 2467-2476.

81. Q. Wu, D. Wu and Y. Guan, Hybrid Titania-Zirconia Nanoparticles Coated Adsorbent for Highly Selective Capture of Nucleosides from Human Urine in Physiological Condition, *Analytical Chemistry*, 2014, **86**, 10122-10130.

82. S. Steckbeck, J. Schneider, L. Wittig, K. Rischka, I. Grunwald and L. C. Ciacchi, Identification of materials' binding peptide sequences guided by a MALDI-ToF MS depletion assay, *Analytical Methods*, 2014, **6**, 1501-1509.

83. Y. Razvag, V. Gutkin and M. Reches, Probing the Interaction of Individual Amino Acids with Inorganic Surfaces Using Atomic Force Spectroscopy, *Langmuir*, 2013, **29**, 10102-10109.

84. A. I. K. Eriksson, K. Edwards and V. A. Hernandez, Cooperative adsorption behavior of phosphopeptides on TiO2 leads to biased enrichment, detection and quantification, *Analyst*, 2015, **140**, 303-312.

85. I. Stokroos, L. Litinetsky, J. J. L. van der Want and J. S. Ishay, Magnetic minerals - Keystone-like crystals in cells of hornet combs, *Nature*, 2001, **411**, 654-654.

86. J. S. Ishay, K. Riabinin, M. Kozhevnikov, H. van der Want and I. Stokiroos, A keystone-like grain in hornet comb cells: Its nature and physical properties, *Biomacromolecules*, 2003, **4**, 649-656.

87. J. S. Ishay, Z. Barkay, N. Eliaz, M. Plotkin, S. Volynchik and D. J. Bergman, Gravity orientation in social wasp comb cells (Vespinae) and the possible role of embedded minerals, *Naturwissenschaften*, 2008, **95**, 333-342.

88. A. M. Horst, A. C. Neal, R. E. Mielke, P. R. Sislian, W. H. Suh, L. Maedler, G. D. Stucky and P. A. Holden, Dispersion of TiO2 Nanoparticle Agglomerates by Pseudomonas aeruginosa, *Applied and Environmental Microbiology*, 2010, **76**, 7292-7298.

89. M. A. Kiser, H. Ryu, H. Jang, K. Hristovski and P. Westerhoff, Biosorption of nanoparticles to heterotrophic wastewater biomass, *Water Research*, 2010, **44**, 4105-4114.

90. L. Petrone, Molecular surface chemistry in marine bioadhesion, *Advances in Colloid and Interface Science*, 2013, **195**, 1-18.

91. M. J. McWhirter, P. J. Bremer, I. L. Lamont and A. J. McQuillan, Siderophore-mediated covalent bonding to metal (oxide) surfaces during biofilm initiation by Pseudomonas aeruginosa bacteria, *Langmuir*, 2003, **19**, 3575-3577.

92. M. J. McWhirter, A. J. McQuillan and P. J. Bremer, Influence of ionic strength and pH on the first 60 min of Pseudomonas aeruginosa attachment to ZnSe and to TiO2 monitored by ATR-IR spectroscopy, *Colloids and Surfaces B-Biointerfaces*, 2002, **26**, 365-372.

93. Y. Shabtai and G. Fleminger, ADSORPTION OF RHODOCOCCUS STRAIN GIN-1 (NCIMB-40340) ON TITANIUM-DIOXIDE AND COAL FLY-ASH PARTICLES, *Applied and Environmental Microbiology*, 1994, **60**, 3079-3088.

94. G. Gertler, I. Brudo, R. Kenig and G. Fleminger, A TiO2-binding protein isolated from Rhodococcus strain GIN-1 (NCIMB 40340) - Purification, properties and potential applications, *Materialwissenschaft Und Werkstofftechnik*, 2003, **34**, 1138-1144.

95. M. S. Jimenez, L. Rodriguez, J. R. Bertolin, M. T. Gomez and J. R. Castillo, Evaluation of gel electrophoresis techniques and laser ablation-inductively coupled plasma-mass spectrometry for screening analysis of Zn and Cu-binding proteins in plankton, *Analytical and Bioanalytical Chemistry*, 2013, **405**, 359-368.

96. A. Raab, B. Ploselli, C. Munro, J. Thomas-Oates and J. Feldmann, Evaluation of gel electrophoresis conditions for the separation of metal-tagged proteins with subsequent laser ablation ICP-MS detection, *Electrophoresis*, 2009, **30**, 303-314.

97. A. B. Nowakowski, W. J. Wobig and D. H. Petering, Native SDS-PAGE: high resolution electrophoretic separation of proteins with retention of native properties including bound metal ions, *Metallomics*, 2014, **6**, 1068-1078.

98. C. M. H. Ferreira, I. S. S. Pinto, E. V. Soares and H. M. V. M. Soares, (Un)suitability of the use of pH buffers in biological, biochemical and environmental studies and their interaction with metal ions - a review, *Rsc Advances*, 2015, **5**, 30989-31003.

99. E. Z. Jahromi, W. White, Q. Wu, R. Yamdagni and J. Gailer, Remarkable effect of mobile phase buffer on the SEC-ICP-AES derived Cu, Fe and Zn-metalloproteome pattern of rabbit blood plasma, *Metallomics*, 2010, **2**, 460-468.

100. A. Sanz-Medel, A. B. S. Cabezuelo, R. Milacic and T. B. Polak, The chemical speciation of aluminium in human serum, *Coordination Chemistry Reviews*, 2002, **228**, 373-383.

101. A. Sarmiento-Gonzalez, J. Ruiz Encinar, A. M. Cantarero-Roldan, J. M. Marchante-Gayon and A. Sanz-Medel, HPLC-ICPMS and Stable Isotope-Labeled Approaches To Assess Quantitatively Ti(IV) Uptake by Transferrin in Human Blood Serum, *Analytical Chemistry*, 2008, **80**, 8702-8711.

102. Y. Valasatava, A. Rosato, G. Cavallaro and C. Andreini, MetalS(3), a database-mining tool for the identification of structurally similar metal sites, *Journal of Biological Inorganic Chemistry*, 2014, **19**, 937-945.

103. J. Pande, M. M. Szewczyk and A. K. Grover, Phage display: Concept, innovations, applications and future, *Biotechnology Advances*, 2010, **28**, 849-858.

104. S. R. Meyers, P. T. Hamilton, E. B. Walsh, D. J. Kenan and M. W. Grinstaff, Endothelialization of titanium surfaces, *Advanced Materials*, 2007, **19**, 2492-+.

105. O. Stoevesandt and M. J. Taussig, Affinity proteomics: the role of specific binding reagents in human proteome analysis, *Expert Review of Proteomics*, 2012, **9**, 401-414.

106. D. Raimunda, T. Khare, C. Giometti, S. Vogt, J. M. Argueello and L. Finney, Identifying metalloproteins through X-ray fluorescence mapping and mass spectrometry, *Metallomics*, 2012, **4**, 921-927.

107. K. M. Dean, Y. Qin and A. E. Palmer, Visualizing metal ions in cells: An overview of analytical techniques, approaches, and probes, *Biochimica Et Biophysica Acta-Molecular Cell Research*, 2012, **1823**, 1406-1415.

108. E. L. Que, R. Bleher, F. E. Duncan, B. Y. Kong, S. C. Gleber, S. Vogt, S. Chen, S. A. Garwin, A. R. Bayer, V. P. Dravid, T. K. Woodruff and T. V. O'Halloran, Quantitative mapping of zinc fluxes in the mammalian egg reveals the origin of fertilization-induced zinc sparks, *Nature Chemistry*, 2015, **7**, 130-139.

109. J. Zhou, Y. Hu, Y. Lin, H. Liu and P. Xie, Preparation and application of a partially degradable gel in mass spectrometry-based proteomic analysis, *Journal of Chromatography B-Analytical Technologies in the Biomedical and Life Sciences*, 2011, **879**, 2957-2962.

110. J. V. Olsen, B. Blagoev, F. Gnad, B. Macek, C. Kumar, P. Mortensen and M. Mann, Global, in vivo, and site-specific phosphorylation dynamics in signaling networks, *Cell*, 2006, **127**, 635-648.

111. A. G. Marshall, C. L. Hendrickson and G. S. Jackson, Fourier transform ion cyclotron resonance mass spectrometry: A primer, *Mass Spectrometry Reviews*, 1998, **17**, 1-35.

112. J. C. Tran, L. Zamdborg, D. R. Ahlf, J. E. Lee, A. D. Catherman, K. R. Durbin, J. D. Tipton, A. Vellaichamy, J. F. Kellie, M. Li, C. Wu, S. M. M. Sweet, B. P. Early, N. Siuti, R. D. LeDuc, P. D. Compton, P. M. Thomas and N. L. Kelleher, Mapping intact protein isoforms in discovery mode using top-down proteomics, *Nature*, 2011, **480**, 254-U141.

CHAPTER 3. MINERAL BINDING OF *RHODOCOCCUS RUBER* GIN-1

3.1. Introduction

It is thought that the first use of inorganic elements by organisms was at mineral surfaces.[1-4] The organisms would have propagated near these minerals to obtain the products of reactions catalyzed at their surfaces. Some active centers of metalloenzymes resemble the structures of minerals presumed to be present in precipitates from hydrothermal solutions in the ocean billions of years ago.[1, 2]

Rhodococcus ruber GIN-1 was isolated for its ability to bind to metal oxides from coal fly ash.[5] The original goal of this work was to adsorb the cells to the metal oxides within coal fly ash, forming cell/metal oxide agglomerates that could be separated so that the metals could be recovered. Further work by the same group discovered that *R. ruber* GIN-1 selectively binds to titanium dioxide over other metal oxides.[6] The amount of cells adsorbed to titanium dioxide was twice as much as that for other oxides, and the rate of absorption to titanium dioxide was exceedingly quick compared to other oxides.

Further work isolated and identified one potential titanium dioxide binding protein.[7, 8] When the protein was first isolated, a group of three proteins were found to bind to titanium dioxide powder but only one protein was isolated by TiO_2-affinity column chromatography.[7] This protein was identified as a cell-surface homolog of dihydrolipoamide dehydrogenase. The identity of the other two proteins remains unclear.

Previous work in our lab by Kathryn Cole identified possible TiO_2 binding proteins as ~70 kDa Elongation Factor G, ~55 kDa glutamate-ammonia ligase, ~55 kDa dihydrolipoamide dehydrogenase, and ~50 kDa Elongation Factor EF1A. While working

with *R. ruber* GIN-1 a potential new siderophore was identified with help from Akira Ilnishi. *Rhodococcus* are known to produce rhodobactin and heterobactin.[9, 10]

We hypothesize that *R. ruber* GIN-1 intentionally uses titanium. This current study works towards the elucidation of other possible titanium dioxide binding proteins as well as the titanium content of the cells, and the identity of a possible new siderophore. This work shows the first known *R. ruber* GIN-1 cell envelope protein involved in TiO_2 binding.

3.2. Materials

All solutions were made using Barnstead NANOpure Diamond (18.2 MΩ-cm) water. Crystal Sea was purchased from Marine Enterprises International. Sachtopore 100 Å (anatase) and Sachtopore 1000 Å (rutile) beads were purchased from Huntsman Pigments and Additives. Protein digests were performed using Trypsin Gold, Mass Spectrometry Grade from Promega. High performance liquid chromatography was performed using HPLC grade water and acetonitrile, and mass spectrometry grade formic acid on an Agilent 1260 Infinity HPLC. Mass spectrometry was performed using an Agilent 6520 Q-TOF with an electrospray ionization source.

Inductively Coupled Plasma Optical Emission Spectroscopy (ICP-OES) standards were prepared using Ti standard for ICP (1000 ppm from Fluka), Iron AA Standard (1000 ppm from Ricca Chemical Company), and iCAP 6000 Multi-Element Test Solution (1ppm Al, 1ppm Cu, 1ppm Mn, 0.2 ppm Ca, 0.2 ppm Mg, and 0.2 ppm Zn) from Thermo Scientific. All dilutions were performed using Barnstead NANOpure Diamond (18.2 MΩ-cm) water. Trace metal grade nitric acid was purchased from Fisher

Scientific. ICP-OES data was obtained on an iCAP 7400 ICP-OES from Thermo Scientific, which has a limit of detection of 0.005 mg/L (0.005 ppm) for most elements.

3.3. Methods

Rhodococcus ruber GIN-1 streaked from Kathryn Cole's stock was grown for one week at 30 °C on LB agar plates. The cultured cells had the characteristic red color of GIN-1. A single colony from these plates was used to inoculate a 10 mL growth in Seawater Media (29.9 g/L Crystal Sea, 1.68 g/L K_2HPO_4, 0.72 g/L KH_2PO_4, 1 g/L $(NH_4)_2SO_4$, 10 g/L Dextrose, 8 g/L Yeast Extract).[6] The 10 mL culture was grown for 24 hours in a shaking incubator at 225 rpm and 30 °C. The 10 mL culture was used to inoculate a 100 mL culture which was grown for 24 hours under the same conditions. The 100 mL culture was used to inoculate a 1 L culture which was grown at 225 rpm and 30 °C until the end of the log growth phase, approximately 28 hours, at which point the cells were pelleted at 3000 rpm and 4 °C for 30 minutes.

The pelleted cells were resuspended in 100 mL of 50 mM Tris-HCl, 2.5 mM $MgSO_4$, and 20% (w/v) sucrose pH=7.4. Mutanolysin was added at 1000 units per 2 ml of cell volume and the resuspended pellet was incubated at 37 °C for 2 hours. The mutanolysin lysed cells were centrifuged at 1377 x*g* and 4 °C for 20 minutes. The pellet was discarded and the supernatant kept.

Two grams of titanium dioxide (TiO_2) powder, 1 g anatase and 1 g rutile, was added to the supernatant. The supernatant/TiO_2 mixture was incubated for 30 minutes at 30 °C. The mixture was centrifuged at 24,000 x*g* and 4 °C for 20 minutes. The supernatant (non-mineral binding supernatant) was stored at 4 °C.

The TiO_2 solid was resuspended and washed with 100 mL PBS buffer pH=7.4 to release any non-specific binding proteins. The resuspended solid was centrifuged at 24,000 x*g* and 4 °C for 20 minutes. The supernatant was stored at 4 °C. This step was repeated once more for a total of two washes.

The TiO_2 solid was resuspended and washed with 100 mL 8M urea and 1% (w/v) sodium dodecylsulfate to release specific binding proteins. The resuspended solid was centrifuged at 24,000 x*g* and 4 °C for 20 minutes. The supernatant was dialyzed into 50 mM Tris 0.15 M NaCl pH=7.4 buffer, and was stored at 4 °C. The solid was discarded.

The non-mineral binding supernatant, PBS buffer washes and the urea wash were precipitated with 100% (w/v) trichloroacetic acid (TCA) to a final volume of 20% TCA. The TCA precipitated samples were centrifuged at 14,000 rpm at 4 °C in an Eppendorf centrifuge. The TCA pellets were washed twice with acetone, dried, and resuspended in 200 μL of 2x SDS Gel-loading buffer. The samples were run on SDS-PAGE and significant bands were subjected to trypsin digestion following manufacturer protocol,[11] followed by LC-MS/MS and identification by MASCOT software.

The titanium content of *R. ruber* GIN-1 was analyzed by Inductively Coupled Plasma – Optical Emission Spectroscopy (ICP-OES). At the end of their growth, cells were pelleted as before, and resuspended in 100 mL 50 mM Tris-HCl, 2.5 mM $MgSO_4$, and 20% (w/v) sucrose pH=7.4. The resuspended cells were incubated with 1 g of each of the Sachtopore beads for 1 hour at 30 °C. This mixture was pelleted and resuspended with 100 mL 8M urea and 1% (w/v) sodium dodecylsulfate to release the cells from the beads. This suspension was then centrifuged at 19.3 x*g* to pellet the Sachtopore beads

without pelleting the cells in a swinging bucket rotor. This was monitored using scanning electron microscopy (SEM) on a sample of the mixture before and after TiO_2 binding. The supernatant was poured off. The supernatant containing the R. ruber cells was lyophilized in the Schafmeister lab with help of Jae Eun Cheong. The lyophilized cells (0.5848 g) were digested in 10 mL of 50% trace metal grade nitric acid.

The digested sample as well as 1:10, 1:100, 1:1000 dilutions were analyzed by ICP-OES. Five standards were prepared for ICP-OES; 0.005 ppm Al, 0.005 ppm Cu, 0.005 ppm Mn, 0.005 ppm Ti, 0.01 ppm Fe, and 0.05 ppm Zn (Std 1), 0.129 ppm Al, 0.129 ppm Cu, 0.129 ppm Mn, 0.129 ppm Ti, 0.133 ppm Fe, and 0.163 ppm Zn (Std 2), 0.253 ppm Al, 0.253 ppm Cu, 0.253 ppm Mn, 0.253 ppm Ti, 0.255 ppm Fe, and 0.276 ppm Zn (Std 3), 0.376 ppm Al, 0.376 ppm Cu, 0.376 ppm Mn, 0.376 ppm Ti, 0.378 ppm Fe, and 0.388 ppm Zn (Std 4), and 0.500 ppm Al, 0.500 ppm Cu, 0.500 ppm Mn, 0.500 ppm Ti, 0.500 ppm Fe, and 0.500 ppm Zn (Std 5). All glassware was demetalated by soaking in an acid bath and thoroughly rinsing with water.

R. ruber GIN-1 growth media was used to isolate siderophores. The Seawater growth media was analyzed for siderophores using a C18 SepPak Column wet with 10 mL 70% methanol. The column was rinsed with 10 mL water, loaded with 5 mL of growth media, rinsed with 5 mL water, and eluted with 1 mL of each of the following: 10% methanol, 20% methanol, 30% methanol, 50% methanol, 70% methanol, and 100% methanol. CAS assay was used to identify fractions containing siderophores according to literature precedent.[12] Siderophore isolation was performed by Kayleigh Jones. The fractions were then analyzed by LC-MS/MS. Siderophores from *R. ruber* GIN-1 had been previously isolated by Akira Ilnishi. These samples were analyzed again by LC-MS/MS.

The LC-MS was run under the following conditions. The LC was held constant at 95% H_2O:5% Acetonitrile for two minutes, a gradient of 95% H_2O:5% Acetonitrile to 5% H_2O:95% Acetonitrile over a period of ten minutes, and ended held at 5% H_2O:95% Acetonitrile for two minutes. The mass spectrometer was held the following settings in positive ion mode: capillary voltage=4000 V, drying gas temp.=325 °C, fragmentor voltage=215 V, and the collision energy was set using the formula (slope)*(m/z)/100 + offset where for ions z=2 the slope=3.9, z=3 the slope=3.5, z>3 the slope=3.0 and the offset=2.7 for all ions.

3.4. Results

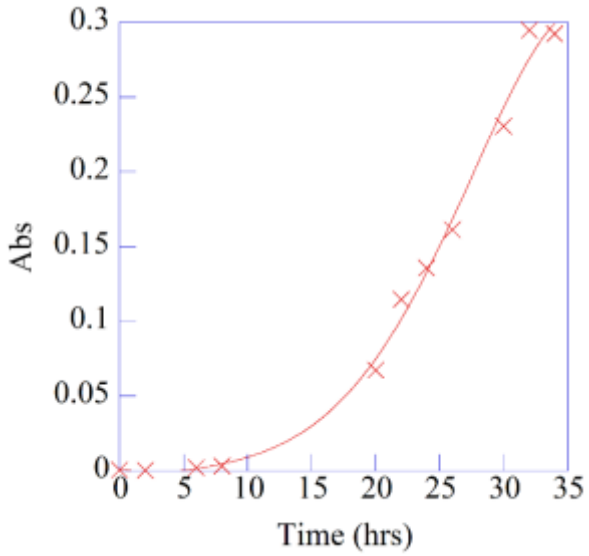

Figure 3.1 Growth curve of Rhodococcus ruber GIN-1.

The band with the highest molecular weight from the urea wash lanes was identified as a *R. ruber* mycolyltransferase with a molecular weight of ~36 kDa. The band with smallest molecular weight from the urea wash lanes was best identified as 30S ribosomal protein S16 from *Rhodococcus* with a molecular weight of ~16 kDa. The band

with the smallest molecular weight from the urea wash lanes best matches a 50S ribosomal protein L14 with a molecular weight of ~14 kDa.

Table 3.1 *Concentrations of metals in R. ruber GIN-1 after exposure to TiO_2.*

Concentrations given in ppm (mg/kg dry weight) are corrected for dilution. Values listed as N/A were either below the detection limit or did not fall on the standard curve.

Sample	Al	Ti	Mn	Fe	Cu	Zn
R. ruber	4.06	1.11	0.556	2.86	0.180	3.76
1:10	5.81	1.20	0.684	3.76	N/A	5.47
1:100	4.27	N/A	N/A	5.13	N/A	15.4
1:1000	N/A	N/A	N/A	N/A	N/A	N/A
Average	4.71	1.16	0.620	3.92	0.180	8.21

Table 3.2 *Mass Spec ions and fragment ions from siderophore sample isolated by Akira Ilnishi.*

MS Ion (m/z)	Associated Fragment Ions (m/z)
415.2024 z=2 (829.3970 z=1)	137.0229 z=1 279.1861 z=2 (557.3652 z=1) 540.3460 z=1 676.3515 z=1

In parentheses are the m/z that would be observed for the multiply charged species above them.

Table 3.3 *Mass Spec ions and fragment ions from siderophore sample isolated by Kayleigh Jones.*

In parentheses are the m/z that would be observed for the multiply charged species above them.

MS Ion (m/z)	Associated Fragment Ions (m/z)
417.2107 z=2 (833.4136 z=1)	254.1551 z=1 617.3147 z=1 668.3091 z=1
424.2333 z=2 (847.4588 z=1)	374.6941 z=2 (748.3814 z=1) 748.3836 z=1
428.2573 z=2 (855.5068 z=1)	203.1028 z=1 617.3368 z=1 685.4134 z=1
473.7427 z=2 (946.4776 z=1)	359.6847 z=2 (718.3606 z=1) 718.3587 z=1 833.3891 z=1

3.5. Discussion

Of the three proteins identified as titanium dioxide binding proteins the ~36 kDa *R. ruber* mycolyl transferase is likely the only significant result which agrees well with its position from SDS-PAGE. The other two ribosomal proteins would likely not be found on the cell envelope and their overall score from the MASCOT program was relatively low. This means that while the masses of these proteins match their position identified by SDS-PAGE they may not be the actual identity of these bands. This could be due to a low signal to noise ratio. The bands were identifiable but light in color possibly causing low signal and if the mass spectrometer was dirty this could have increased the noise. Both of these individually cause problems for the MASCOT identification software. The mycolyl transferase would however likely be found on the cell envelope as the cell envelope of *Rhodococcus* has covalently linked mycolic acids at the outermost layer.[13] Mycolyl transferase catalyzes the transfer of the mycolyl reside from one molecule of trehalose monomycolate to another forming trehalose dimonomycolate and trehalose.[14] The mycolyl transferase of *Mycobacterium tuberculosis* has been studied for its contribution to pathogenesis.[15] How this protein contributes to titanium binding is uncertain. The crystal structure of mycolyl transferase from *Corynebacterium glutamicum* (Figure 3.2) shows multiple aspartic and glutamic acids on the protein surface that could participate in titanium dioxide binding.[16]

The protein originally identified by Siegmann *et al.* was a ~52 kDa dihydrolipoamide dehydrogenase cell-surface homolog.[8] There were bands present in our study above the ~36 kDa mycolyl transferase but none that were obviously different between the PBS wash and urea wash lanes as seen in the previous studie by Siegmann *et*

al. or Kathryn Cole. A better method for the isolation of titanium dioxide binding proteins would involve competitive binding. After isolation of the cell envelope proteins, competitive binding in the presence of titanium dioxide and magnetite would allow for separation of non-specific metal oxide binding proteins from those specific for titanium dioxide.

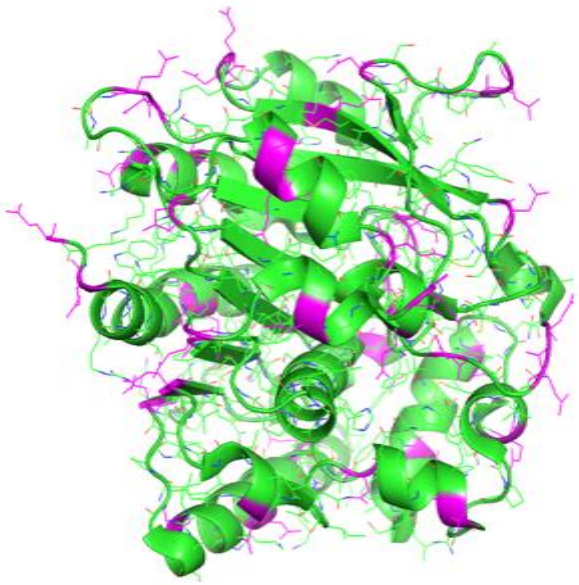

Figure 3.2 Crystal structure of mycolyl transferase from *Corynebacterium glutamicum*.

Aspartic acids and glutamic acids highlighted in magenta. Prepared using PyMol from the coordinates for PDB 4H18.[16]

Results from ICP-OES showed a titanium concentration of 1 ppm compared to an iron concentration of 4 ppm, and a zinc concentration 8 ppm. Assuming the organism is 80% water the concentrations are 6 μM, 18 μM, and 31 μM, respectively. Iron and zinc concentrations are higher than the titanium concentration but the titanium concentration is appreciable. Whether or not *R. ruber* GIN-1 uses the sequestered titanium for any

reason is unknown. In addition, all of these concentrations are probably higher as the cells were lyophilized from a solution containing urea. Bacterial iron concentrations are usually around 200 ppm dry weight.[17] Further studies of the titanium uptake by *R. ruber* GIN-1 should include a step isolating the cells from the urea solution.

Mass spectrometry of siderophore samples isolated by Akira Ilnishi originally performed by the Keck facility at Yale identified a 416.4733 m/z, and analysis of the same sample in the Shepartz lab at Yale identified a 415.18 m/z. These were both doubley positive species with neutral exact masses of 830.9310 Da, and 828.3444 Da, respectively. Neither of these peaks have the same mass to charge as a doubly positive rhodobactin molecule which would be observed at 416.1858 m/z and has a neutral exact mass of 830.3559 Da. When this sample was analyzed on our Agilent QTOF instrument a 415.2024 m/z was identified which corresponds to a neutral exact mass of 828.3892 Da. The only fragment from tandem mass spectrometry experiments that is identifiable as being from rhodobactin is the 137.0229 m/z, which matches a catechol group with a carbonyl ($C_7H_5O_3^+$). The 415.2024 m/z cannot be an oxidized form of rhodobactin. This would require only one catechol to oxidize to form the quinone and the catechol fragment is the only fragment that has been identified. This reduced form of the 415.2024 m/z would have a neutral mass of 830.4048 Da which does not match rhodobactin at 830.3559 Da. This gives evidence for a known class of iron siderophores and known titanium binding group.

It is important to note that the original characterization of rhodobactin by Dhungana *et al.* has some flaws.[9] Their characterization by ESI-MS also identifies catechol at 137.01 m/z but they claim the molecular ion is observed at 830.37 m/z. The

neutral exact mass for the structure they provide is 830.36 Da and this would need at least the addition of one proton to observe via ESI-MS, making the observable peak at 831.36 m/z. They have either misinterpreted their own data or accidentally written the neutral mass where the ion exact mass should be.

The growth media loaded onto the C18 SepPak was fluorescent as previously reported by Akira Ilnishi. The 70% methanol wash fraction was the most fluorescent fraction isolated from the SepPak. The results of tandem mass spectrometry experiments on this fraction are reported in Table 3.3. The fragments from this experiment cannot be confidently identified based only on this data alone but a set of most likely chemical formulas could be proposed for each fragment. Table 3.4 lists ten possible chemical formulas for the neutral species of the 415.2024 m/z, but there are 17 different molecular formulas that fall within 3 ppm of the measured 415.2024 m/z as determined using mMass software which considers isotopic pattern.[18] Only C, H, N, and O were considered as possible elements within the molecular formula, as the isotope pattern does not support the presence of sulfur with an increased M+2 isotope peak. Without further mass spec fragmentation (MS^3 or higher) or NMR confirmation further identification is not possible.[19] The most likely reason for the difference between the primary masses identified in the samples isolated by Kayleigh and those isolated by Akira Ilnishi is that they were isolated from different growth medias. Those isolated by Kayleigh were isolated from the Seawater media and those isolated by Akira were from M6LB media. The M6LB media is iron limited which would cause overproduction of siderophore but the Seawater media is not iron limited.

Table 3.4 *Possible molecular formulas of 415.2024 m/z within instrument error.*

Molecular Formula	Monoisotopic mass
$C_{52}H_{52}N_4O_6$	828.389
$C_{53}H_{48}N_8O_2$	828.390
$C_{54}H_{54}NO_7$	828.390
$C_{51}H_{56}O_{10}$	828.387
$C_{50}H_{50}N_7O_5$	828.387
$C_{55}H_{50}N_5O_3$	828.391
$C_{41}H_{52}N_{10}O_9$	828.392
$C_{49}H_{54}N_3O_9$	828.386
$C_{48}H_{48}N_{10}O_4$	828.386
$C_{57}H_{52}N_2O_4$	828.393

The work presented here shows promise for an abundance of biological titanium chemistry and forms the basis for further study. The Rhodococcus cell envelope protein was identified as a titanium dioxide binding protein but how this is facilitated is unclear. *Rhodococcus ruber GIN-1* uptakes an appreciable amount of titanium but more controls are needed, and likely makes use of a new and yet unidentified siderophore. More work needs to be performed on *Rhodococcus ruber* GIN-1 to coalesce the work presented here.

REFERENCES CITED

1. B. Herschy, A. Whicher, E. Camprubi, C. Watson, L. Dartnell, J. Ward, J. R. G. Evans and N. Lane, An Origin-of-Life Reactor to Simulate Alkaline Hydrothermal Vents, *Journal of Molecular Evolution*, 2014, **79**, 213-227.
2. W. Martin, J. Baross, D. Kelley and M. J. Russell, Hydrothermal vents and the origin of life, *Nature Reviews Microbiology*, 2008, **6**, 805-814.
3. A. D. Gordon, A. Smirnov, S. L. Shumlas, S. Singireddy, M. DeCesare, M. A. A. Schoonen and D. R. Strongin, Reduction of Nitrite and Nitrate on Nano-dimensioned FeS, *Origins of Life and Evolution of Biospheres*, 2013, **43**, 305-322.
4. S. D. Senanayake and H. Idriss, Photocatalysis and the origin of life: Synthesis of nucleoside bases from formamide on TiO2(001) single surfaces, *Proceedings of the National Academy of Sciences of the United States of America*, 2006, **103**, 1194-1198.
5. J. Shabtai, G. Fleminger and J. Fleming, Species of a Microorganism of the Genus Rhodococcus, 1994, **U.S. Pat. No. 5,290,697**.
6. Y. Shabtai and G. Fleminger, Adsorption of Rhodococcus Strain GIN-1 (NCIMB-40340) on Titanium-Dioxide and Coal Fly-Ash Particles, *Applied and Environmental Microbiology*, 1994, **60**, 3079-3088.
7. G. Gertler, I. Brudo, R. Kenig and G. Fleminger, A TiO2-binding protein isolated from Rhodococcus strain GIN-1 (NCIMB 40340) - Purification, properties and potential applications, *Materialwissenschaft Und Werkstofftechnik*, 2003, **34**, 1138-1144.

8. A. Siegmann, A. Komarska, Y. Betzalel, I. Brudo, S. Jindou, G. Mor and G. Fleminger, The titanium binding protein of Rhodococcus ruber GIN1 (NCIMB 40340) is a cell-surface homolog of the cytosolic enzyme dihydrolipoamide dehydrogenase, *Journal of Molecular Recognition*, 2009, **22**, 138-145.

9. S. Dhungana, R. Michalczyk, H. Boukhalfa, J. G. Lack, A. T. Koppisch, J. M. Fairlee, M. T. Johnson, C. E. Ruggiero, S. G. John, M. M. Cox, C. C. Browder, J. H. Forsythe, L. A. Vanderberg, M. P. Neu and L. E. Hersman, Purification and characterization of rhodobactin: a mixed ligand siderophore from Rhodococcus rhodochrous strain OFS, *Biometals*, 2007, **20**, 853-867.

10. C. J. Carrano, M. Jordan, H. Drechsel, D. G. Schmid and G. Winkelmann, Heterobactins: A new class of siderophores from Rhodococcus erythropolis IGTS8 containing both hydroxamate and catecholate donor groups, *Biometals*, 2001, **14**, 119-125.

11. P. Corporation, Trypsin Gold, Mass Spectrometry Grade: Instructions for use V5280, 2015).

12. B. Schwyn and J. B. Neilands, Universal Chemical-Assay for the Detection and Determination of Siderophores, *Analytical Biochemistry*, 1987, **160**, 47-56.

13. L. C. Sutcliffe, A. K. Brown and L. G. Dover, The Rhodococcal Cell Envelope: Composition, Organisation and Biosynthesis, *Biology of Rhodococcus*, 2010, **16**, 29-71.

14. J. T. Belisle, V. D. Vissa, T. Sievert, K. Takayama, P. J. Brennan and G. S. Besra, Role of the major antigen of Mycobacterium tuberculosis in cell wall biogenesis, *Science*, 1997, **276**, 1420-1422.

15. D. H. Anderson, G. Harth, M. A. Horwitz and D. Eisenberg, An interfacial mechanism and a class of inhibitors inferred from two crystal structures of the Mycobacterium tuberculosis 30 kDa major secretory protein (antigen 85B), a mycolyl transferase, *Journal of Molecular Biology*, 2001, **307**, 671-681.

16. E. Huc, C. de Sousa-D'Auria, I. L. de la Sierra-Gallay, C. Salmeron, H. van Tilbeurgh, N. Bayan, C. Houssin, M. Daffe and M. Tropis, Identification of a Mycoloyl Transferase Selectively Involved in O-Acylation of Polypeptides in Corynebacteriales, *Journal of Bacteriology*, 2013, **195**, 4121-4128.

17. S. C. Andrews, Iron storage in bacteria, *Advances in Microbial Physiology, Vol 40*, 1998, **40**, 281-351.

18. M. Strohalm, D. Kavan, P. Novak, M. Volny and V. Havlicek, mMass 3: A Cross-Platform Software Environment for Precise Analysis of Mass Spectrometric Data, *Analytical Chemistry*, 2010, **82**, 4648-4651.

19. A. R. Johnson and E. E. Carlson, Collision-Induced Dissociation Mass Spectrometry: A Powerful Tool for Natural Product Structure Elucidation, *Analytical Chemistry*, 2015, **87**, 10668-10678.

CHAPTER 4. POTENTIAL METAL CONCENTRATION BY THE FEATHER DUSTER WORM *SABELLASTARTE SP.*

4.1. Introduction

Some metals essential for organisms are scarce in the environment. This fact makes it necessary for organisms to acquire and concentrate these elements. The demands of scarce nutrients are met through varied mechanisms throughout different species.[1-4] The mechanisms can vary due to the diverse metals required or different strategies can be employed by different species for the same metal.

Certain organisms are exceptional at sequestering diverse metals from the environment and have been proposed to be used for metal pollution detection.[5-7] These organisms' high sequestration of metals is likely linked to their high demand for iron and zinc and their static lifestyle. While motile organisms can search out necessary nutrients, these sedentary organisms must take advantage of times when nutrients are rich. Thus, the accumulation of abiological or even toxic elements in these organisms provides an indicator of exposure. One family of organisms proposed as marine pollution indicators is Sabellidae, or the feather duster worms (Figure 4.1).[5] Feather duster worms' bodies reside inside of a tube they construct from secreted adhesive matter and usually detrital sand and shell, but one genus, *Glomerula*, secretes a calcium carbonate tube.[8] Their radioles extend past the mouth of the tube and fan out around them to filter feed on the passing currents and can be retreated into the tube in defense. Sabellidae live in different seas around the world in the intertidal zones and their fossils date to the Jurassic period.[8, 9]

Figure 4.1 *Sabellastarte magnifica* or the Magnificent feather duster worm.[10]

There has been one report by Popham and D'Auria of feather duster worms as "sentinel organisms," sequestering and accumulating titanium from the environment.[5] In this study feather duster worms, *Eudistylia vancouveri*, were collected from near (~20 m) and far from an outfall of a storm water drainage sewer of the municipality of North Vancouver, British Columbia. The metal concentrations they obtained are presented in Table 4.3 In these samples titanium was concentrated to 72.5 ppm dry weight in the samples near the sewer but no titanium was detected in the far samples. The samples near the sewer contained 8-fold higher vanadium concentrations and 6-fold higher iron concentrations than the samples far from the sewer. The concentration of titanium from the environment is an essential step if an organism is going to utilize it. It is unknown if Sabellidae, or any other organism, uses titanium as an essential element but feather duster worms may provide a good model to study the mechanism of sequestration of titanium by

organisms. Feather duster worms are readily available from aquarium supply stores and relatively easy to maintain in tanks. This study investigates the metal concentration of a *Sabellastarte sp*. obtained from Adventure Aquarium in Camden, New Jersey. This work is the first study of the ability of *Sabellastarte sp*. to sequester titanium. Based on the work of Popham and D'Auria, Sabellidae in general should be good model organisms for titanium sequestration.

4.2. Materials

A single feather duster worm specimen (designated W), *Sabellastarte sp.*, and a feather duster worm tube specimen (designated T) of unknown origin were provided by Alicia Longo at Adventure Aquarium in Camden, New Jersey. The worm (W) had died of natural causes on the day of collection and the tube (T) was from an organism that had died at some earlier time. Feather duster worms expel themselves from their tubes when they die. The feather duster worm was preserved in 1% formalin and a sample of water from the tank (designated as Tank Water) from the day the worm died was acquired.

Trace metal grade nitric acid was purchased from Fisher Scientific. Inductively Coupled Plasma Optical Emission Spectroscopy (ICP-OES) standards were prepared using Ti standard for ICP (1000 ppm from Fluka) Iron AA Standard (1000 ppm from Ricca Chemical Company) and iCAP 6000 Multi-Element Test Solution (5 ppm Ni, 1ppm Al, 1ppm Cu, 1ppm Mn, 0.2 ppm Ca, 0.2 ppm Mg, and 0.2 ppm Zn) from Thermo Scientific. All dilutions were performed using Barnstead NANOpure Diamond (18.2 MΩ-cm) water. ICP-OES data was obtained on an iCAP 7400 ICP-OES from Thermo Scientific which has a limit of detection equal to 0.0053 mg/L for most elements.

4.3. Methods

The whole feather duster worm and tube were lyophilized separately in the Schafmeister lab with help from Jae Eun Cheong. The whole lyophilized feather duster worm (0.1547 g dry weight) and a piece of the feather duster worm tube (0.1479 g dry weight) were completely digested in 50% Trace Metals Nitric Acid by refluxing for 2 hours and letting cool overnight. Samples were syringe filtered and dilutions of 1/10, 1/100, and 1/1000 were prepared of both the feather duster worm (W 1:10, W 1:100, and W 1:1000 respectively) and the feather duster worm tube (T 1:10, T 1:100, and T 1:1000 respectively) for analysis by ICP-OES. Standards containing 0.120 ppm Mg, 0.600 ppm Al, 0.075 ppm Ti, 0.600 ppm Mn, 0.100 ppm Fe, 3.000 ppm Ni, 0.600 ppm Cu, and 0.120 ppm Zn (Std 1), an a second containing 0.160 ppm Mg, 0.800 ppm Al, 0.100 ppm Ti, 0.600 ppm Mn, 0.125 ppm Fe, 4.000 ppm Ni, 0.800 ppm Ni, and 0.160 ppm Zn (Std 2) were prepared. These concentrations were based on the titanium concentration results of Popham and D'Auria.[5] The tank water sample was diluted minimally with nitric acid to a final concentration of 3% nitric acid.

4.4. Results

The ICP-OES results from the samples as run are shown in Table 3.1. Values reported as a negative number are considered to be a value of zero for further calculations. Values reported as N/A in Table 3.1 are concentrations too high for the instrument to measure. The values obtained from the ICP-OES were then used to calculate the concentrations of the metals in the dry weight of the feather duster worm and tube, as well as the initial concentration in the tank water, Table 3.2.

Table 4.1 *ICP-OES metal concentrations in mg/L of each sample as run before accounting for dilution.*

Sample	Mg	Al	Ti	Mn	Fe	Ni	Cu	Zn
Blank	0.000	0.000	0.000	0.000	0.000	0.000	0.000	0.000
Std 1	0.117	0.591	0.089	0.600	0.106	3.002	0.601	0.120
Std 2	0.162	0.806	0.105	0.800	0.128	3.998	0.799	0.160
W 1:10	N/A	0.181	0.077	0.037	0.490	0.011	0.056	0.887
W 1:100	4.815	0.021	0.001	0.004	0.047	0.005	0.017	0.204
W 1:1000	0.667	0.000	-0.005	0.001	0.001	0.003	0.023	0.060
T 1:10	2.897	0.082	0.036	0.047	0.037	0.006	0.019	0.218
T 1:100	0.633	0.008	0.004	0.006	0.036	0.002	0.036	0.069
T 1:1000	0.197	-0.005	-0.006	0.001	-0.002	0.003	0.022	0.026
Tank Water	N/A	0.002	-0.008	0.000	0.000	0.006	0.005	0.079

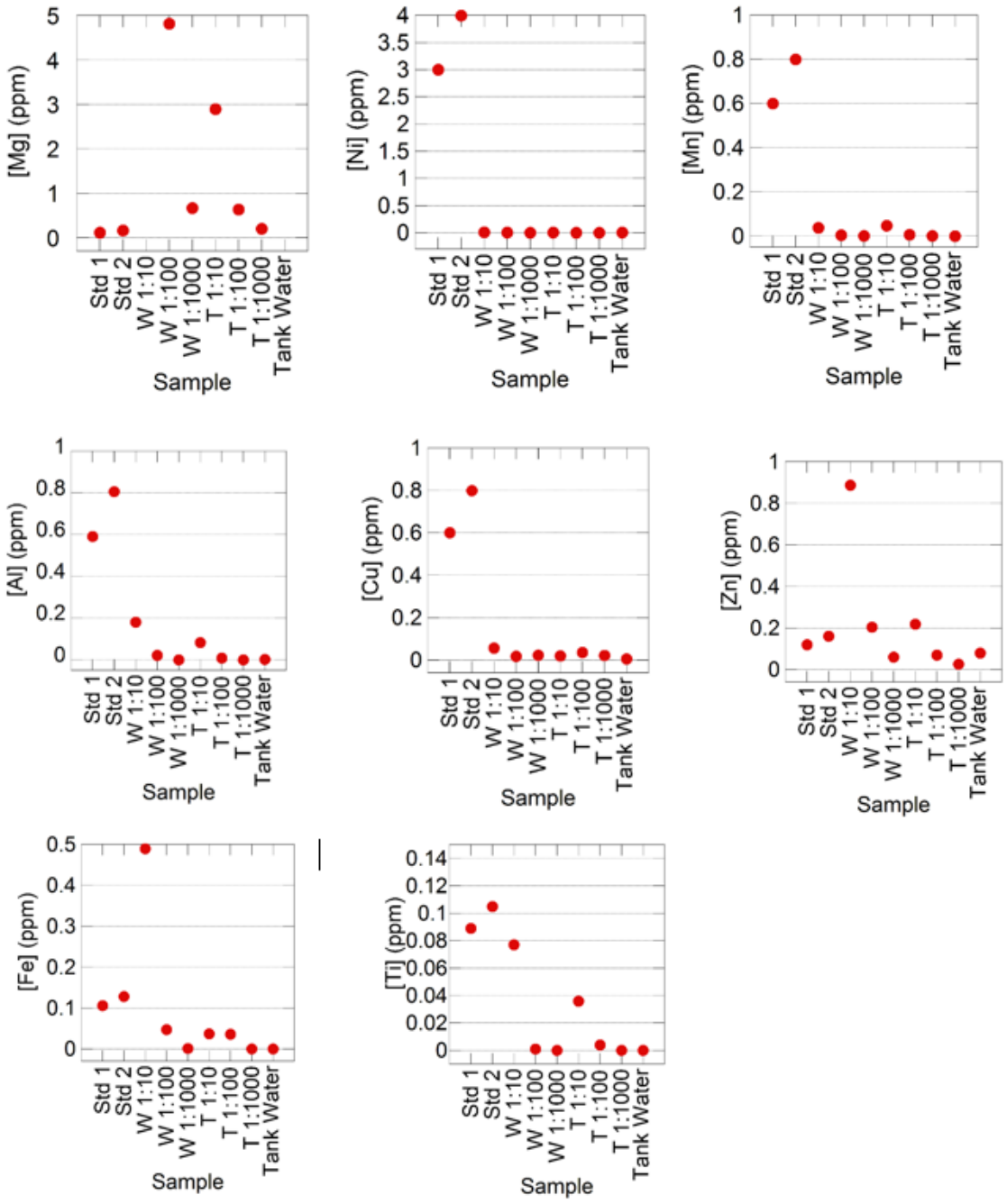

Figure 4.2 Plot of the measured concentration (ppm) of magnesium, aluminum, titanium, manganese, iron, nickel, copper, and zinc in the standards (Std 1 and Std 2), feather duster worm (W1:10, W 1:100, and W 1:1000), feather duster worm tube (T 1:10, T 1:100, T 1:1000), and tank water samples.

Table 4.2 *Sample metal concentrations corrected to original sample in mg/g dry weight and mg/L for the tank water.*

Sample	Mg	Al	Ti	Mn	Fe	Ni	Cu	Zn
W 1:10	N/A	0.058	0.025	0.012	0.158	0.004	0.018	0.286
W 1:100	15.533	0.068	0.003	0.013	0.152	0.015	0.055	0.657
W 1:1000	21.529	0.000	0.000	0.016	0.028	0.093	0.758	1.943
T 1:10	0.979	0.028	0.012	0.016	0.012	0.002	0.006	0.074
T 1:100	2.137	0.026	0.012	0.022	0.123	0.008	0.120	0.233
T 1:1000	6.666	0.000	0.000	0.019	0.000	0.088	0.759	0.881
Tank Water	N/A	0.003	0.000	0.000	0.000	0.006	0.005	0.082

Table 4.3 *Most probable concentrations of metal ions in feather duster worm (W) and feather duster worm tube (T) in mg/kg. Values from Popham and D'Auria are shown for comparison. Values reported here as N/A were not reported in the study by Popham.*[5]

Sample	Mg	Al	Ti	Mn	Fe	Ni	Cu	Zn
W	15000	60.0	20.0	10.0	150.0	1.0	20.0	300.0
T	1000	30.0	10.0	20.0	10.0	1.0	100.0	200.0
Popham (near sewer)	N/A	N/A	72.5	21.7	1554.0	1.08	26.0	193.0
Popham (control)	N/A	N/A	0.000	9.9	271.0	0.61	10.0	96.0

4.5. Discussion

Popham and D'Auria's measurements were obtained via X-ray Emission Spectroscopy (XES) of multiple freeze-dried and pulverized feather duster worms without tubes from two different sites. One was close to (~20 m) a storm water drainage sewer (near sewer) and the second an undefined further distance away (control) and their obtained values are shown in Table 4.3. Popham and D'Auria do not report the environmental metal ion concentrations, but generally titanium is present at around 0.001 ppm in sea water.[11] The concentration of titanium reported by Popham and D'Auria was 0.0725 mg/kg dry weight. Our study was limited to the single feather duster worm specimen and a single feather duster worm tube obtained from Adventure Aquarium.

The specimen from this study, *Sabellastarte sp.*, and the specimens studied by Popham and D'Auria, *Eudistylia vancouveri*, are distantly related but do show some similarities in metal sequestration (Table 4.3). Manganese, nickel, copper, and zinc concentrations are on the same order of magnitude in the worm, near sewer, and far sewer specimens. Assuming the concentrations of all metals are higher near the sewer outlet than further away, this result can be interpreted as signifying that feather duster worms are not sensitive to variances in the concentration of these three metals. The concentrations of titanium in the worm, and the near sewer specimens are all on the same order of magnitude but the far sewer specimen shows no titanium. The tank water from our study had no detectable titanium but the worm still showed appreciable amounts, meaning *Sabellastarte sp*. may be more sensitive to low titanium concentrations than *Eudistylia vancouveri*. Iron concentrations are on the same order of magnitude in the

worm and far sewer specimen but the near sewer specimen is higher. The sequestration of iron in feather duster worms may be correlated to their environmental iron concentration.

When the feather duster worm was removed from the 1% formalin it was gelatinous and the radioles were indeterminate from the body. The amount of titanium detected in this study (0.025 ppm) in the feather duster worm agrees well with previously published results (0.0725 ppm).[5] Assuming the feather duster worm is 80% water by mass the concentration of titanium is 0.0027 mg/g.

The concentrations of metal ions in the tank water were all much lower than the standards, with the exception of magnesium, which was higher. All of the metals were found in higher amounts in the feather duster worm than the tank water, with the possible exception of nickel, displaying the feather duster worms' ability to sequester metals in very low abundance from the water. The measured concentrations of metals in the feather duster worm and feather duster worm tube were not covered by the standard curve but can be trusted to at least the measured order of magnitude. The high water magnesium concentration from intentional doping of the tank water makes it impossible to ascertain if magnesium was concentrated in the worm or not. The metal concentrations within the worm are similar to those present within the tube but we cannot determine if these are related because of the uncertainty in the provenance of the tube.

Essential metals like iron and zinc were measured on the order 0.1 mg/g dry weight, and copper and nickel on the order of 0.01 mg/g dry weight. Titanium and aluminum were also measured on the order of 0.01 mg/g dry weight. There is evidence that titanium is sequestered from the environment but not in high quantities. Titanium

may or may not be necessary for this organism but if it is, it is only necessary in small quantities.

The concentrations of these metal ions in feather duster worms agree well between the study by Popham and D'Auria and this study, despite its limitations. This study, reinforced by Popham and D'Auria, demonstrates that Sabellidae do concentrate metal ions from their environment and may be useful as indicator organisms. The data presented in this work establishes that Sabellidae can sequester titanium present in small quantities from the environment but titanium is known to present in a range of concentrations depending on the environment.[12] The ability of these organisms to sequester titanium from environments with environmentally relevant high concentrations and titanium-depleted environments makes them a good model for study. The effects of titanium on the on the Sabellidae should be further studied, focusing on their possible use as a sentinel organism and the elucidation of the necessity of titanium and sequestration mechanism. A range of genus and species should also be considered for these studies.

REFERENCES CITED

1. K. N. Raymond, B. E. Allred and A. K. Sia, Coordination Chemistry of Microbial Iron Transport, *Accounts of Chemical Research*, 2015, **48**, 2496-2505.
2. M. A. Saito, E. M. Bertrand, S. Dutkiewicz, V. V. Bulygin, D. M. Moran, F. M. Monteiro, M. J. Follows, F. W. Valois and J. B. Waterbury, Iron conservation by reduction of metalloenzyme inventories in the marine diazotroph Crocosphaera watsonii, *Proceedings of the National Academy of Sciences of the United States of America*, 2011, **108**, 2184-2189.
3. F. Yoneyama, M. Yamamoto, W. Hashimoto and K. Murata, Azotobacter vinelandii gene clusters for two types of peptidic and catechol siderophores produced in response to molybdenum, *Journal of Applied Microbiology*, 2011, **111**, 932-938.
4. in *Biological Inorganic Chemistry: Structure and Reactivity*, eds. I. Bertini, H. B. Gray, E. I. Stiefel and J. S. Valentine, University Science Books, 2007, ch. VIII.
5. J. D. Popham and J. M. Dauria, A new sentinel organism for vanadium and titanium, *Marine Pollution Bulletin*, 1982, **13**, 25-27.
6. E. G. McEvoy and P. Sundberg, Patterns of trace-metal accumulation in Swedish marine nemerteans, *Hydrobiologia*, 1993, **266**, 273-280.
7. M. Camusso, R. Balestrini and A. Binelli, Use of zebra mussel (Dreissena polymorpha) to assess trace metal contamination in the largest Italian subalpine lakes, *Chemosphere*, 2001, **44**, 263-270.

8. O. Vinn, H. A. Ten Hove and H. Mutvei, On the tube ultrastructure and origin of calcification in sabellids (Annelida, Polychaeta), *Palaeontology*, 2008, **51**, 295-301.

9. C. J. Glasby and T. Timm, Global diversity of polychaetes (Polychaeta; Annelida) in freshwater, *Hydrobiologia*, 2008, **595**, 107-115.

10. N. N. Hobgood, *Journal*, 2010, *Sabellastarte magnifica* (Magnificent Feather Duster worm)Sabellastarte magnifica (Magnificent Feather Duster worm).

11. J. Emsley, *The Elements*, Clarendon Press, Oxford, U.K., 3rd edn., 1998.

12. K. M. Buettner and A. M. Valentine, Bioinorganic Chemistry of Titanium, *Chemical Reviews*, 2012, **112**, 1863-1881.

CHAPTER 5. FERRIREDUCTASE ACTIVITY OF NICATRANSFERRIN, A MODEL, MONOLOBAL TRANSFERRIN

5.1. Introduction

Nearly every organism known on Earth requires iron to live, serving a multitude of biological functions.[1-3] While iron is abundant, it suffers from being mostly insoluble in oxic aqueous environments.[4] It is also toxic to organisms if left unbound, as it participates in the Haber-Weiss cycle.[5] In order to increase the availability of iron and prevent unwanted chemistry, organisms have evolved complex systems to sequester iron with biological ligands.

Higher organisms, like humans, use the transferrin (Tf) family of proteins to sequester and safely traffic iron. The broad use of the family of Tf proteins motivates work into their structure and function.[6, 7] Human serum transferrin (hsTf) is comprised of N-terminus and C-terminus clamp-shaped lobes tethered together by a short amino acid chain, each lobe being able to bind one Fe(III) ion. Each binding site consists of two tyrosines, a histidine, an aspartate, and a synergistic anion, usually carbonate (Figure 5.1). Once each lobe has bound an ion, the holoTf binds to the membrane bound transferrin receptor. The receptor binds two holoTf complexes and the cell then envelops the holoTf-transferrin receptor complex. Once inside the cell, this endosome becomes acidified and the Fe(III) ions are reduced by the ferrireductase Steap3, bound by an unknown small molecule and exported from the endosome (Figure 5.2). The order and mechanism of the reduction and release of iron are debated.[6]

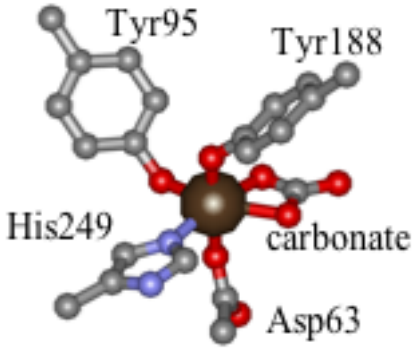

Figure 5.1 Iron binding site of human serum transferrin.

Created using PyMol with the coordinates from PDB 2HAU and labeled with numbering from hsTf N-lobe.[8]

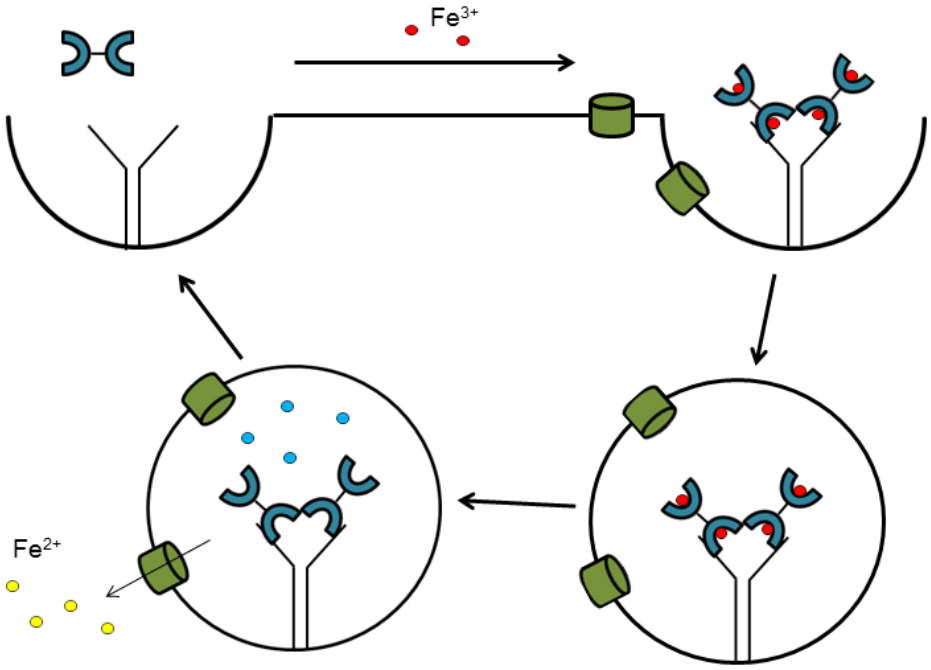

Figure 5.2 Schematic of the transferrin cycle.

Ascidians, also called sea squirts, or tunicates for their protective outer layer, are a class of invertebrate organisms that phylogenetically are the closest relative of vertebrates.[9-11] *Ciona intestinalis* are hermaphroditic and release both eggs and sperm into the water. The *C. intestinalis* larvae float freely with currents and develop a notochord in their tadpole stage. During this tadpole stage the ascidian swims, and fixes itself to a surface, reabsorbing its notochord for nutrients.[12] While attached to the surface, ascidians filter feed using two syphons, and are known to sometimes sequester large amounts of metals like V, Fe, and Ti.[13] *Ciona intestinalis* also has genes for both a monolobal transferrin (nicaTf) and bilobal transferrin.[14] In this study we observe and characterize the nicaTf dependent reduction of Fe(III) to Fe(II), a process previously unobserved for transferrin proteins.

Recent studies have advocated that *Ciona intestinalis* may in fact be two different species, the other being *Ciona robusta*.[15, 16] The new work suggests that *C. intestinalis* predominates mainly in the Northeast and Northwest Atlantic Ocean while *C. robusta* occurs primarily in the Pacific Ocean along the coasts of Japan, New Zealand, and the western coast of North America. The genetic sequence of *C. intestinalis* was obtained primarily from a single organism collected off the coast of California.[17] This sequence was used for cloning of the protein used in this study.[18] It is likely that the organism used for genomic sequencing is *C. robusta*, but we will refer to it as *C. intestinalis* in order to agree with the name attached to the genomic sequence. The GenBank genomic sequence for nicaTf matches the amino acid sequence of nicaTf as isolated from a specimen obtained from Marine Biological Laboratory in Woods Hole, suggesting a conservation of this protein between the two species.[14]

To further understand the transferrin cycle, we have studied nicatransferrin (nicaTf), a monolobal transferrin from the model ascidian *Ciona intestinalis*.[14, 18-20] The bilobal human serum transferrin has a molecular mass of 80 kDa and the monolobal nicatransferrin has molecular mass of 37.7 kDa. NicaTf shares a 32% sequence homology with the N-lobe of hsTf. The residues for disulfides, synergistic anion binding, and iron binding are conserved (Figure 5.3). NicaTf binds one equivalent of iron but does not show the characteristic LMCT at 465 nm shown by serum transferrin. NicaTf instead has an as of yet unidentified absorbance at 330 nm that is independent of iron binding.[14] The conservation of residues combined with an evolutionarily ancient amino acid sequence may aid in our understanding of how the transferrin cycle evolved and a better understanding of the transferrin cycle as it functions today. Recent experiments showed incomplete iron loading of nicaTf. This led to the suspicion that nicaTf is reducing iron. This work examines the kinetics and implications of nicaTf dependent iron reduction. We hypothesize that this iron reduction may due to the lack of a known Steap3 protein in *C. intestinalis*.

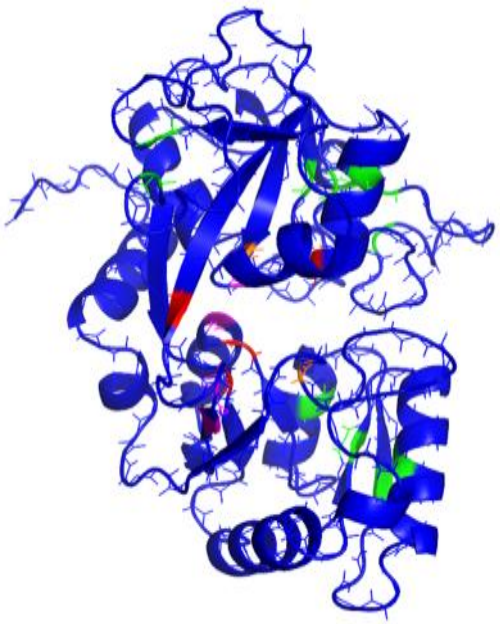

Figure 5.3 I-TASSER model of nicaTf.[21] Residues in green identify conserved cysteines that participate in disulfide bonds.

Residues in red identify conserved iron binding residues. Residues in magenta identify conserved synergistic anion binding residues. Residues in orange identify conserved lobe opening trigger residues.

5.2. Materials

Nicatransferrin was expressed and purified as previously described.[18] NicaTf was then further purified using size exclusion chromatography on a Superdex-75 10/30 GL column. The nicaTf was used as isolated from fractions with no impurities. Tris and HEPES were purchased from American Bioanalytical. $FeCl_3$ was purchased from Fisher. Nitrilotriacetic acid and ferrozine were purchased from Acros Organics. Sodium Chloride was purchased from J.T. Baker. NADH was purchased from Amresco. All solutions were made using water (18.2 mΩcm) from a Barnsted Nanopure. Solution pH was obtained using a Thermo Scientific Orion Ross Ultra semi-micro pH electrode. UV-vis data were

collected using a Cary Bio 50 UV-vis using the Cary scanning kinetics program. The reaction was maintained at temperature using a RTE111 water bath.

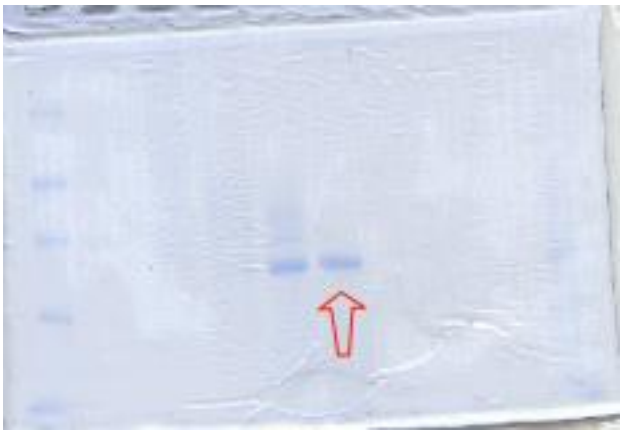

Figure 5.4 SDS-PAGE of purified nicaTf. NicaTf from the fraction denoted by the arrow was used but not nicaTf from lane to the left as it is impure.

5.3. Methods

Reduction of Fe(III) to Fe(II) by nicaTf was detected using UV-Vis spectroscopy to monitor formation of the Fe(II)-Ferrozine ($Fe(Fz)_3$) complex by its characteristic peak at 562 nm.[22, 23] UV-Vis spectra were collected typically every 30 seconds for 1 hour immediately followed by collection every 3 minutes for 2 hours between 700 and 350 nm. The spectra were collected at 15, 20, 25, 30, and 35 °C using a cell connected to a recirculating water bath. Experiments lasting 24 hours were also conducted but showed no change in kinetic fits. The UV-Vis spectra were fit using SpecFit software.[24]

Final concentrations of 4 μM nicaTf, 100 μM Fe(nitrilotriacetic acid)$_2$,[25] 1 mM ferrozine were used for iron reduction experiments. Experiments were performed in both 50 mM HEPES, 0.15 M NaCl pH=7.4 and 50 mM Tris, 0.15 M NaCl pH=7.4. Iron

reduction was also performed with the addition of 100 μM NADH in which case the volume and concentrations were constant with the previous assays. After the reduction assay, some samples were used in DTNB (5,5'-dithiobis(2nitrobenzoic acid)) assay experiments in order to detect free thiol.[26] These experiments were repeated using a molecular crowding agent, Ficoll PM70, with a final concentration of 0.75 mg/mL to evaluate the possible effects of plasma proteins on the kinetics. The plasma protein concentration of *Ciona intestinalis* was determined by Bradford assay to be between 0.5 and 1.0 mg/mL.[27]

5.4. Results

On visual inspection of the UV-Vis spectra it is apparent that the experiments performed in Tris buffer show a smaller change in the absorbance at the lambda max of the $Fe(Fz)_3$ complex over time than the spectra for the experiments performed in HEPES buffer. It is also apparent that control experiments without nicaTf in Tris buffer show no change in absorbance over time, but the control experiments without nicaTf in HEPES buffer do show a small change in absorbance. 24 hour experiments in both HEPES and Tris buffer show no difference in rates as determined by SpecFit.

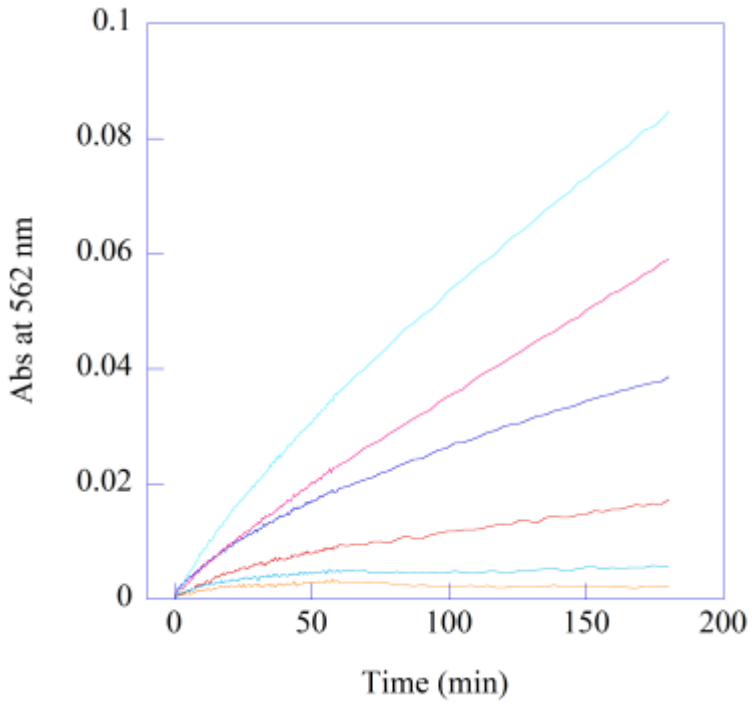

Figure 5.5 Formation of $Fe(Fz)_3$ over time at 25 °C. HEPES buffer without nicaTf (green), with nicaTf (blue), and with nicaTf and NADH (light blue).

Tris buffer without nicaTf (orange), with nicaTf (red), and with nicaTf and NADH (maroon).

Kinetic experiments performed using a molecular crowding agent showed no difference in rate of iron reduction.

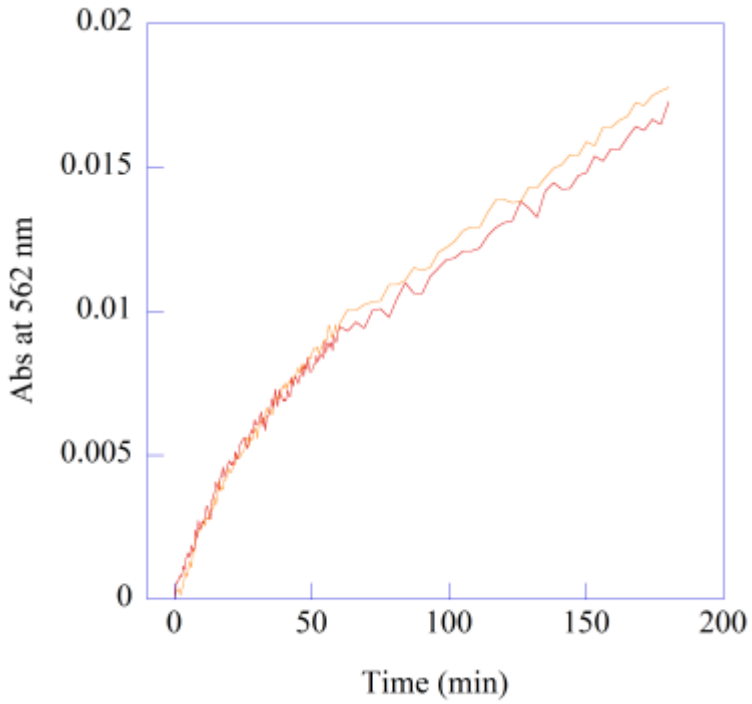

Figure 5.6 Molecular crowding at 25 °C. Tris buffer with nicaTf (red) and with nicaTf and Ficoll PM70 (orange).

Experiment run in 50 mM Tris, 0.15 M NaCl pH=7.4 with or without 0.75 mg/mL Ficoll PM70.

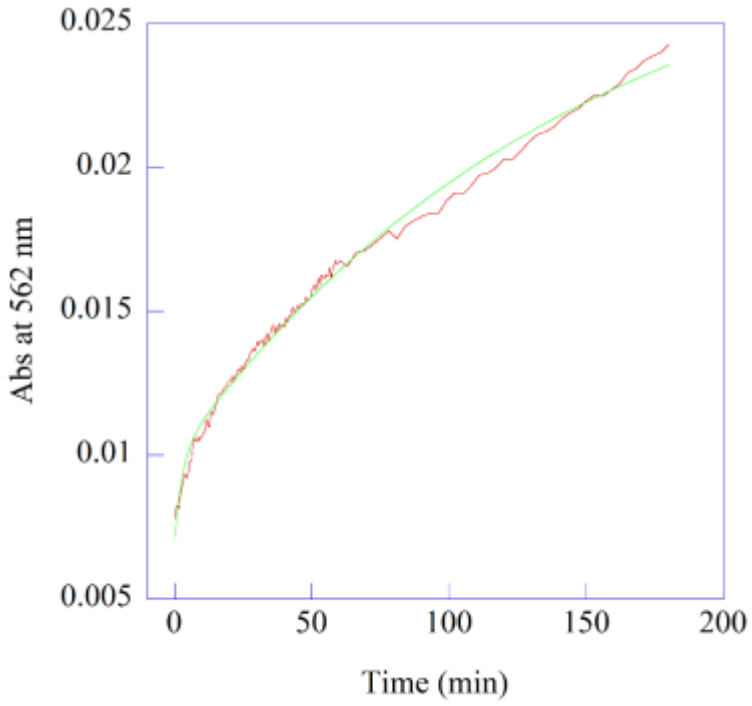

Figure 5.7 Kinetic data versus fit. Cross section of data fit at 562 nm for experiment run in 50 mM Tris, 0.15 M NaCl pH=7.4 at 25 °C.

Data (red) and Fit (green) have difference residuals no greater than $5x10^{-4}$ au.

Kinetic fitting software SpecFit identified two sequential first order reactions (A∏B∏C) as the best fit for the nicaTf dependent reduction of Fe(III) using the data present from 350 to 700 nm. This fit for data collected over three hours was identical to that collected for twenty-four hours.

Table 5.1 *Kinetic rate constants for experiments performed in Tris buffer.*

Temp (°C)	k_1 average (/min)	Std. dev.	k_2 average (/min)	Std. dev.	Δ[Fe(II)]
35	9.7E-02	5.1E-02	4.6E-03	3.6E-03	1.2E-06
30	7.0E-02	1.7E-02	5.5E-03	3.7E-03	8.6E-07
25	6.8E-02	8.9E-03	6.0E-03	3.2E-03	5.7E-07
20	4.8E-02	8.5E-03	2.4E-03	3.2E-03	3.9E-07
15	4.6E-02	7.9E-03	8.1E-03	5.8E-03	2.5E-07

Table 5.2 *Kinetic rate constants for experiments performed in Tris buffer with NADH.*

Temp (°C)	k_1 average (/min)	Std. dev.	k_2 average (/min)	Std. dev.	Δ[Fe(II)]
35	1.5E-01	2.6E-02	1.5E-03	4.4E-04	4.2E-06
30	8.5E-02	9.4E-03	2.2E-03	7.1E-04	2.9E-06
25	7.9E-02	1.0E-02	2.5E-03	8.0E-04	2.0E-06
20	6.5E-02	1.0E-02	3.2E-03	3.8E-04	1.4E-06
15	6.3E-02	6.0E-03	2.0E-03	9.2E-04	1.0E-06

Table 5.3 *Kinetic rate constants for experiments performed in HEPES buffer.*

Temp (°C)	k_1 average (/min)	Std. dev.	k_2 average (/min)	Std. dev.	Δ[Fe(II)]
35	7.1E-02	3.1E-02	4.6E-03	3.3E-03	2.6E-06
30	6.2E-02	3.6E-02	4.2E-03	2.2E-03	2.0E-06
25	6.3E-02	1.7E-02	4.4E-03	2.0E-03	1.6E-06
20	5.6E-02	1.7E-02	4.3E-03	2.1E-03	1.1E-06
15	5.4E-02	1.1E-02	4.5E-03	1.9E-03	7.5E-07

Table 5.4 *Kinetic rate constants for experiments performed in HEPES buffer with NADH.*

Temp (°C)	k_1 average (/min)	Std. dev.	k_2 average (/min)	Std. dev.	Δ[Fe(II)]
35	1.7E-01	3.0E-02	3.2E-03	1.1E-03	6.8E-06
30	1.1E-01	3.4E-02	2.9E-03	1.2E-03	4.7E-06
25	5.3E-02	1.0E-02	2.9E-03	7.4E-04	3.5E-06
20	6.9E-02	2.2E-02	3.9E-03	1.1E-03	2.4E-06
15	3.8E-02	1.3E-02	2.6E-03	8.9E-04	1.6E-06

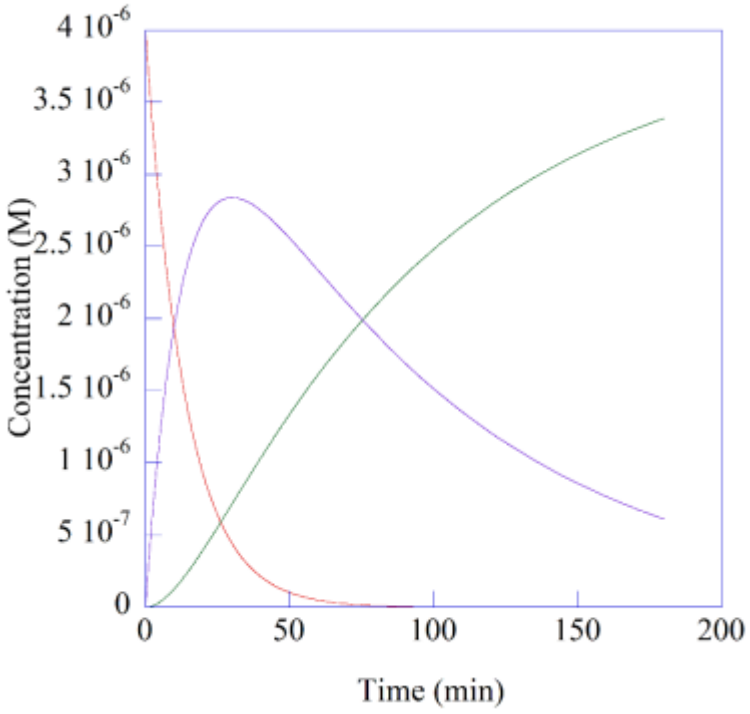

Figure 5.8 Concentration profile of species from kinetic fitting.

Species “A” is red, species “B” is purple, and species “C” is green. Experiment run in 50 mM Tris, 0.15 M NaCl pH=7.4 at 25 °C.

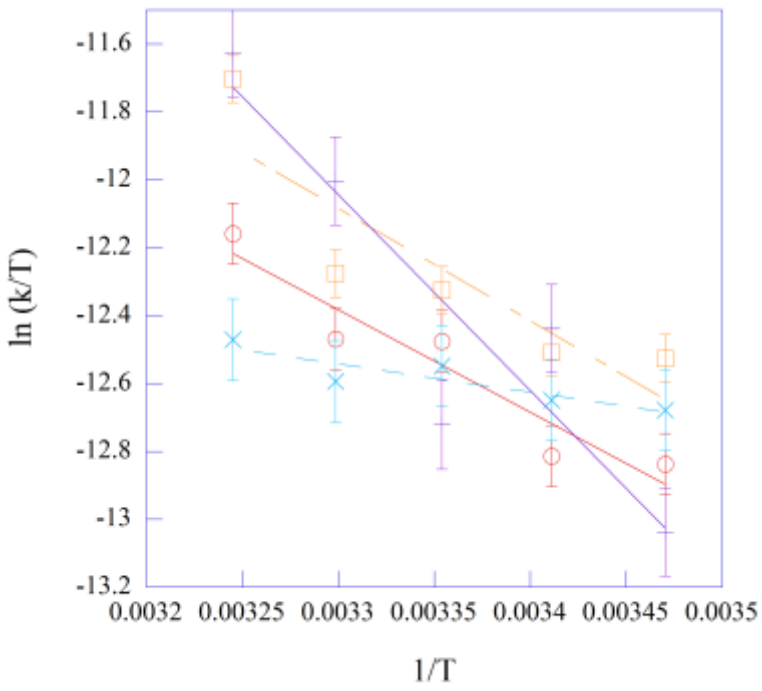

Figure 5.9 Eyring plot of kinetic fit values for k_1.

Tris buffer without NADH (red) and with NADH (orange). HEPES buffer without NADH (blue) and with NADH (purple).

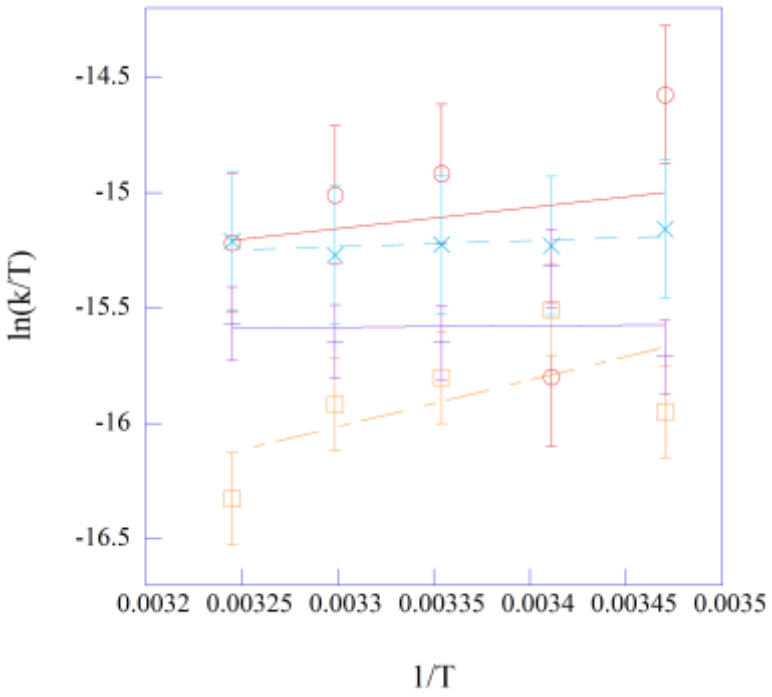

Figure 5.10 Eyring plot of kinetic fit values for k_2.

Tris buffer without NADH (red) and with NADH (orange). HEPES buffer without NADH (blue) and with NADH (purple).

Table 5.5 *Enthalpy and entropy of activation.*

	Tris	Tris w/NADH	HEPES	HEPES w/NADH
$\Delta H^{\ddagger}$ (kJ/mole)	25	28	6.9	48
$\Delta S^{\ddagger}$ (kJ/K mole)	-0.22	-0.21	-0.28	-0.14

DTNB assays of the protein samples before and after the reduction experiment showed one free thiol per protein molecule. The remaining thiols are likely buried inside the protein beyond detection.

5.5. Discussion

The enhanced reduction that occurs in experiments performed in HEPES buffer in both the presence and absence of nicaTf can be explained due to HEPES redox activity. It has been demonstrated that the piperazine ring present in some of Good's buffers can form radical cations.[28-30] HEPES was first shown to be oxidized by Cu(II) in the presence of Cu(I) stabilizing chelators.[31]

Molecular crowding experiments are important in determining whether or not the rate of reaction is diffusion limited *in vivo*. [32] This is important to consider as most biochemical assays are carried out under dilute concentrations that are not representative of cellular or plasma protein concentrations. Molecular crowding experiments showed no difference in the rates of iron reduction. This observation is unsurprising given the relatively high concentration of iron compared to nicaTf. The molecular crowding agent should inhibit the mobility of nicaTf but will limit the mobility of the iron much less and with such high relative concentrations this should not limit the rate of reaction.

From the kinetic fitting the "A" complex can be thought of as the holo-nicaTf complex. Complex "A" then proceeds through an unidentified "B" complex resulting in the "C" complex. The "C" complex in the model displays an absorption spectra that matches with previous studies.[23] The A∏B reaction is thought to be the iron reduction step and has a half-life of about 10 minutes. This reaction half-life fits well with the transferrin cycle which takes approximately 20 minutes from iron binding to transferrin release from the cell.

The use of ferrozine as an Fe(II) chelator will shift the equilibrium of this reaction towards the products. Experiments, not shown here, in which ferrozine was not added

until 1 hour after the reaction was initiated were also performed. In these experiments the absorbance rapidly rose upon the addition of ferrozine. This rise in absorbance fell slightly lower than the expected absorbance, had the ferrozine been in the reaction since the beginning. This indicates that the ferrozine does shift the reaction but is dominated by the nicaTf dependent reduction. The shift caused by ferrozine may also analogous to the small molecule thought to shuttle the reduced iron from transferrin to the cell in humans.[6]

The identity of the "B" complex is uncertain. It has an observable absorption peak with a lambda max equivalent to the $Fe(Fz)_3$. This may indicate that there is a ternary nicaTf-Fe-Fz species, similar to small molecule ternary iron species that have been previously described.[33, 34] The reduction of iron by the protein would cause a change in coordination preference facilitating the release of iron as Fe(Fz). Complex "B" may be one of or a combination of these two species which go on to form the $Fe(Fz)_3$ species.

Eyring plots of the kinetic data (Figure 5.4) show similar enthalpies of activation of k_1 for trials conducted in Tris buffer and Tris buffer with NADH, 25 and 28 kJ/mole respectively. There is a large difference in the enthalpies of activation of the HEPES buffer with and without NADH, 48 and 6.9 kJ/mole respectively. HEPES may interact with iron and act as a reductant with the concomitant formation of radical cations, lowering the activation energy in the presence of Fe(II) stabilizing chelators.

Experiments conducted in HEPES with NADH have highest activation energy but also the highest rates of reaction. It seems improbable that the addition of NADH would increase the activation energy this much. HEPES with NADH has the slowest k_1 value at 15 °C but has the highest formation of $Fe(Fz)_3$ at 15 °C. These experiments also have the largest standard deviations of all the data. The large activation energy may be due to the

reaction occurring too fast for our instrument set-up to observe accurately, and the software may be observing the end of a process too quick for our experimental parameters.

The kinetics of the nicaTf dependent reduction of Fe(III) place it within the time regime expected for the transferrin cycle, with a half-life of 10 minutes, but the mechanism of this process is still uncertain and an unidentified intermediate persists. The 10-minute half-life is for that of human serum transferrin. However, *Ciona intestinalis* has no apparent transferrin receptor. With no receptor it is possible that the reduction of Fe(III) to Fe(II) allows for the passage of iron through a membrane porin, such as a Ca(II) channel. This would likely require some sort of cellular recognition.

How nicaTf facilitates this reduction in unclear. DTNB assay results suggest that thiols are not oxidized but it is possible that thiols beyond the detection of the assay do participate. The role of the chromophore that absorbs at ~330 nm is uncertain as the ferrozine reagent has a high absorbance below 350 nm. After reacting for 24 hours in 50 mM Tris, 0.15 M NaCl pH=7.4 at 25 °C, nicaTf has been observed to reduce 2.5 equivalents of iron with the absorbance still increasing.

These experiments show that the reduction of iron may in fact take place while the iron is bound to transferrin. Mechanistically, a change in oxidation state would alter the ligand preference of the iron, decreasing the stability with transferrin, in preference for softer, more thermodynamically stable ligands. Considering that nicatransferrin and human serum transferrin likely evolved along the same pathway, it seems logical that human serum transferrin would also reduce iron before release.

Ciona intestinalis does not have a known transferrin receptor. How this affects the transport of iron is uncertain. *Ciona intestinalis* also lacks the protein Steap3 or a homolog thereof. The Steap3 protein is known to be the reductant donor in humans and compensating for this loss may be the reason for nicatransferrin autoreduction. *Ciona intestinalis* does have a divalent metal transporter 1 (DMT1) which in humans is responsible for the transport of iron(II) into the cell. It remains possible that there is some cell wall protein that recognizes nicatransferrin which then releases iron(II) to DMT1.

REFERENCES CITED

1. M. D. Garrick and L. M. Garrick, Cellular iron transport, *Biochimica Et Biophysica Acta-General Subjects*, 2009, **1790**, 309-325.
2. S. C. Andrews, A. K. Robinson and F. Rodriguez-Quinones, Bacterial iron homeostasis, *Fems Microbiology Reviews*, 2003, **27**, 215-237.
3. R. M. Welch, Micronutrient Nutrition of Plants, *Critical Reviews in Plant Sciences*, 1995, **14**, 49-82.
4. P. L. Brown and C. Ekberg, *Hydrolysis of Metal Ions*, Wiley-VCH Verlag GmbH & Co. KGaA, Weinheim, Germany, 2016.
5. J. P. Kehrer, The Haber-Weiss reaction and mechanisms of toxicity, *Toxicology*, 2000, **149**, 43-50.
6. A. N. Steere, S. L. Byrne, N. D. Chasteen and A. B. Mason, Kinetics of iron release from transferrin bound to the transferrin receptor at endosomal pH, *Biochimica Et Biophysica Acta-General Subjects*, 2012, **1820**, 326-333.
7. L. A. Lambert, H. Perri, P. J. Halbrooks and A. B. Mason, Evolution of the transferrin family: Conservation of residues associated with iron and anion binding, *Comparative Biochemistry and Physiology B-Biochemistry & Molecular Biology*, 2005, **142**, 129-141.
8. J. Wally, P. J. Halbrooks, C. Vonrhein, M. A. Rould, S. J. Everse, A. B. Mason and S. K. Buchanan, The crystal structure of iron-free human serum transferrin provides insight into inter-lobe communication and receptor binding, *Journal of Biological Chemistry*, 2006, **281**, 24934-24944.

9. I. Goodbody, Physiology of Ascidians, *Advances in Marine Biology*, 1974, **12**, 1-149.

10. F. Delsuc, H. Brinkmann, D. Chourrout and H. Philippe, Tunicates and not cephalochordates are the closest living relatives of vertebrates, *Nature*, 2006, **439**, 965-968.

11. N. H. Putnam, T. Butts, D. E. K. Ferrier, R. F. Furlong, U. Hellsten, T. Kawashima, M. Robinson-Rechavi, E. Shoguchi, A. Terry, J. K. Yu, E. Benito-Gutierrez, I. Dubchak, J. Garcia-Fernandez, J. J. Gibson-Brown, I. V. Grigoriev, A. C. Horton, P. J. de Jong, J. Jurka, V. V. Kapitonov, Y. Kohara, Y. Kuroki, E. Lindquist, S. Lucas, K. Osoegawa, L. A. Pennacchio, A. A. Salamov, Y. Satou, T. Sauka-Spengler, J. Schmutz, T. Shin-I, A. Toyoda, M. Bronner-Fraser, A. Fujiyama, L. Z. Holland, P. W. H. Holland, N. Satoh and D. S. Rokhsar, The amphioxus genome and the evolution of the chordate karyotype, *Nature*, 2008, **453**, 1064-U1063.

12. A. Kowalevsky, *Mémoires de l'Académie impériale des sciences de St. Pétersbourg 7*, 1866, **10**, 1.

13. E. P. Levine, Occurrence of Titanium, Vanadium, Chromium, and Sulfuric Acid in Ascidian Eudistoma Ritteri, *Science*, 1961, **133**, 1352-1353.

14. R. Uppal, K. V. Lakshmi and A. M. Valentine, Isolation and characterization of the iron-binding properties of a primitive monolobal transferrin from Ciona intestinalis, *Journal of Biological Inorganic Chemistry*, 2008, **13**, 873-885.

15. R. Pennati, G. F. Ficetola, R. Brunetti, F. Caicci, F. Gasparini, F. Griggio, A. Sato, T. Stach, S. Kaul-Strehlow, C. Gissi and L. Manni, Morphological

Differences between Larvae of the Ciona intestinalis Species Complex: Hints for a Valid Taxonomic Definition of Distinct Species, *Plos One*, 2015, **10**.

16. R. Brunetti, C. Gissi, R. Pennati, F. Caicci, F. Gasparini and L. Manni, Morphological evidence that the molecularly determined Ciona intestinalis type A and type B are different species: Ciona robusta and Ciona intestinalis, *Journal of Zoological Systematics and Evolutionary Research*, 2015, **53**, 186-193.

17. P. Dehal, Y. Satou, R. K. Campbell, J. Chapman, B. Degnan, A. De Tomaso, B. Davidson, A. Di Gregorio, M. Gelpke, D. M. Goodstein, N. Harafuji, K. E. M. Hastings, I. Ho, K. Hotta, W. Huang, T. Kawashima, P. Lemaire, D. Martinez, I. A. Meinertzhagen, S. Necula, M. Nonaka, N. Putnam, S. Rash, H. Saiga, M. Satake, A. Terry, L. Yamada, H. G. Wang, S. Awazu, K. Azumi, J. Boore, M. Branno, S. Chin-bow, R. DeSantis, S. Doyle, P. Francino, D. N. Keys, S. Haga, H. Hayashi, K. Hino, K. S. Imai, K. Inaba, S. Kano, K. Kobayashi, M. Kobayashi, B. I. Lee, K. W. Makabe, C. Manohar, G. Matassi, M. Medina, Y. Mochizuki, S. Mount, T. Morishita, S. Miura, A. Nakayama, S. Nishizaka, H. Nomoto, F. Ohta, K. Oishi, I. Rigoutsos, M. Sano, A. Sasaki, Y. Sasakura, E. Shoguchi, T. Shin-i, A. Spagnuolo, D. Stainier, M. M. Suzuki, O. Tassy, N. Takatori, M. Tokuoka, K. Yagi, F. Yoshizaki, S. Wada, C. Zhang, P. D. Hyatt, F. Larimer, C. Detter, N. Doggett, T. Glavina, T. Hawkins, P. Richardson, S. Lucas, Y. Kohara, M. Levine, N. Satoh and D. S. Rokhsar, The draft genome of Ciona intestinalis: Insights into chordate and vertebrate origins, *Science*, 2002, **298**, 2157-2167.

18. A. D. Tinoco, C. W. Peterson, B. Lucchese, R. P. Doyle and A. M. Valentine, On the evolutionary significance and metal-binding characteristics of a monolobal

transferrin from Ciona intestinalis, *Proceedings of the National Academy of Sciences of the United States of America*, 2008, **105**, 3268-3273.

19. J. P. Gaffney and A. M. Valentine, The challenges of trafficking hydrolysis prone metals and ascidians as an archetype, *Dalton Transactions*, 2011, **40**, 5827-5835.
20. J. P. Gaffney and A. M. Valentine, Contrasting Synergistic Anion Effects in Vanadium(V) Binding to Nicatransferrin versus Human Serum Transferrin, *Biochemistry*, 2009, **48**, 11609-11611.
21. J. Y. Yang, R. X. Yan, A. Roy, D. Xu, J. Poisson and Y. Zhang, The I-TASSER Suite: protein structure and function prediction, *Nature Methods*, 2015, **12**, 7-8.
22. L. L. Stookey, Ferrozine - A New Spectrophotometric Reagent for Iron, *Analytical Chemistry*, 1970, **42**, 779.
23. C. R. Gibbs, Characterization and Application of Ferrozine Iron Reagent as a Ferrous Iron Indicator, *Analytical Chemistry*, 1976, **48**, 1197-1201.
24. R. A. Binstead, B. Jung and A. D. Zuberbuhler, *SpecFit/32*, Spectrum Software Asociates, Marlborough, MA, 2001.
25. G. W. Bates, C. Billups and P. Saltman, Kinetics and Mechanism of Iron(III) Exchange between Chelates and Transferrin Complexes of Citrate and Nitrilotriacetic Acid, *Journal of Biological Chemistry*, 1967, **242**, 2810-&.
26. P. W. Riddles, R. L. Blakeley and B. Zerner, Reassessment of Ellman Reagent, *Methods in Enzymology*, 1983, **91**, 49-60.
27. J. Webb and P. Chrystal, Protein-Binding of Iron in Blood-Plasma of the Ascidian Herdmania momus, *Marine Biology*, 1981, **63**, 107-112.

28. J. K. Grady, N. D. Chasteen and D. C. Harris, Radicals from Good's Buffers, *Analytical Biochemistry*, 1988, **173**, 111-115.

29. M. Kirsch, E. E. Lomonosova, H. G. Korth, R. Sustmann and H. de Groot, Hydrogen peroxide formation by reaction of peroxynitrite with HEPES and related tertiary amines - Implications for a general mechanism, *Journal of Biological Chemistry*, 1998, **273**, 12716-12724.

30. C. M. H. Ferreira, I. S. S. Pinto, E. V. Soares and H. M. V. M. Soares, (Un)suitability of the use of pH buffers in biological, biochemical and environmental studies and their interaction with metal ions - a review, *Rsc Advances*, 2015, **5**, 30989-31003.

31. K. Hegetschweiler and P. Saltman, Interaction of Copper(II) with N-(2-hydroxymethyl)piperazine-N'-ethanesulfonic acid (HEPES), *Inorganic Chemistry*, 1986, **25**, 107-109.

32. H. X. Zhou, G. N. Rivas and A. P. Minton, Macromolecular crowding and confinement: Biochemical, biophysical, and potential physiological consequences, *Annual Review of Biophysics*, 2008, **37**, 375-397.

33. K. A. Mies, J. I. Wirgau and A. L. Crumbliss, Ternary complex formation facilitates a redox mechanism for iron release from a siderophore, *Biometals*, 2006, **19**, 115-126.

34. J. M. Harrington and A. L. Crumbliss, The redox hypothesis in siderophore-mediated iron uptake, *Biometals*, 2009, **22**, 679-689.

CHAPTER 6. INVESTIGATION OF PURPLE GRANULES FROM *EUDISTOMA PURPUROPUNCTATUM*

6.1. Introduction

Ascidians are a group of filter-feeding marine invertebrates that are known to accumulate large quantities of metal ions, most famously vanadium.[1-4] Several of these organisms sequester titanium including *Eudistoma ritteri*, which is the most avid sequesterer acquiring up to 1500 ppm (dry weight) titanium in the whole organism.[5-7] This value represents a ~30 million fold increase over the water it is filtering. While these metal concentrations are not necessarily indicative of their use, the driving force for the organism to sequester such high concentrations is unclear.

Eudistoma purpuropunctatum is a species of ascidian from the same genus as *E. ritteri* that has a characteristic purple color and lives beneath the oxic zone.[8] *E. purpuropunctatum* was named from the Latin *purpuro* meaning purple and *punctatus* meaning spotted as with punctures. In the species' original characterization, it was found that its characteristic purple color was due to small, approximately 10 μm, granule clusters in cells embedded in the tunic and zooid (Figure 6.1). The zooids measure approximately 11 mm in length when relaxed but usually 3-5 mm in preserved samples. The colonies are 1 – 3 cm thick and may be 10 cm or more in length and width with rounded, irregular edges. The colonies range in color from light to dark lavender but occasionally colonies or regions of a colony are without color and appear grayish white. The pigment is primarily located on the surface of the tunic. *Eudistoma purpuropunctatum* lives in areas with fast currents and is not feasible to collect, but preserved specimens are available at certain museums.

Under normal aqueous oxic conditions titanium exists in the Ti(IV) oxidation state, but it is possible that below the oxic zone titanium exists as Ti(III) which exhibits a characteristic purple/blue color due to the d-d electronic transitions of the d^1 ion. We hypothesize that due to the phylogenetic relationship of *E. purpuropunctatum* and *E. ritteri*, *E. purpuropunctatum* may also sequester high amounts of titanium and the purple granules may get their coloration from a Ti(III) containing mineral.

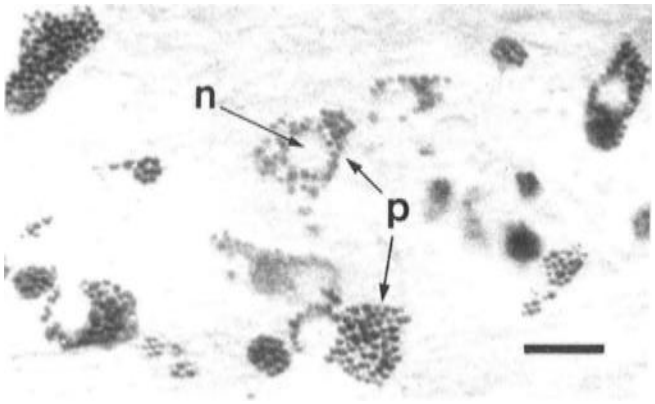

Figure 6.1 Membrane-bound clusters of pigment granules in the tunic of *E. purpuropunctatum*.

p = pigment granules, n = nucleus, scale bar = 10 μm. Adapted from Ref 7.

6.2. Materials

A portion of a paratype organism was obtained from the Smithsonian Institution National Museum of Natural History, Catalog No. 18663. The paratype material was collected by SCUBA from Turn Rock off the coast of Turn Island, Washington at 20 m deep by Ronald L. Shimek on July 20, 1986 and was deposited at the Smithsonian by 1989, preserved in ethanol.

Inductively Coupled Plasma Optical Emission Spectroscopy (ICP-OES) standards were prepared using Ti standard for ICP (1000 ppm from Fluka) Iron AA Standard (1000 ppm from Ricca Chemical Company) and iCAP 6000 Multi-Element Test Solution (1ppm Al, 1ppm Cu, 1ppm Mn, 0.2 ppm Ca, 0.2 ppm Mg, and 0.2 ppm Zn) from Thermo Scientific. All dilutions were performed using Barnstead NANOpure Diamond (18.2 MΩ-cm) water. Trace metal grade nitric acid was purchased from Fisher Scientific. ICP-OES data was obtained on an iCAP 7400 ICP-OES from Thermo Scientific, which has a limit of detection of 0.005 mg/L (0.005 ppm) for most elements.

Light microscopy was performed in the lab of Dr. Nicholas Davatzes in the Earth and Environmental Science Department. Scanning electron microscopy (SEM) and Energy-dispersive X-ray spectroscopy (EDX) were performed in the CoE-NIC facility at Temple University. The CoE-NIC is supported by a DoD DURIP Award N0014-12-1-0777 from the office of Naval Research and is sponsored by the College of Engineering at Temple University. SEM and EDX were performed using a FEI quanta FEG450 scanning electron microscope. Using EDX coupled to SEM, an electron beam was focused to a spot allowing for surface analysis using beam energy of a range of 10 keV equipped with K-alpha X-Ray source.

Laser Electrospray Mass Spectrometry (LEMS) was performed by Rachel Parise in the lab of Dr. Robert Levis.[9] HPLC grade solvents were used for electrospray ionization (ESI). Vaporization of the sample was performed using a Ti:sapphire laser with a wavelength centered at 810 nm, operating at 10Hz, a 70 fs pulse, a pulse power of 1.5 mJ and a spot size of about 100 μm.

6.3. Methods

Prior to specimen preparation for ICP-OES analysis, samples were removed from the specimen for analysis by SEM, LEMS, and other techniques. The remaining portion of the original specimen was lyophilized in the Schafmeister lab with help from Yanfeng Fan. The lyophilized ascidian sample (0.004 g) was digested in 4 mL of 50% trace metal grade nitric acid by refluxing overnight. Dilutions of the sample were prepared for analysis by ICP-OES: 3 mL of the digested sample was diluted to 5 mL (3:2 sample) and 1 mL of that dilution was diluted to 5 mL (1:4 sample). Five standards were prepared for ICP-OES; 0.005 ppm Al, 0.005 ppm Cu, 0.005 ppm Mn, 0.005 ppm Ti, 0.01 ppm Fe, and 0.05 ppm Zn (Std 1), 0.129 ppm Al, 0.129 ppm Cu, 0.129 ppm Mn, 0.129 ppm Ti, 0.133 ppm Fe, and 0.163 ppm Zn (Std 2), 0.253 ppm Al, 0.253 ppm Cu, 0.253 ppm Mn, 0.253 ppm Ti, 0.255 ppm Fe, and 0.276 ppm Zn (Std 3), 0.376 ppm Al, 0.376 ppm Cu, 0.376 ppm Mn, 0.376 ppm Ti, 0.378 ppm Fe, and 0.388 ppm Zn (Std 4), and 0.500 ppm Al, 0.500 ppm Cu, 0.500 ppm Mn, 0.500 ppm Ti, 0.500 ppm Fe, and 0.500 ppm Zn (Std 5). All glassware was demetalated by soaking in an acid bath and thoroughly rinsed with water.

Two small sample pieces (Sample 1 and Sample 2) were cut from the original specimen using a surgical scalpel. The samples were analyzed using reflective light microscopy, SEM, and EDX. Light microscopy images were taken of the sample pieces of the organism that were dried on SEM carbon grids. The light microscope images were used to identify and characterize areas with high and low concentrations of the dark purple/brown granules. Small regions within the areas classified by light microscopy

were then analyzed by SEM and EDX to identify elemental components of the selected regions.

From the original specimen, samples were cut to 150 μm thick using a microtome for analysis by LEMS. The microtomed samples were mounted on glass slides and stored at -80 °C and brought to room temperature for analysis. LEMS uses a nonresonant femtosecond laser to vaporize the sample combined with an ESI source to capture, ionize and transport the vaporized material into the vacuum chamber for analysis by time of flight mass spectrometry. This allows for molecular mapping of solid tissue samples with a resolution equivalent to that of the spot size of the focused laser. The mass spectrometer was operated in positive ion mode. The ESI needle was held at ground and the inlet capillary was held at -4.5 kV. The ESI needle was 3 mm above the sample stage, 5 mm in front of the capillary and the laser spot was 1mm in front of the electrospray source. ESI was performed using 1:1 methanol:water with 0.1% acetic acid with a flow rate of 0.3 μL/min using a syringe pump. The ESI plume was dried with an opposing nitrogen gas flow at 180 °C. The sample stage was biased to -2.0 kV. The specimen was mounted on a stainless steel slide using double stick tape and was vaporized orthogonal to the electrospray plume, where sample is captured in the electrospray droplets and ionized.

6.4. Results

Visual inspection of sample as received showed that the dispersed purple color was not present but rather large spots of purple/brown color (Figure 6.2). Light microscope analysis showed ~10 μm granules of purple/brown color are thinly distributed throughout the specimen along with large clusters of the 10 μm granules (Figure 6.3).

The results of ICP-OES analysis revealed concentrations of aluminum, titanium, and iron of 12000, 2000, and 11000 ppm dry weight, respectively. The concentrations of manganese, copper, and zinc were 130, 130, and 1800 ppm dry weight, respectively.

EDX of the selected smaller regions showed no detectable titanium elemental composition in either the high or low granule concentration spots. The selected regions were mainly comprised of carbon, nitrogen, sulfur, and oxygen, with minor contributions from sodium, calcium, silicon, and iron (Figure 6.16).

LEMS results do not show any protein m/z patterns, or titanium isotope signature. The only easily identifiable pattern is a polymer packet around 970 m/z (Figure 6.17).

Figure 6.2 Image of *Eudistoma purpuropunctatum* specimen received from Smithsonian Institution National Museum of Natural History.

Figure 6.3 Clustering of purple/brown granules (red) and disperse purple/brown granules in tunic (blue).

Table 6.1 *E. purpuropunctatum ICP-OES results as measured.*

Standards and sample dilution results (sample 3:2 and 1:4) reported in ppm (mg/L).

Sample	Al	Ti	Mn	Fe	Cu	Zn
Std 1	-0.015	0.006	0.005	0.008	0.003	0.050
Std 2	0.118	0.131	0.132	0.131	0.132	0.159
Std 3	0.248	0.253	0.254	0.251	0.256	0.274
Std 4	0.377	0.382	0.377	0.385	0.377	0.389
Std 5	0.505	0.495	0.498	0.498	0.498	0.502
3:2	5.590	1.122	0.067	5.655	0.062	0.623
1:4	1.644	0.226	0.015	1.214	0.015	0.208

Table 6.2 *E. purpuropunctatum ICP-OES dilution results (sample 3:2 and 1:4) reported in ppm (mg/kg dry weight)*.

Sample	Al	Ti	Mn	Fe	Cu	Zn
3:2	9800	2000	110	10000	110	1100
1:4	14000	2000	130	11000	130	1800

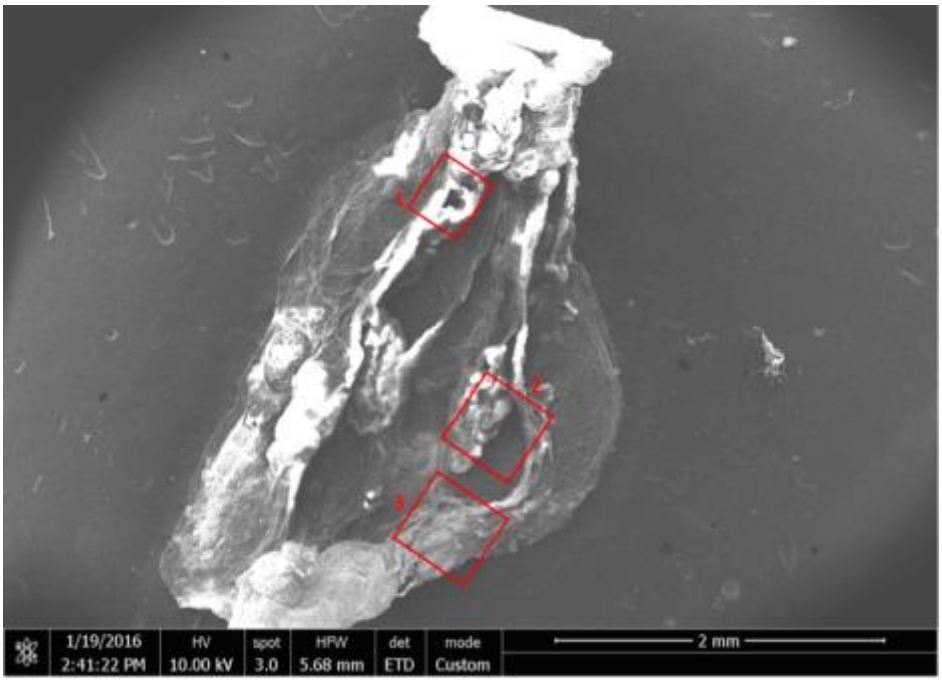

Figure 6.4 SEM image *E. purpuropunctatum* Sample 1 showing relation of Areas 1-3 analyzed by EDX.

Figure 6.5 Light microscope image of Sample 1 at 40x magnification showing approximate locations of Area 1 highlighted in red and spots analyzed by EDX in green.

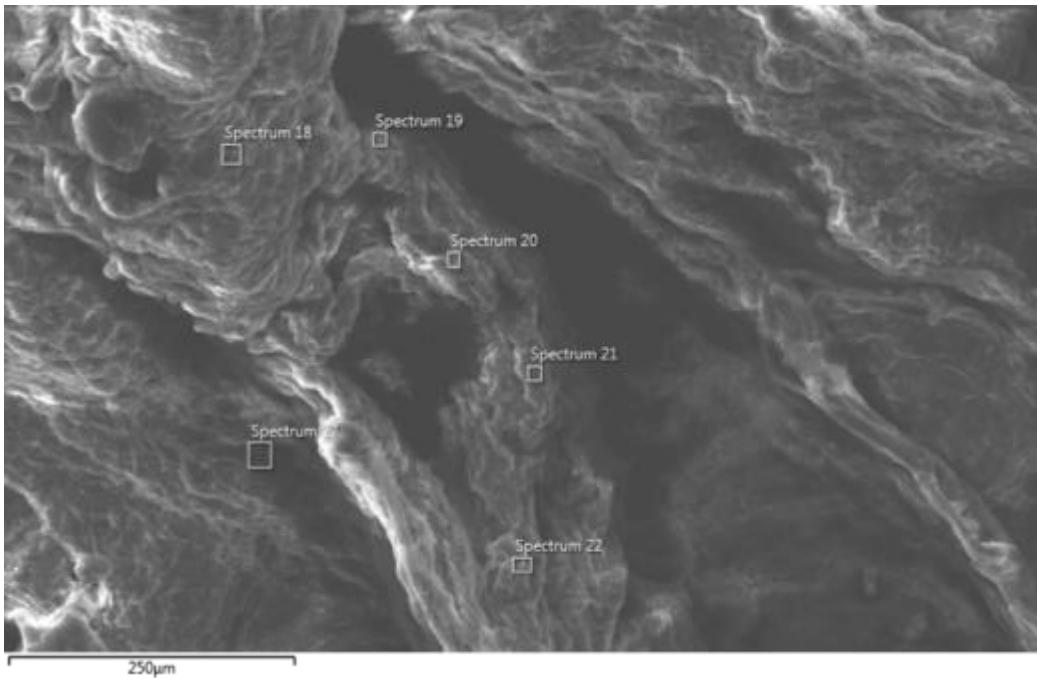

Figure 6.6 SEM image of Sample 1, Area 1 showing spots analyzed by EDX.

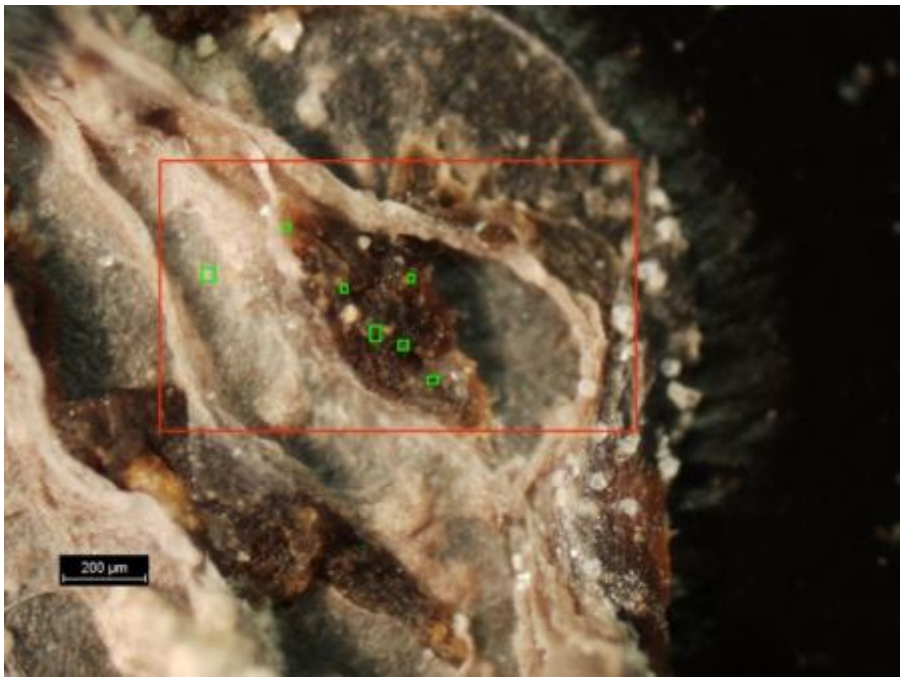

Figure 6.7 Light microscope image of Sample 1 at 40x magnification showing approximate locations of Area 2 highlighted in red and spots analyzed by EDX in green.

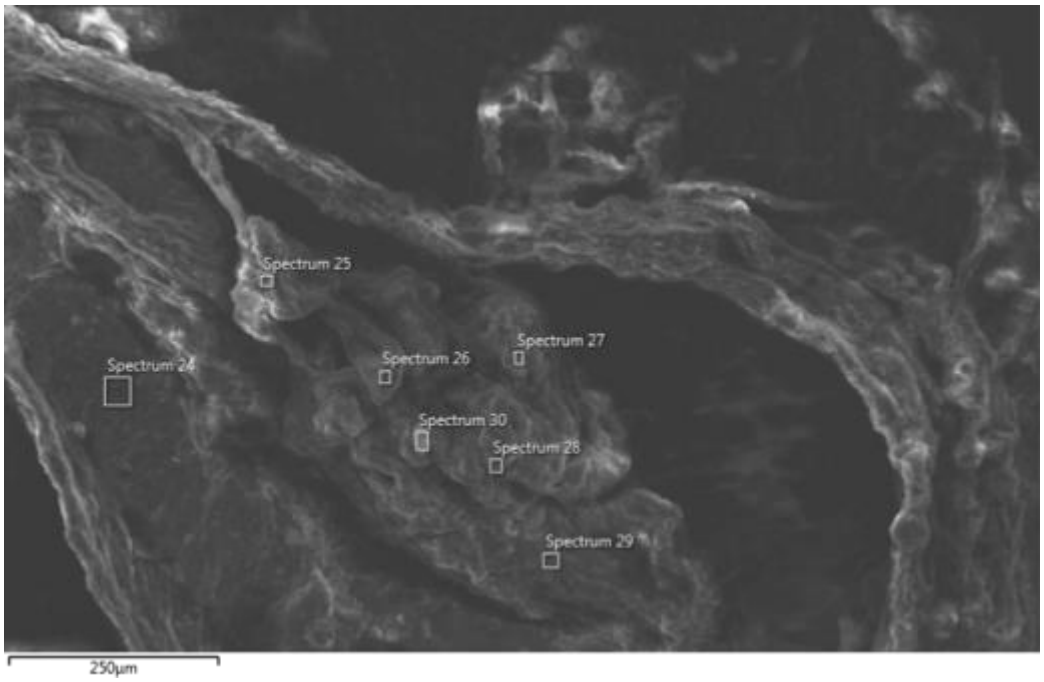

Figure 6.8 SEM image of Sample 1, Area 2 showing spots analyzed by EDX.

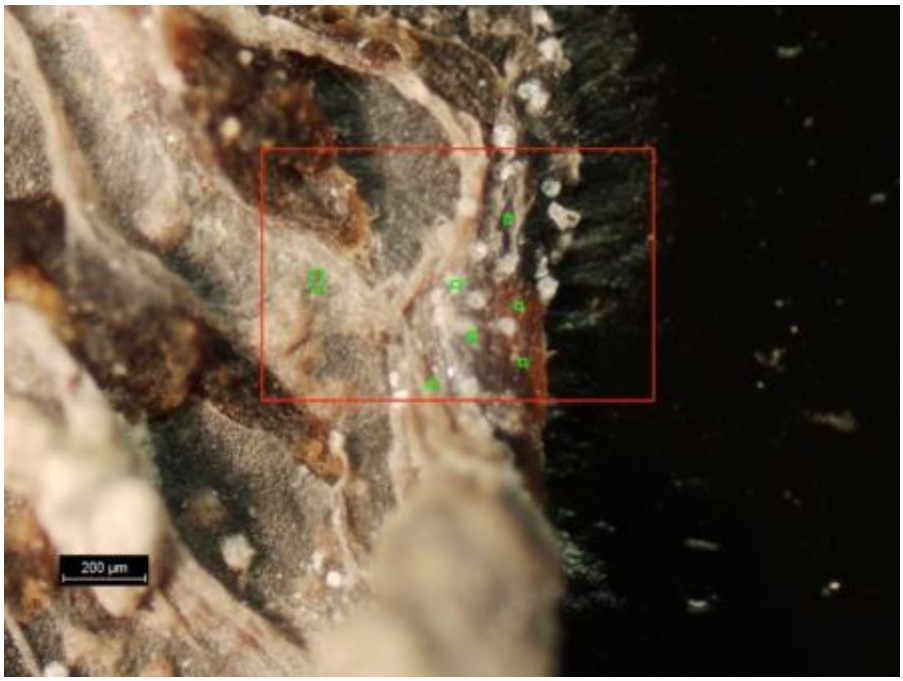

Figure 6.9 Light microscope image of Sample 1 at 40x magnification showing approximate locations of Area 3 highlighted in red and spots analyzed by EDX in green.

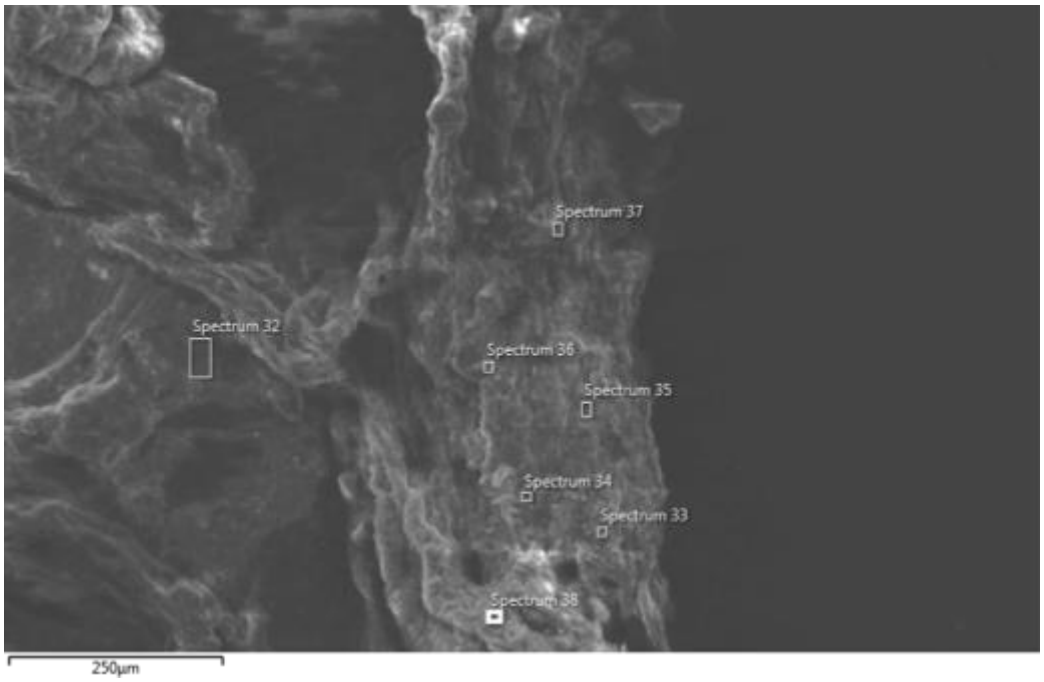

Figure 6.10 SEM image of Sample 1, Area 3 showing spots analyzed by EDX.

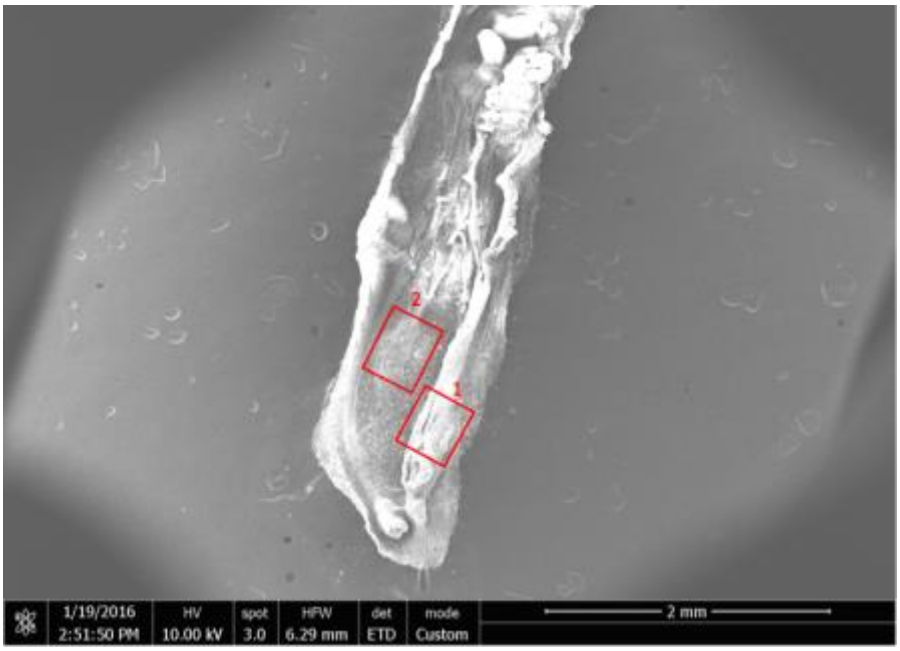

Figure 6.11 SEM image *E. purpuropunctatum* Sample 2 showing relation of Areas 1 and 2 analyzed by EDX.

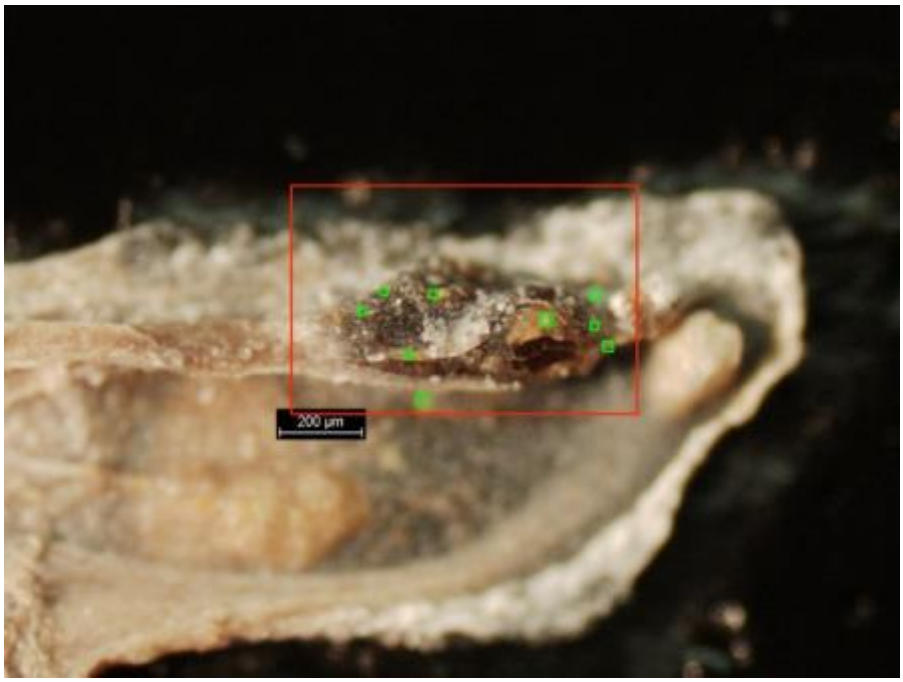

Figure 6.12 Light microscope image of Sample 2 at 40x magnification showing approximate locations of Area 1 highlighted in red and spots analyzed by EDX in green.

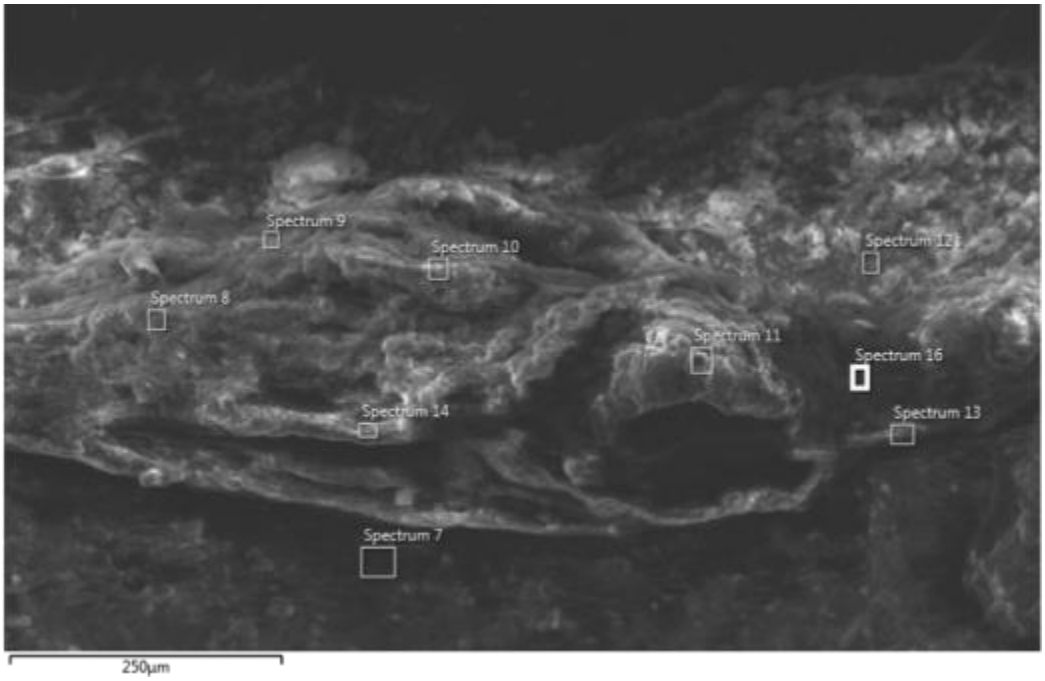

Figure 6.13 SEM image of Sample 2, Area 1 showing spots analyzed by EDX.

Figure 6.14 Light microscope image of Sample 2 at 40x magnification showing approximate locations of Area 2 highlighted in red and spots analyzed by EDX in green.

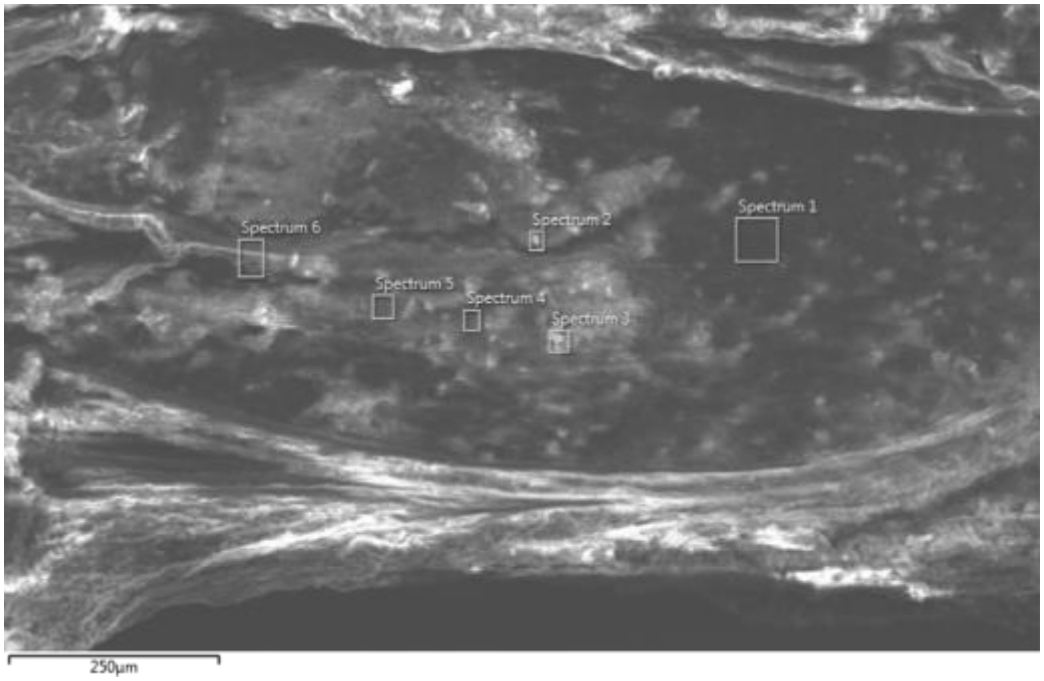

Figure 6.15 SEM image of Sample 2, Area 2 showing spots analyzed by EDX.

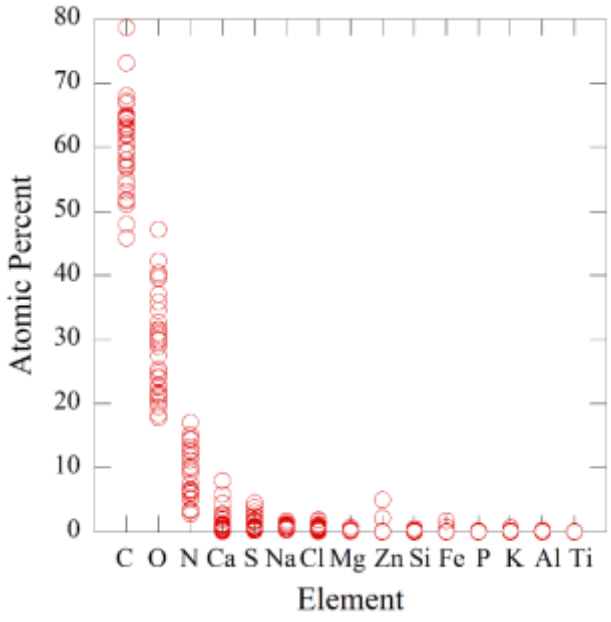

Figure 6.16 Table of atomic percent of each element detected at all spots analyzed by EDX.

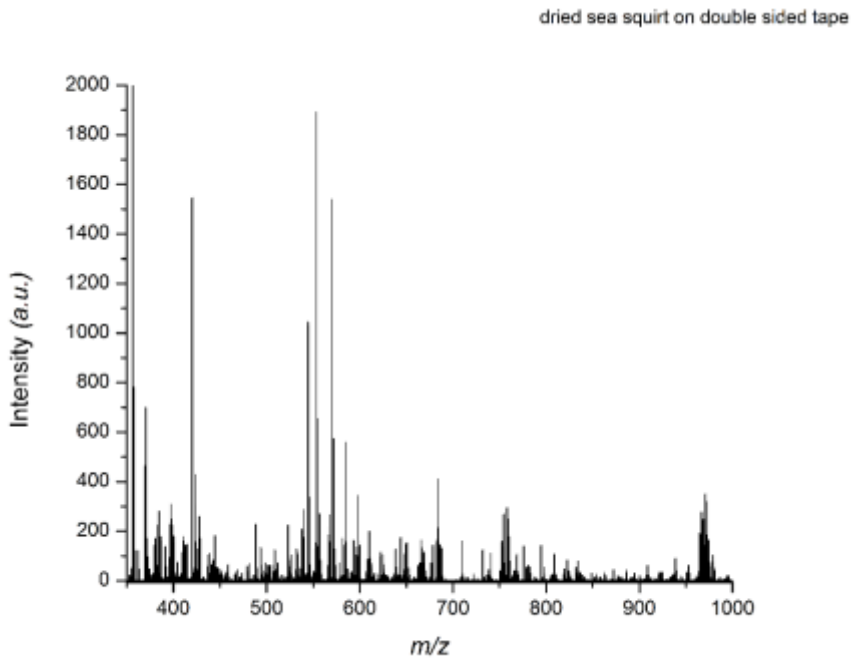

Figure 6.17 LEMS mass spectrum of *E. purpuropunctatum*.

6.5. Discussion

The specimen, as received, may have altered during its approximately 30 year-long storage as it no longer had its characteristic dispersed purple color due to 10 μm granule clusters (Figure 6.2). The specimen appeared to have clusters of large, approximately 1 mm in greatest diameter, particles of a purple/brown color. Examination by light microscopy showed that the visible purple/brown clusters could be aggregates of the initially described dispersed purple granules on the ascidian body. Small granules of purple/brown color that match the initially described 10 μm size can also be observed dispersed throughout the tissue (Figure 6.3). It is unclear to what extent long-term storage affected this specimen. The aggregation of the purple granules could be an effect of this storage or may be part of the specimens' original physiology. In the original description

of *E. purpuropunctatum*, it was stated that not all areas of the specimen might have dispersed purple color. Some areas of the specimen tunic were grayish white in color but in highly colored colonies the purple color was clustered on the body of the organisms. The grayish/white color of the tunic in our sample would suggest that our sample came from an area lacking in pigment, but what may possibly be the clustering of pigment on the zooid bodies would indicate that our sample was once highly colored. It is possible that our sample was of moderate coloration and the granules clustered due to the conditions of its long-term storage. Alternatively, the granules may have migrated out of the tunic but remained associated with the zooid body in the preserved sample, but the ethanol the specimen was preserved in showed no signs of granules.

ICP-OES analysis showed aluminum, iron, titanium, zinc, manganese and copper in decreasing abundance. The unexpectedly high aluminum and iron concentrations, 12000 ppm and 11000 ppm respectively, are unreliable as the measured sample concentrations were above the standard curve, but ascidians have been known to concentrate iron.[4, 10] It is possible that the purple color comes from an aluminum mineral. Aluminum minerals by themselves are colorless, but gem stones like sapphires are aluminum oxides with titanium and iron dopants. The titanium concentration is also unexpectedly high, 2000 ppm, present on the same order of magnitude as zinc. Assuming the organism is 90% water the concentrations in the whole organism would be 1200 ppm aluminum, 200 ppm titanium, and 1100 ppm iron. The reason for the high concentration of these metals is indeterminate. There may be error due to the small, 0.004 mg sample size or possible contamination. Without water from the area and time in which the sample was collected, it is impossible to know the extent of the concentration.

The EDX results indicate that the purple granules do not get their coloration from a titanium, or aluminum containing granule. It does not appear that the granules contain much of any inorganic element. Regions with both high and low granule concentrations show similar elemental compositions with no noticeable and consistent change in element abundance. This result is interpreted to mean that the purple granules are of organic composition.

LEMS results also show no difference between areas of high and low granule concentration. Any m/z detected does not display a titanium isotope pattern. The peaks detected at around 970 m/z appear to be a polymer and are likely from the double stick tape used to hold the sample in place.

The chemical composition of the purple granules remains unknown. All of the sample was used for ICP-OES analysis but showed unusually high concentrations of aluminum and titanium. EDX results seem to indicate that the granules are organic in nature and LEMS results provided little insight. EDX shows 6 spots with aluminum content out of a total of 36 spots analyzed. A total of 20 spots analyzed by EDX were focused on clusters of the purple granules. It is possible that EDX is not a sensitive enough technique to detect the relatively low metal content within the organic framework of the organism. However, if the metal were evenly distributed it should be detectable. This means that the metals are likely localized in areas we did not look. The ICP-OES results also show that *E. purpuropunctatum* sequesters as much if not more titanium than *E. ritteri*.

This work shows that *Eudistoma purpuropunctatum* sequesters high amounts of titanium, even more than *Eudistoma ritteri*. *E. purpuropunctatum* also sequesters an

unexpectedly high amount of iron and aluminum. With the possible caveat of the small available sample size the source of the concentrations of these ions is a mystery. SEM/EDX and LEMS analysis did not identify the environment of titanium, iron, or aluminum. Both of these species should be considered for further studies on titanium sequestration but *E. purpuropunctatum* is hard to retrieve from the environment and may not be amenable to culture.

If more of the *Eudistoma purpuropunctatum* sample could be obtained, the best path forward would be to carefully excise the granules with as little surrounding tissue as possible, and analysis by LC-MS, and NMR. Analysis of a whole organism by synchrotron radiation would allow for elemental mapping of the specimen. A new specimen would be considered best circumstance for future analysis. These results are promising that *E. purpuropunctatum* may sequester high amount of titanium, among other elements, but more work is necessary for them to be confirmed.

REFERENCES CITED

1. D. B. Carlisle, Vanadium and other Metals in Ascidians, *Proceedings of the Royal Society Series B-Biological Sciences*, 1968, **171**, 31.
2. M. J. Smith, D. E. Ryan, K. Nakanishi, P. Frank and K. O. Hodgson, Vanadium in Ascidians and the Chemistry of Tunichromes, *Metal Ions in Biological Systems, Vol 31: Vanadium and Its Role in Life*, 1995, **31**, 423-490.
3. J. P. Gaffney and A. M. Valentine, The challenges of trafficking hydrolysis prone metals and ascidians as an archetype, *Dalton Transactions*, 2011, **40**, 5827-5835.
4. C. Papadopoulou and G. D. Kanias, Tunicate Species as Marine Pollution Indicators, *Marine Pollution Bulletin*, 1977, **8**, 229-231.
5. E. P. Levine, Occurrence of Titanium, Vanadium, Chromium, and Sulfuric Acid in Ascidian Eudistoma Ritteri, *Science*, 1961, **133**, 1352-1353.
6. E. P. Levine, Studies on the structure, reproduction, development and accumulation of metals in the colonial ascidian *Eudistoma ritteri* Van Name, 1945, *Journal of Morphology*, 1962, 105-137.
7. J. H. Swinehart, W. R. Biggs, D. J. Halko and N. C. Schroeder, Vanadium and Selected Metal Contents of some Ascidians, *Biological Bulletin*, 1974, **146**, 302-312.
8. G. Lambert, A New Species of the Compound Ascidian Eudistoma (Ascidiacea, Polycitoridae) from the Northeastern Pacific, *Canadian Journal of Zoology-Revue Canadienne De Zoologie*, 1989, **67**, 2700-2703.
9. E. J. Judge, J. J. Brady and R. J. Levis, Mass Analysis of Biological Macromolecules at Atmospheric Pressure Using Nonresonant Femtosecond Laser

Vaporization and Electrospray Ionization, *Analytical Chemistry*, 2010, **82**, 10203-10207.

10. J. E. Stacey and W. R. Driedzic, Temporal variability in, and impact of food availability on vanadium and iron concentrations in Ciona intestinalis tissues (Tunicata, Ascidiacea), *Journal of Experimental Marine Biology and Ecology*, 2010, **386**, 11-18.

APPENDIX A ATOMIC PERCENTAGES OF SPOTS ANALYZED BY EDX

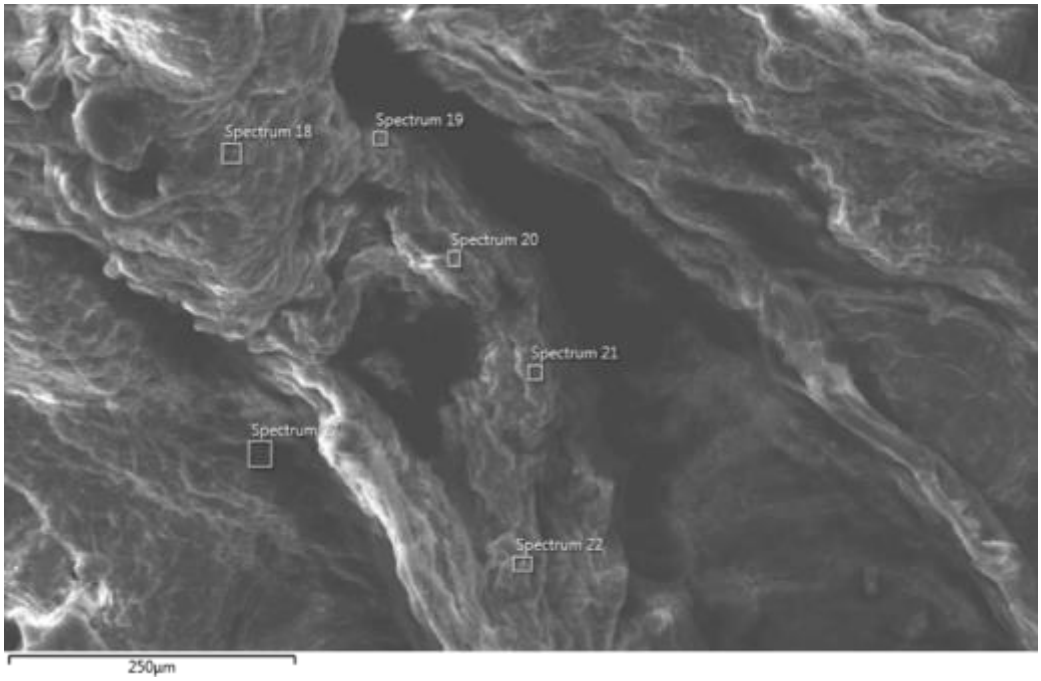

Figure 6.18 Sample 1, Area 1 SEM showing spots analyzed by EDX.

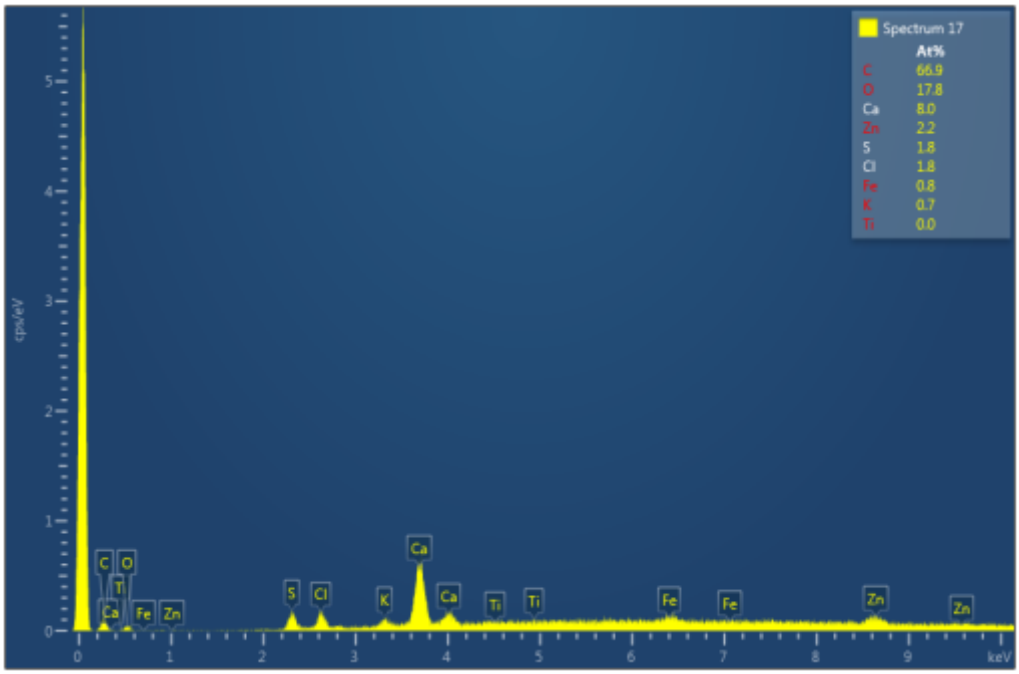

Figure 6.19 Sample 1, Area 1, Spot 17 EDX atomic percentage.

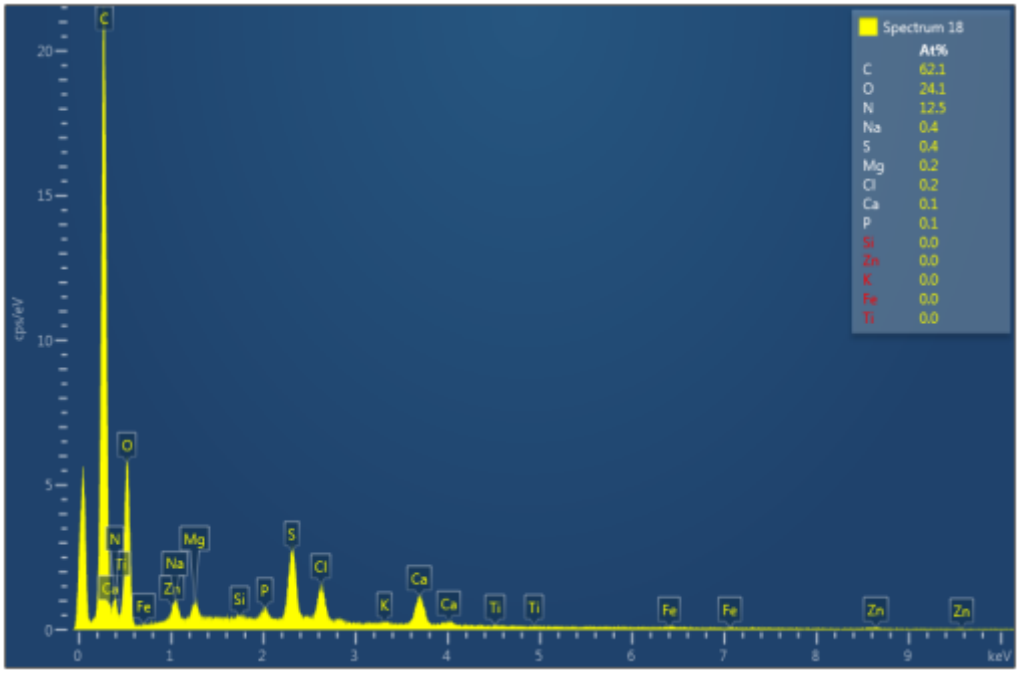

Figure 6.20 Sample 1, Area 1, Spot 18 EDX atomic percentage.

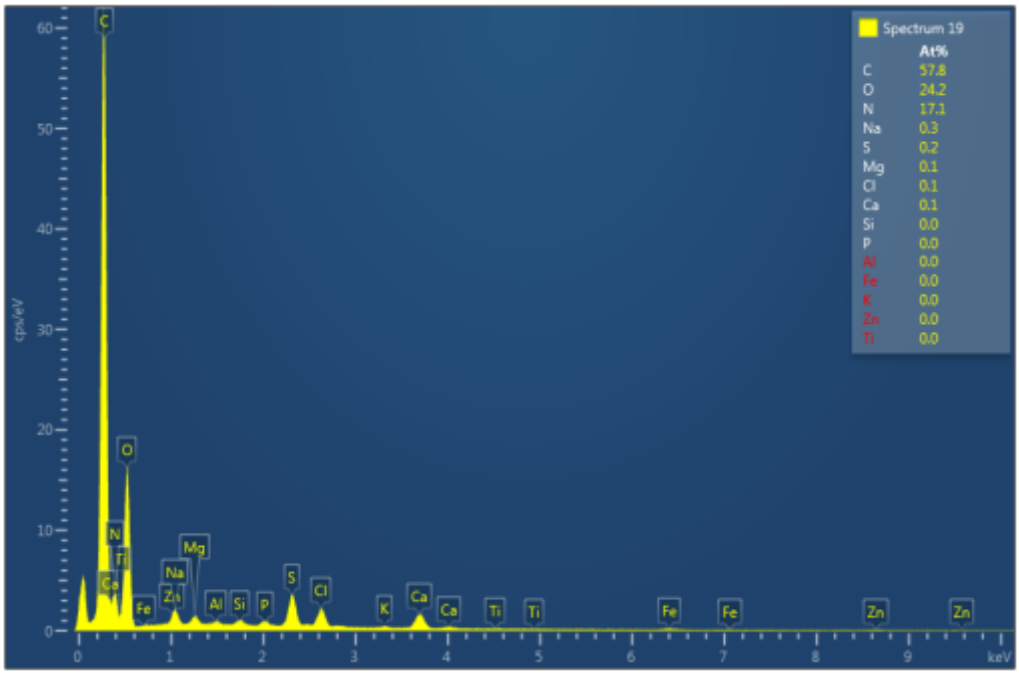

Figure 6.21 Sample 1, Area 1, Spot 19 EDX atomic percentage.

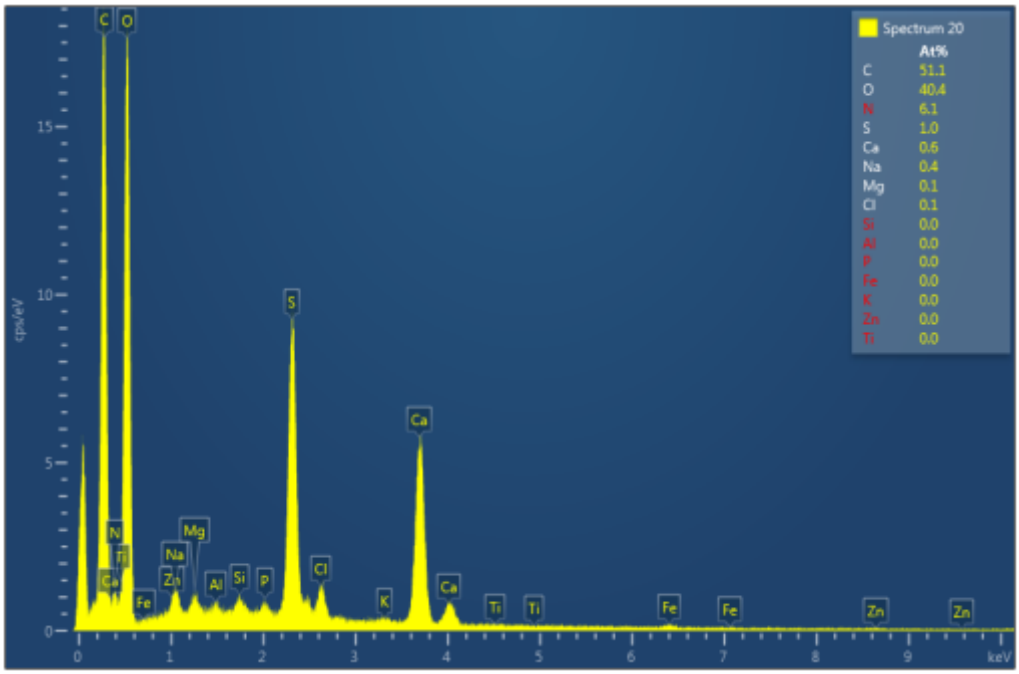

Figure 6.22 Sample 1, Area 1, Spot 20 EDX atomic percentage.

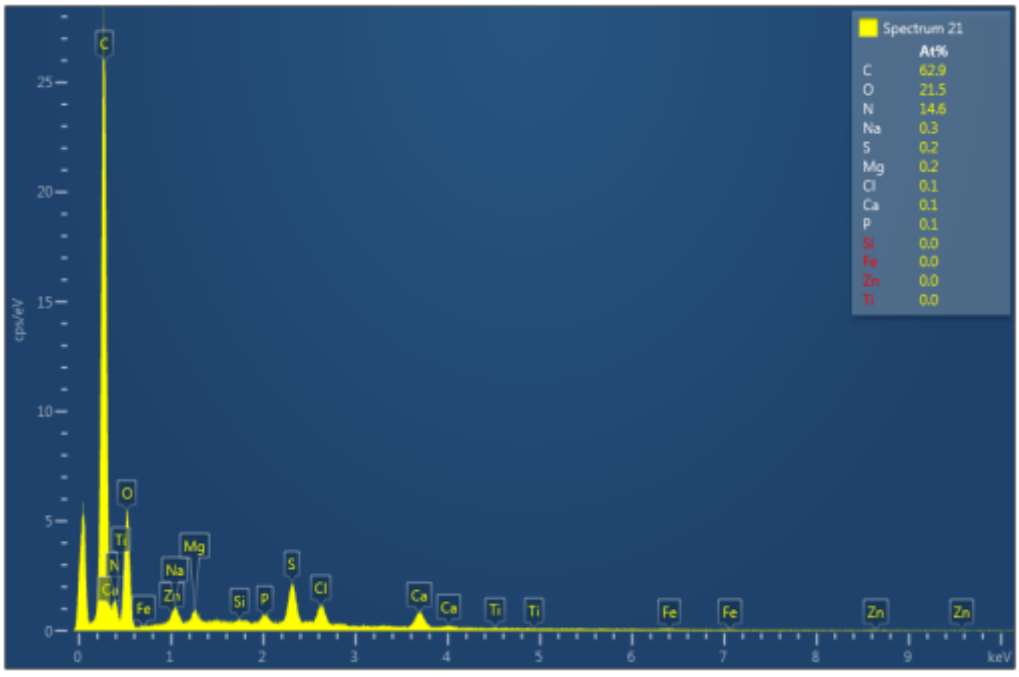

Figure 6.23 Sample 1, Area 1, Spot 21 EDX atomic percentage.

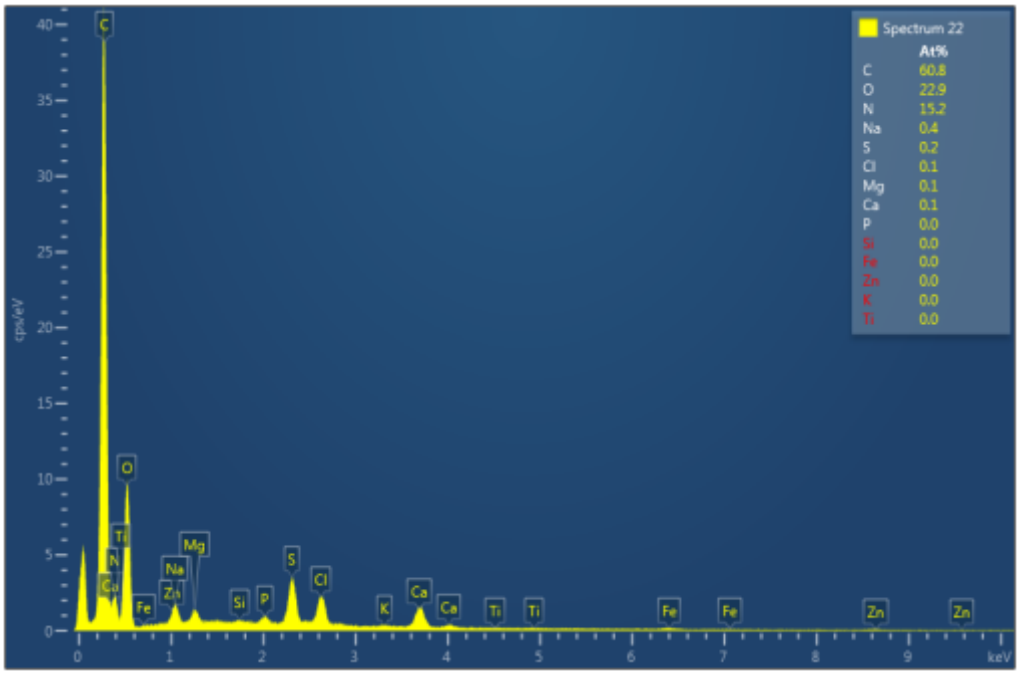

Figure 6.24 Sample 1, Area 1, Spot 22 EDX atomic percentage.

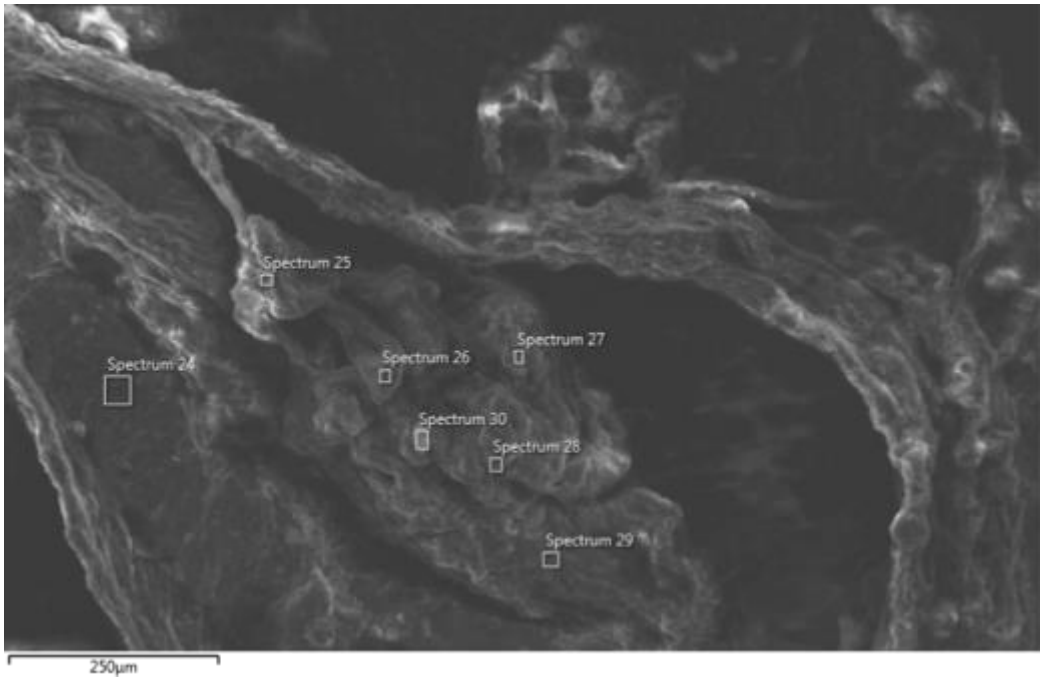

Figure 6.25 Sample 1, Area 1 SEM showing spots analyzed by EDX.

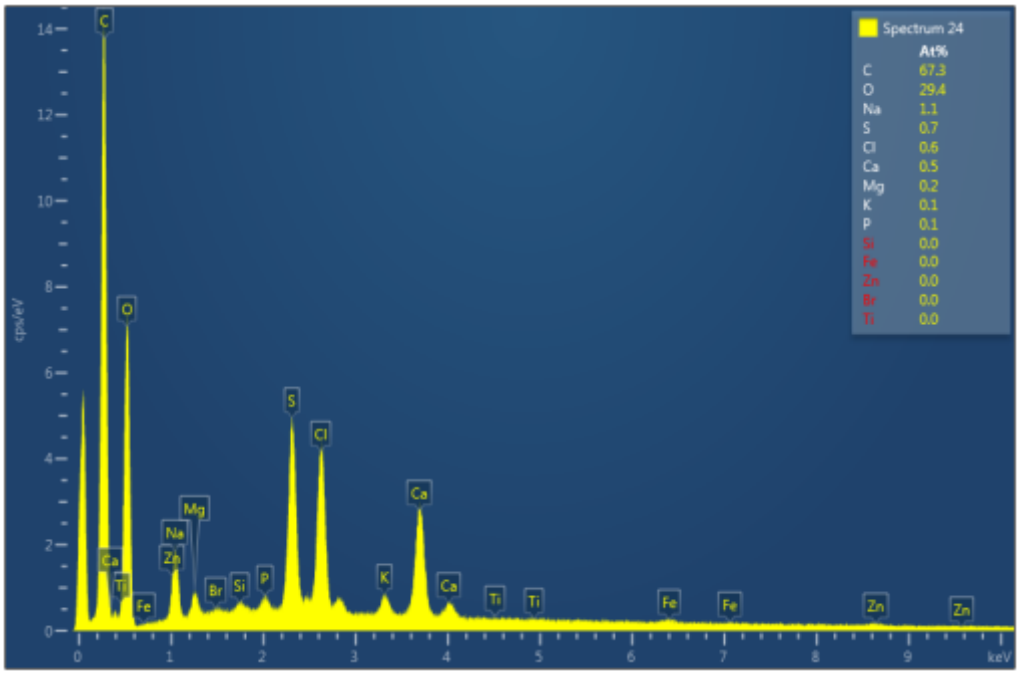

Figure 6.26 Sample 1, Area 2, Spot 24 EDX atomic percentage.

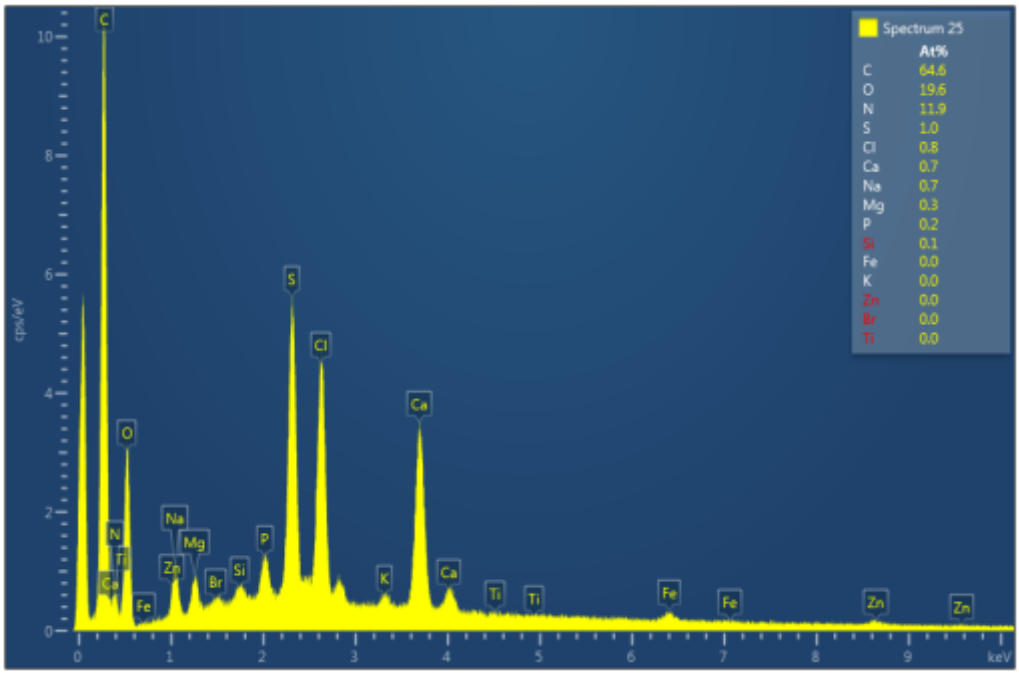

Figure 6.27 Sample 1, Area 2, Spot 25 EDX atomic percentage.

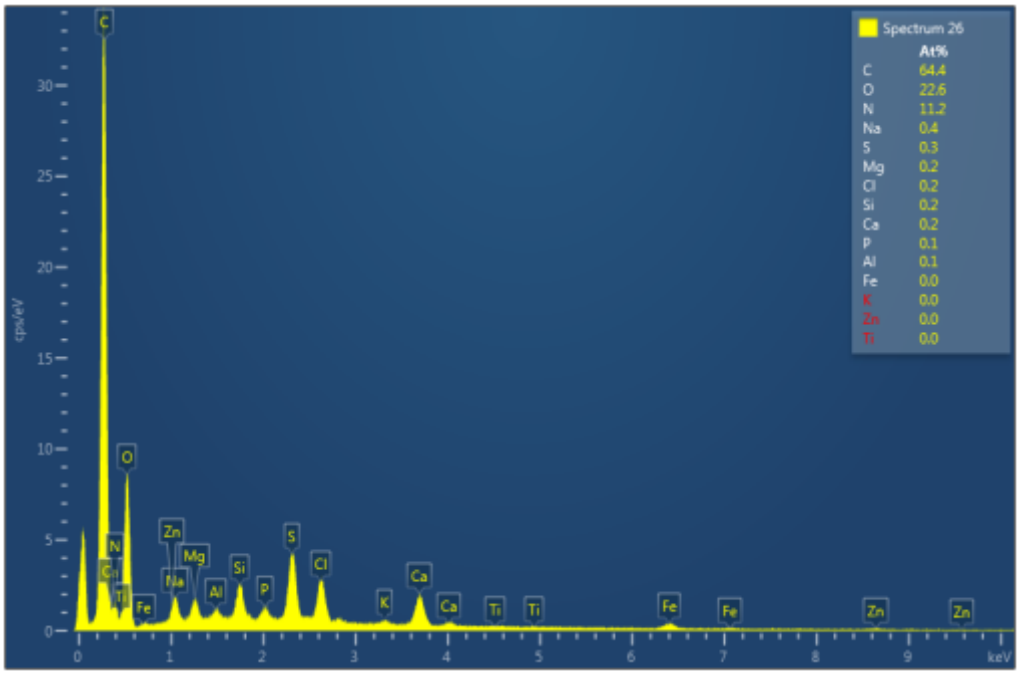

Figure 6.28 Sample 1, Area 2, Spot 26 EDX atomic percentage.

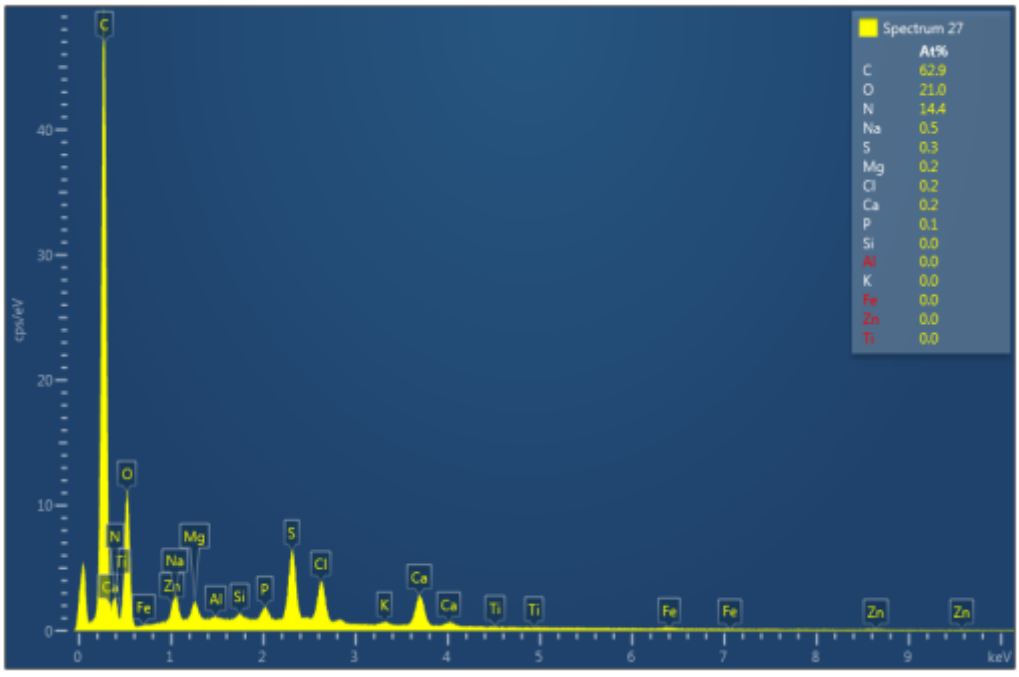

Figure 6.29 Sample 1, Area 2, Spot 27 EDX atomic percentage.

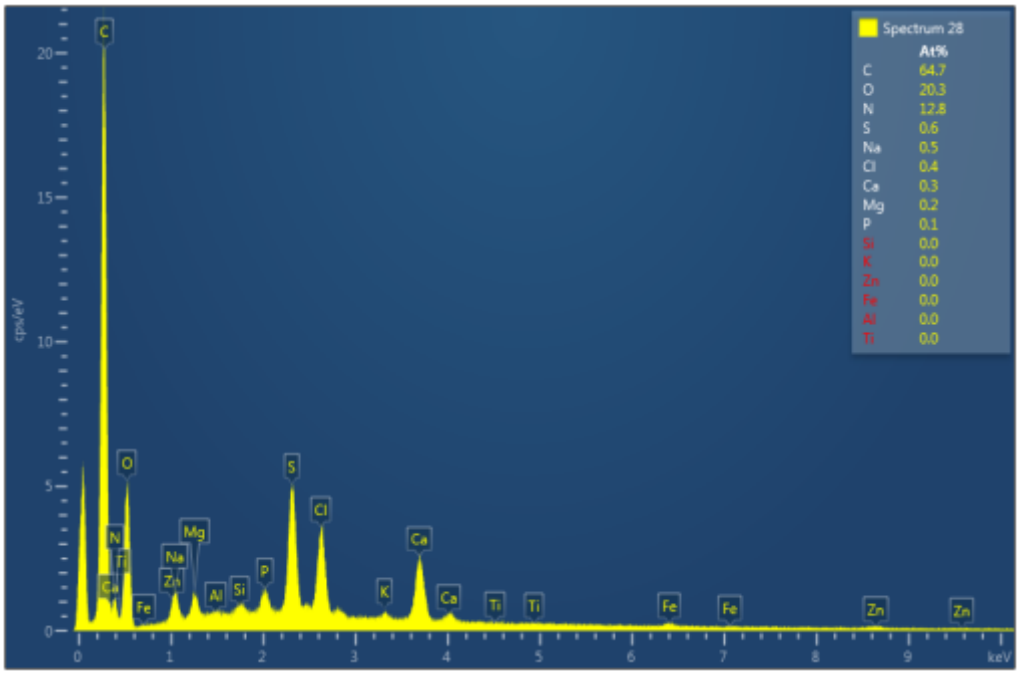

Figure 6.30 Sample 1, Area 2, Spot 28 EDX atomic percentage.

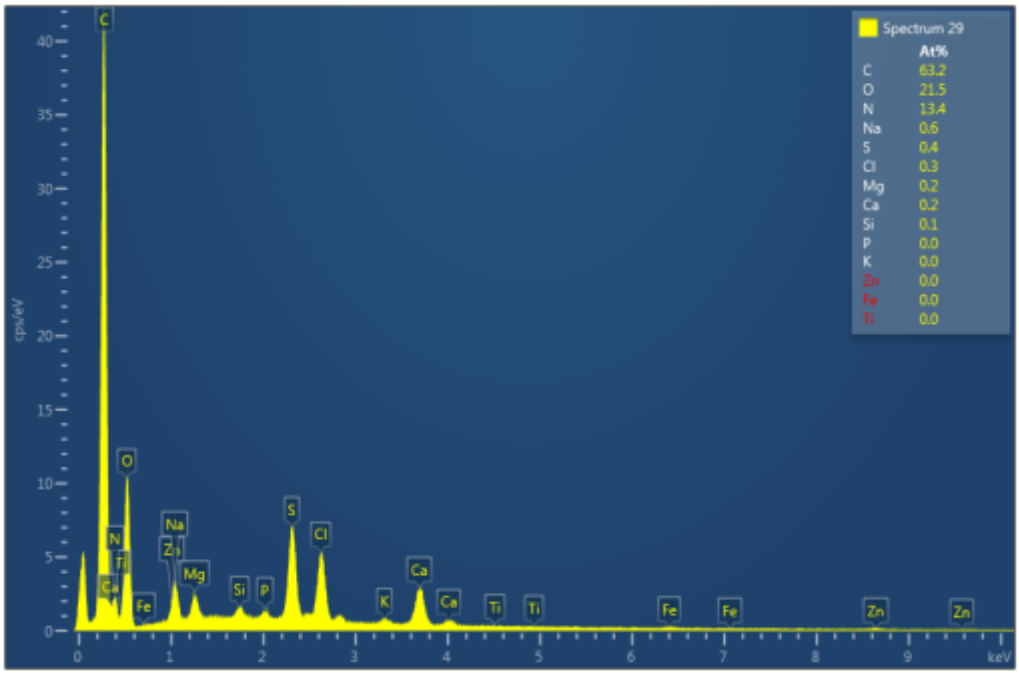

Figure 6.31 Sample 1, Area 2, Spot 29 EDX atomic percentage.

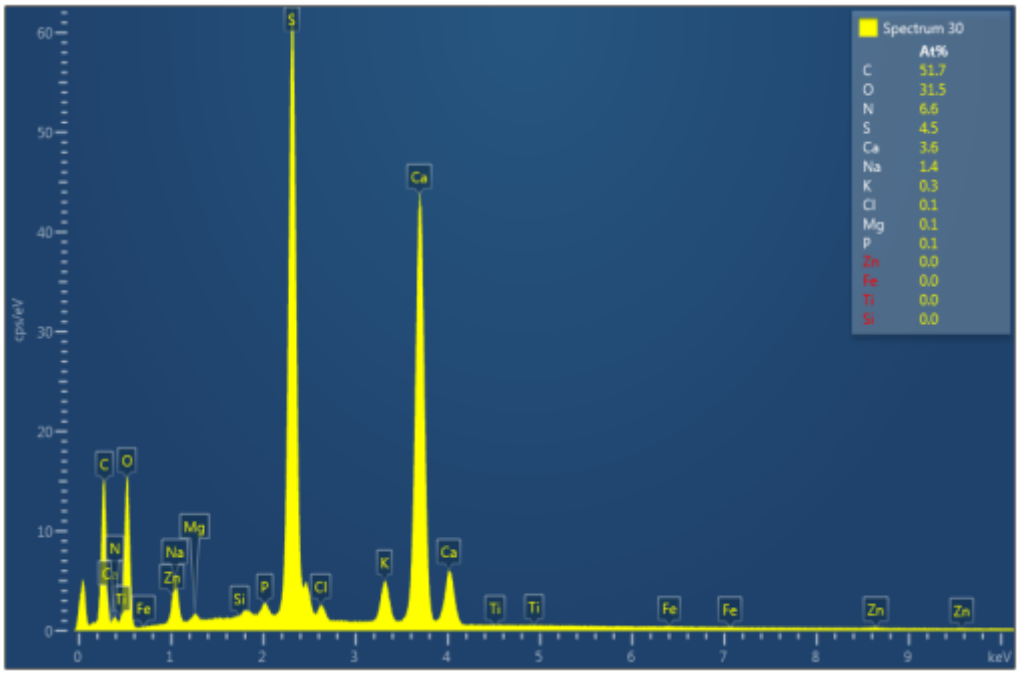

Figure 6.32 Sample 1, Area 2, Spot 30 EDX atomic percentage.

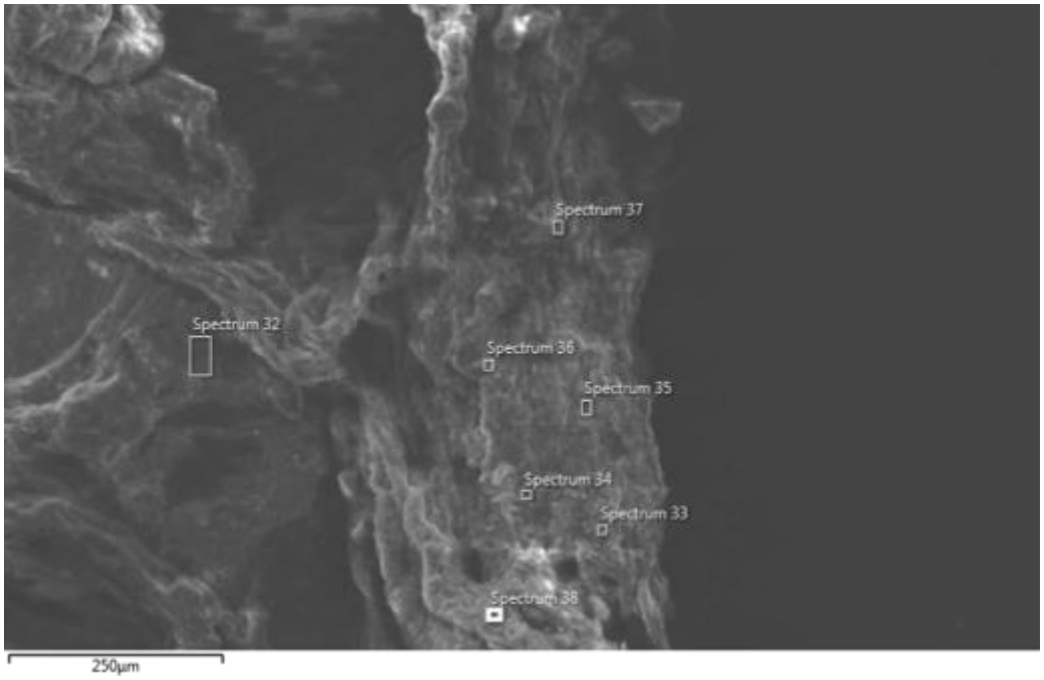

Figure 6.33 Sample 1, Area 3 SEM showing spots analyzed by EDX.

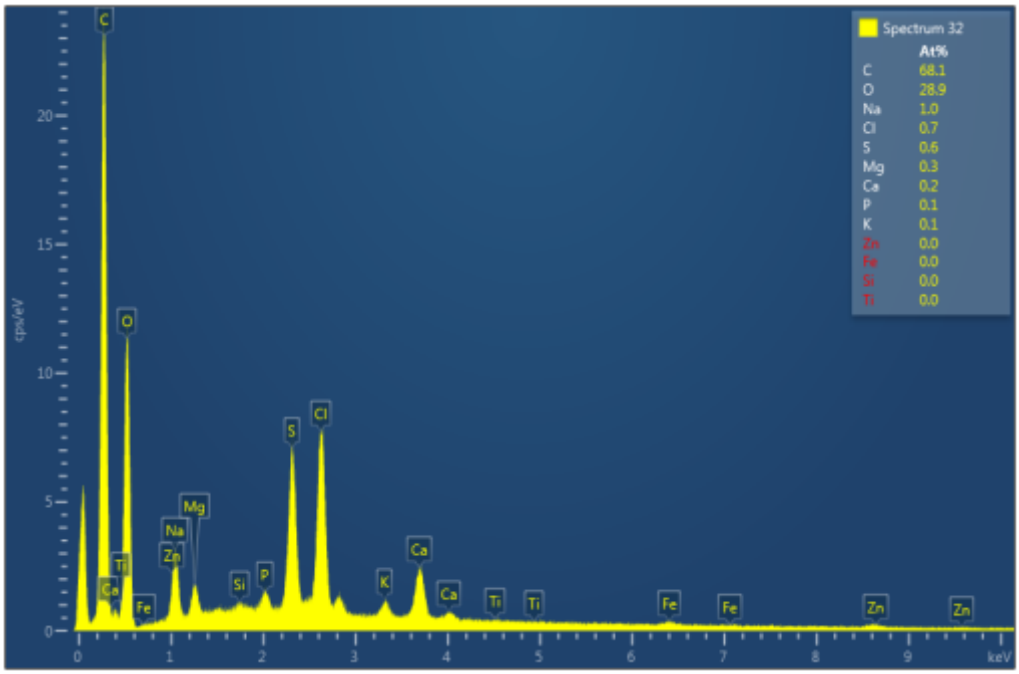

Figure 6.34 Sample 1, Area 3, Spot 32 EDX atomic percentage.

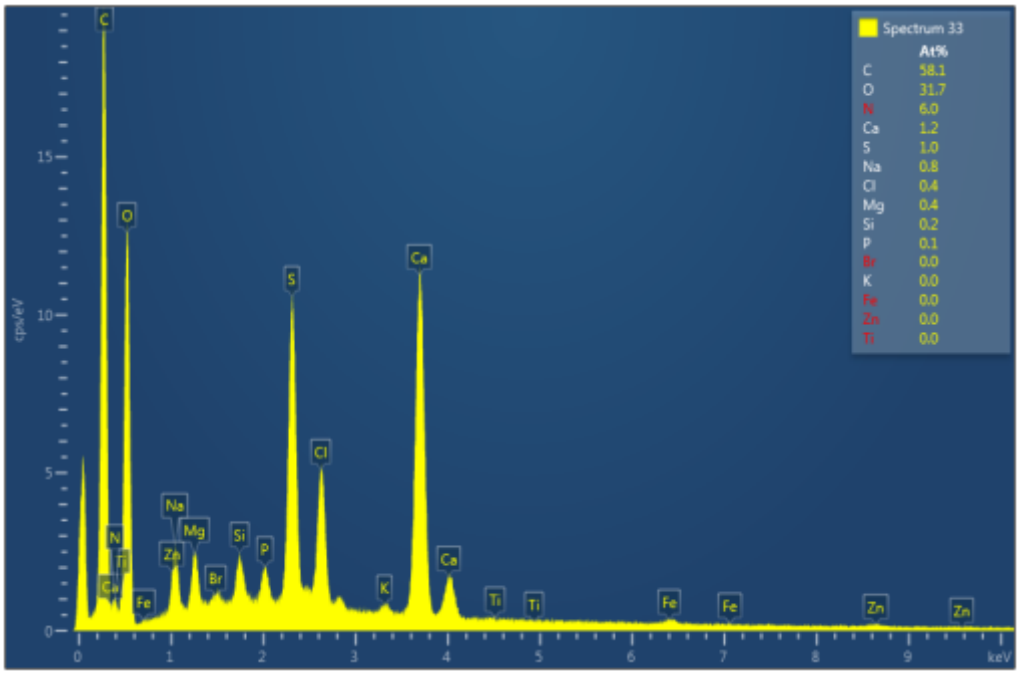

Figure 6.35 Sample 1, Area 3, Spot 33 EDX atomic percentage.

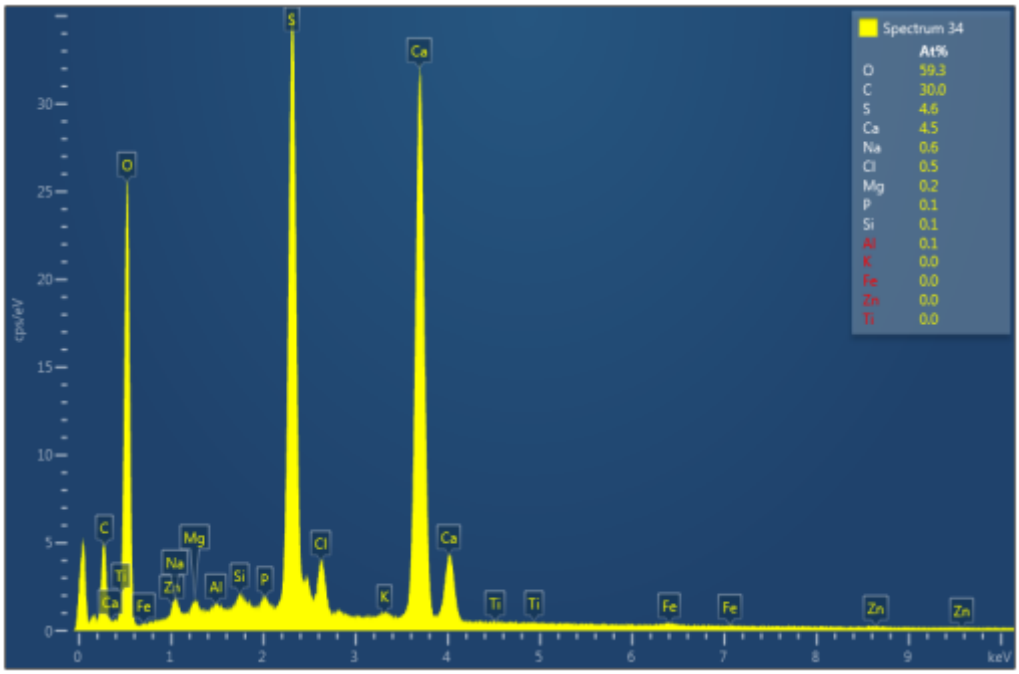

Figure 6.36 Sample 1, Area 3, Spot 34 EDX atomic percentage.

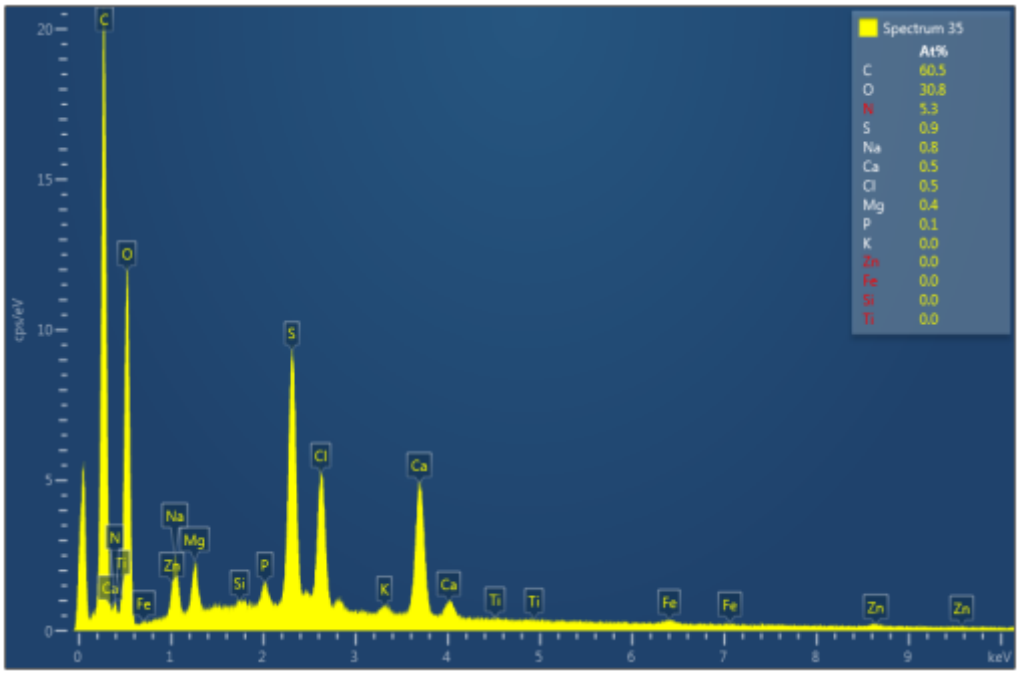

Figure 6.37 Sample 1, Area 3, Spot 35 EDX atomic percentage.

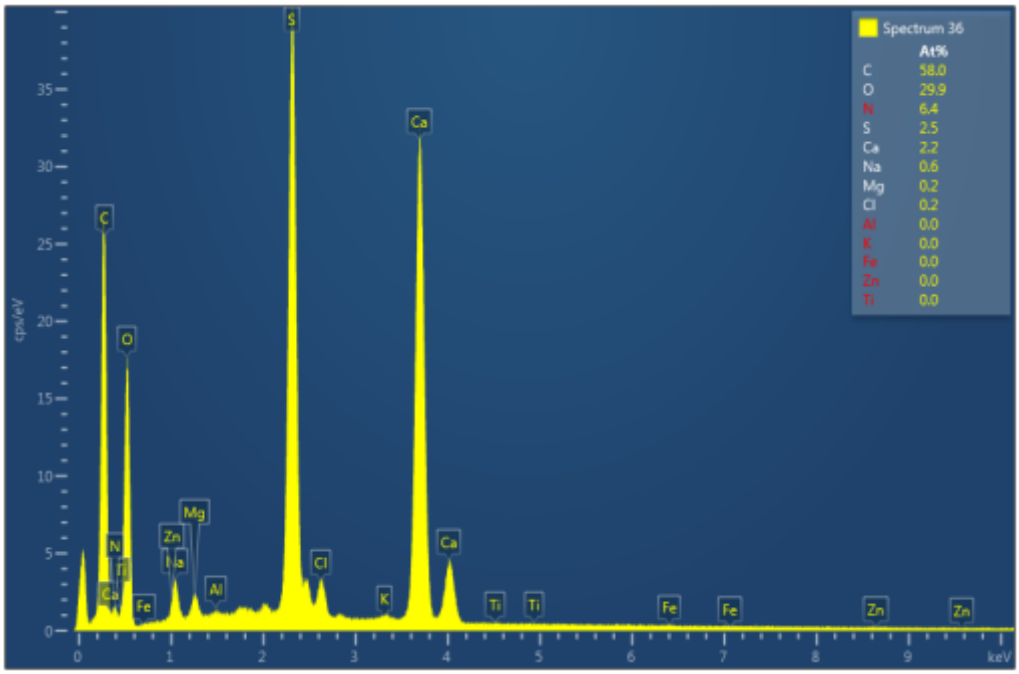

Figure 6.38 Sample 1, Area 3, Spot 36 EDX atomic percentage.

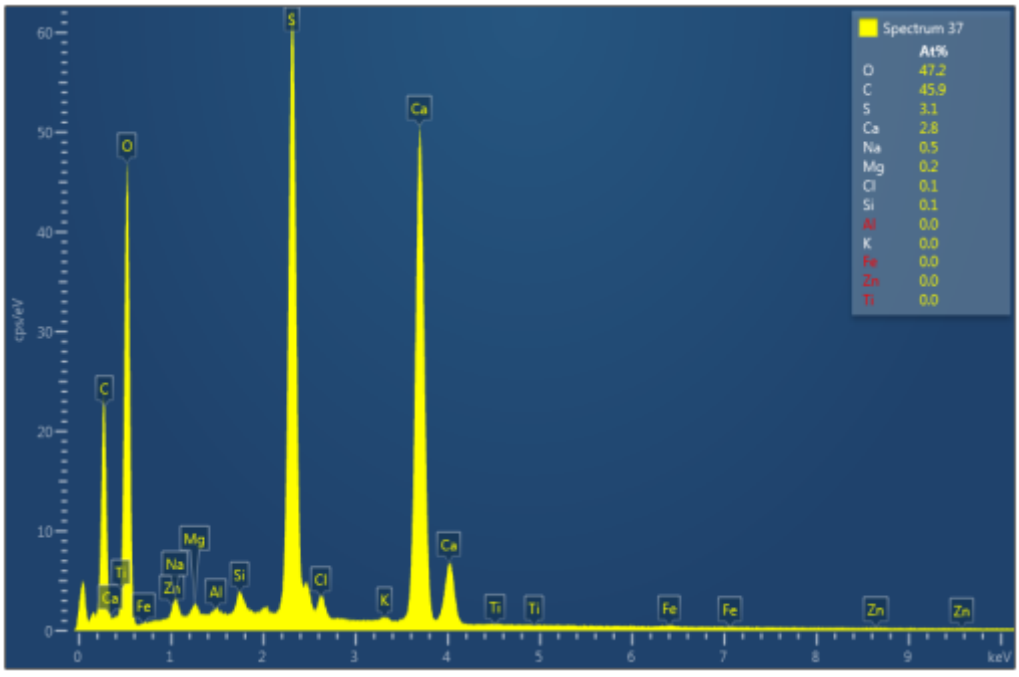

Figure 6.39 Sample 1, Area 3, Spot 37 EDX atomic percentage.

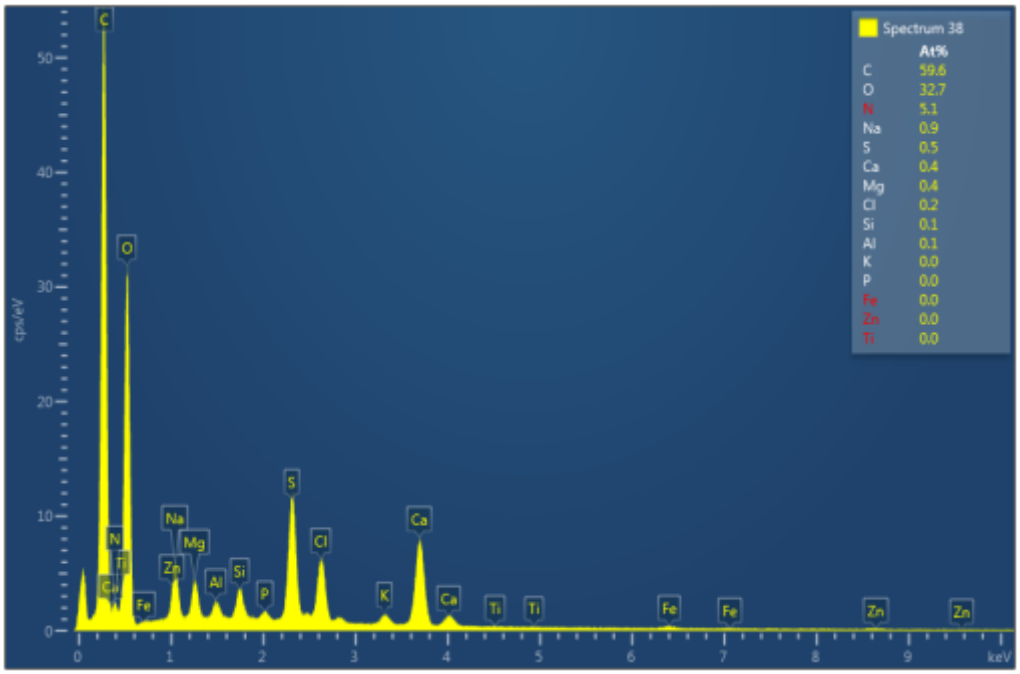

Figure 6.40 Sample 1, Area 3, Spot 38 EDX atomic percentage.

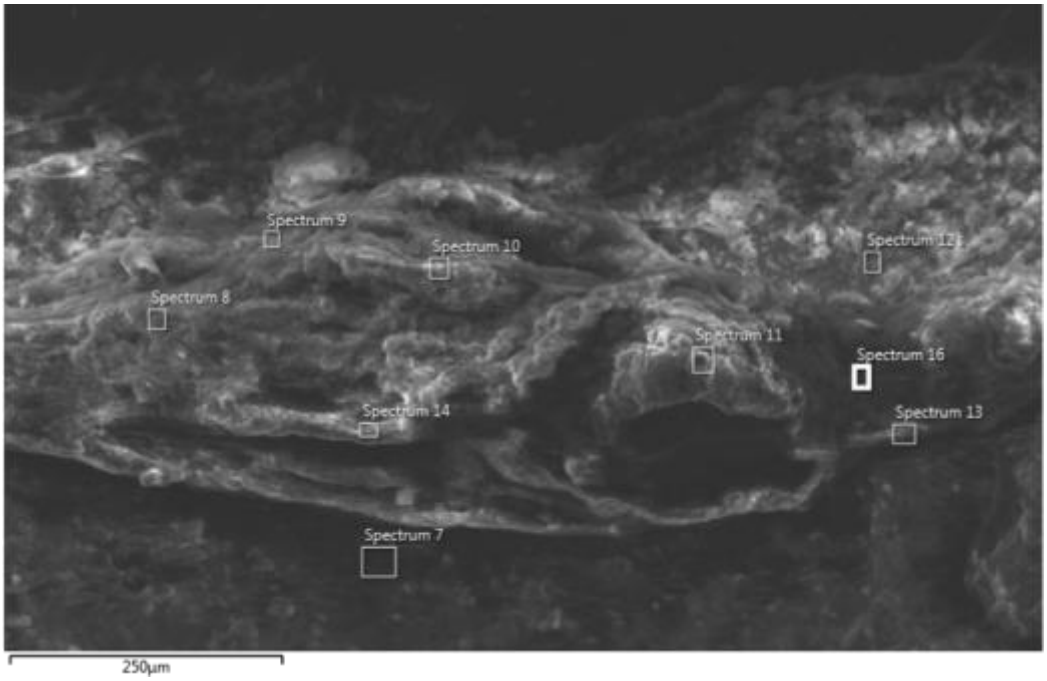

Figure 6.41 Sample 2, Area 1 SEM showing spots analyzed by EDX.

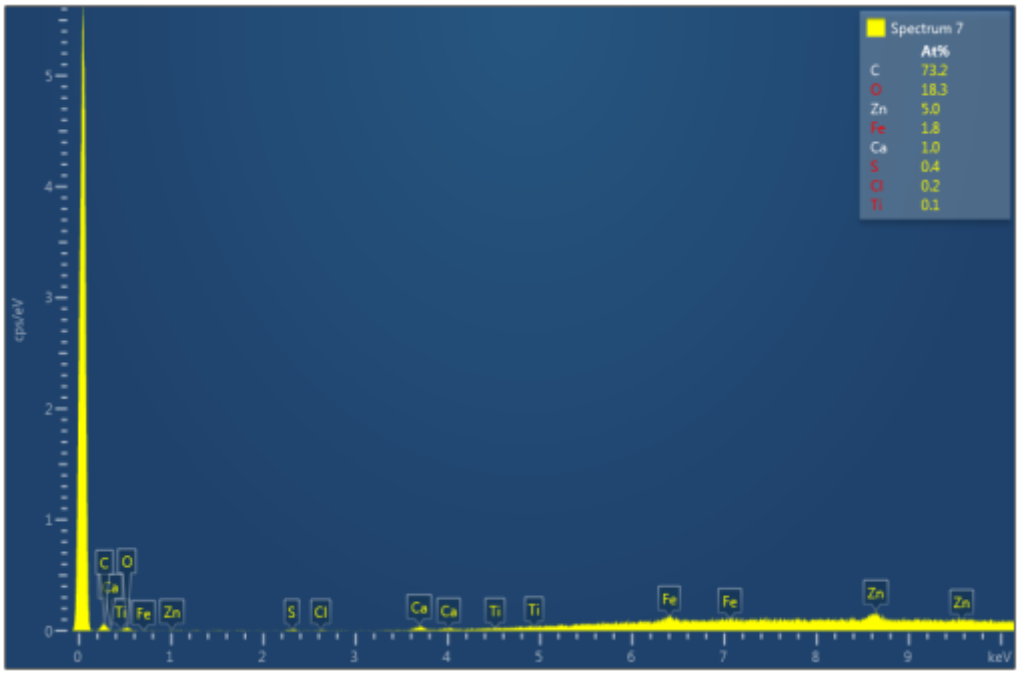

Figure 6.42 Sample 2, Area 1, Spot 7 EDX atomic percentage.

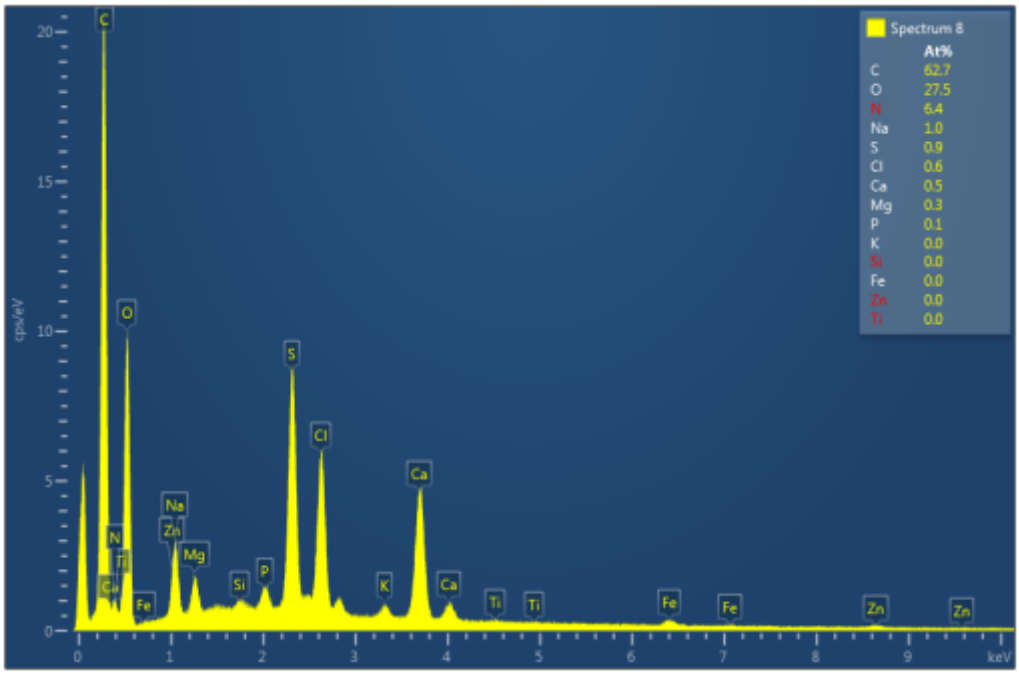

Figure 6.43 Sample 2, Area 1, Spot 8 EDX atomic percentage.

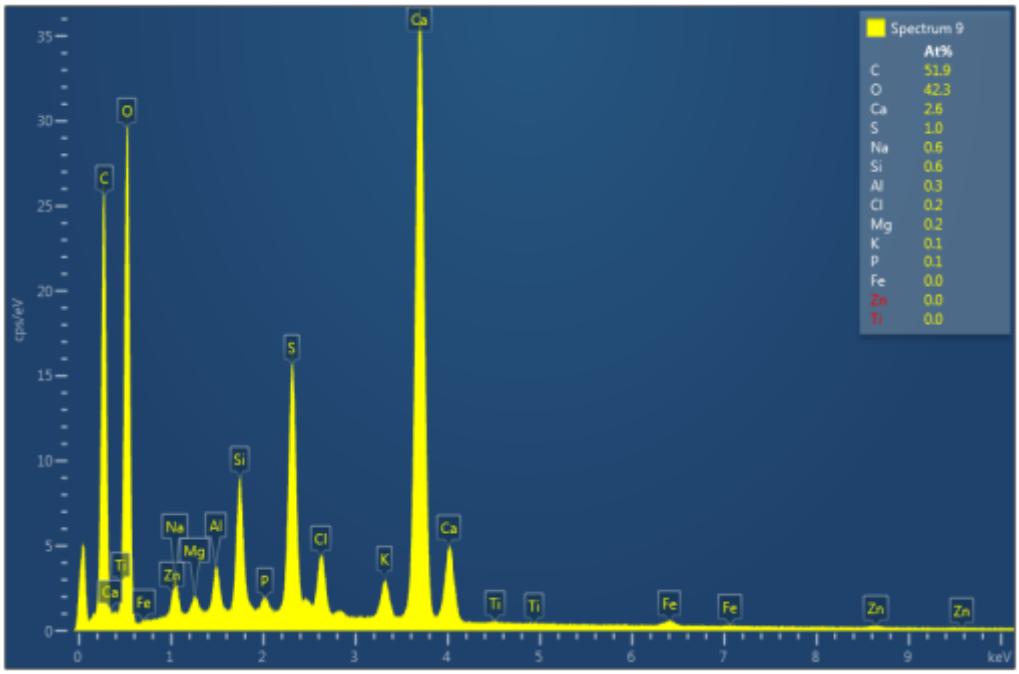

Figure 6.44 Sample 2, Area 1, Spot 9 EDX atomic percentage.

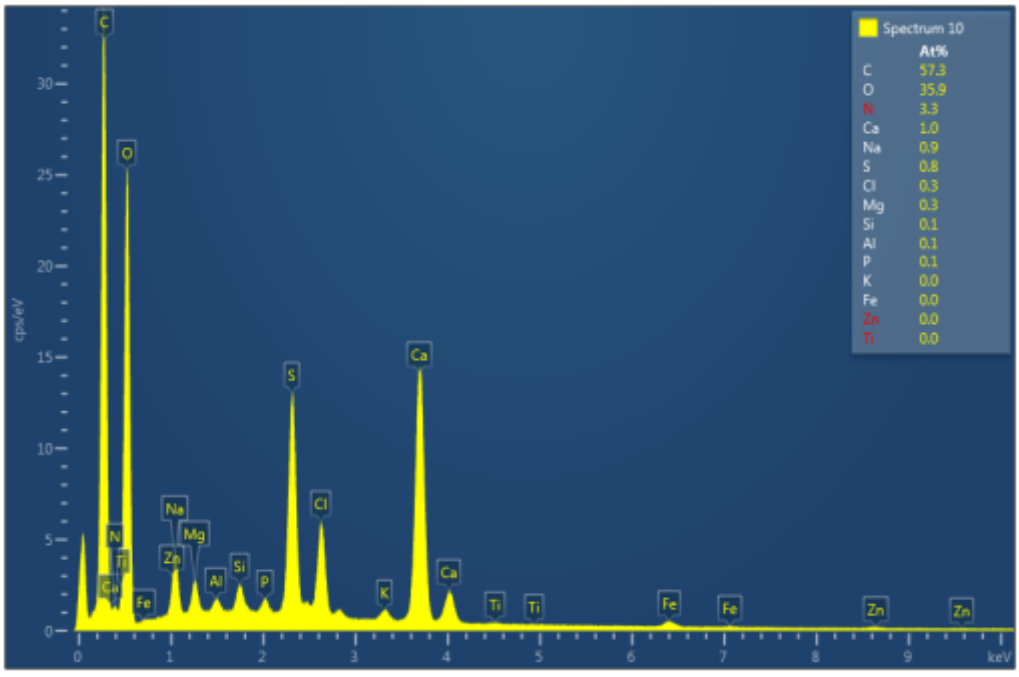

Figure 6.45 Sample 2, Area 1, Spot 10 EDX atomic percentage.

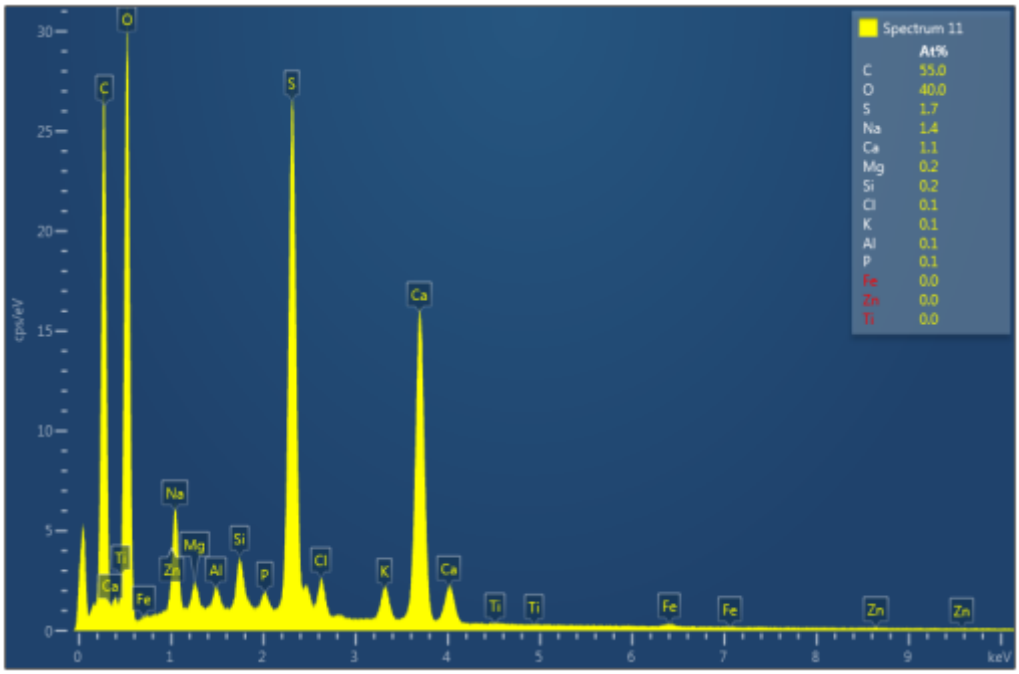

Figure 6.46 Sample 2, Area 1, Spot 11 EDX atomic percentage.

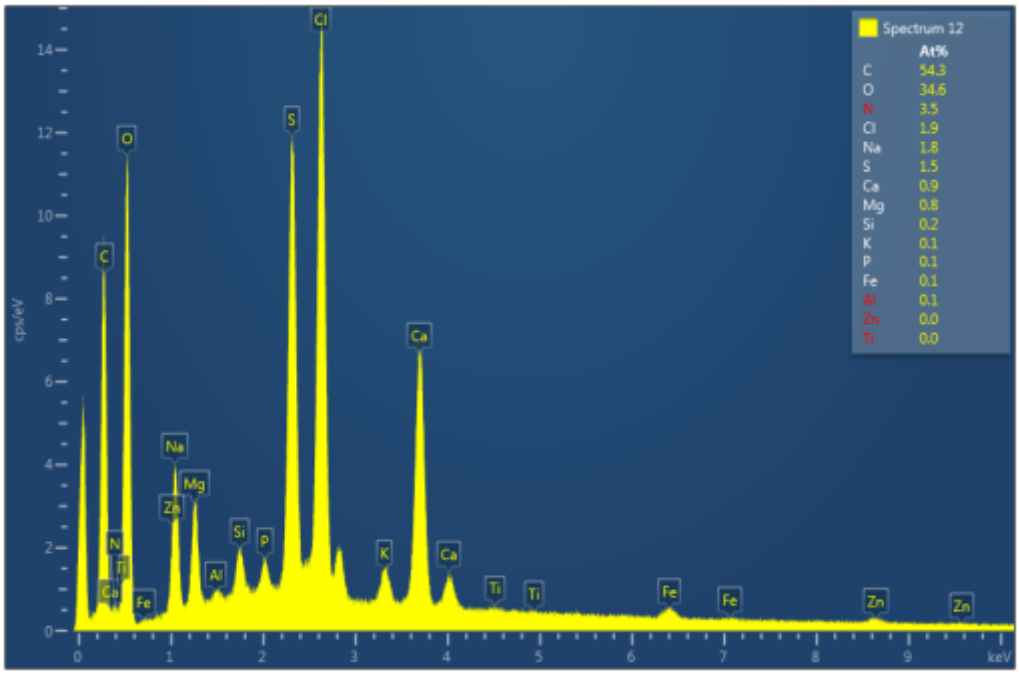

Figure 6.47 Sample 2, Area 1, Spot 12 EDX atomic percentage.

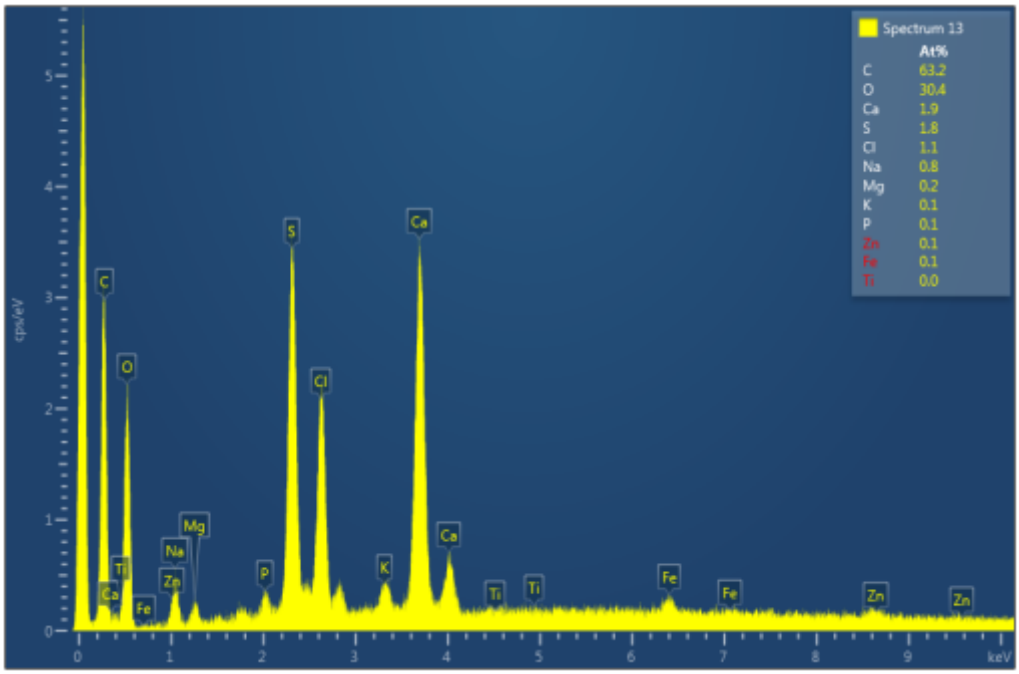

Figure 6.48 Sample 2, Area 1, Spot 13 EDX atomic percentage.

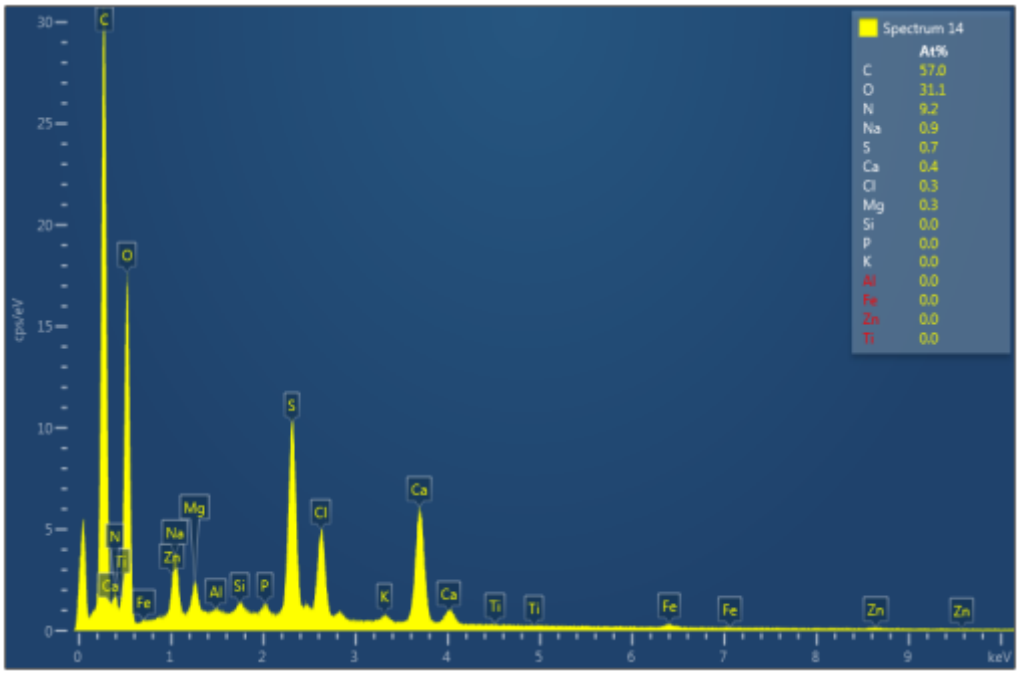

Figure 6.49 Sample 2, Area 1, Spot 14 EDX atomic percentage.

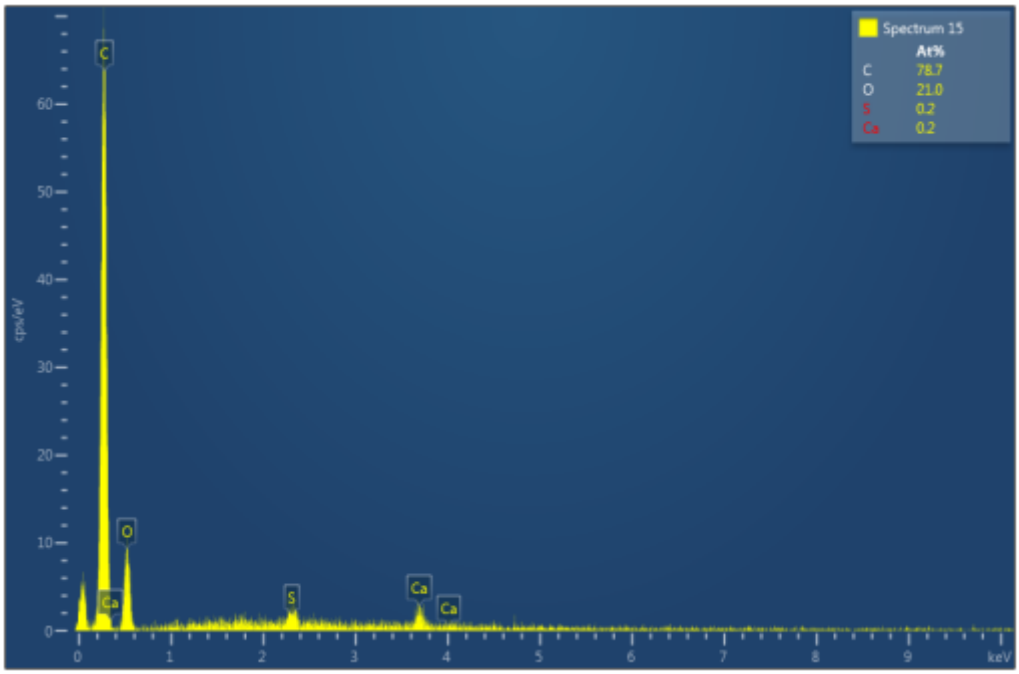

Figure 6.50 Sample 2, Area 1, Spot 15 EDX atomic percentage.

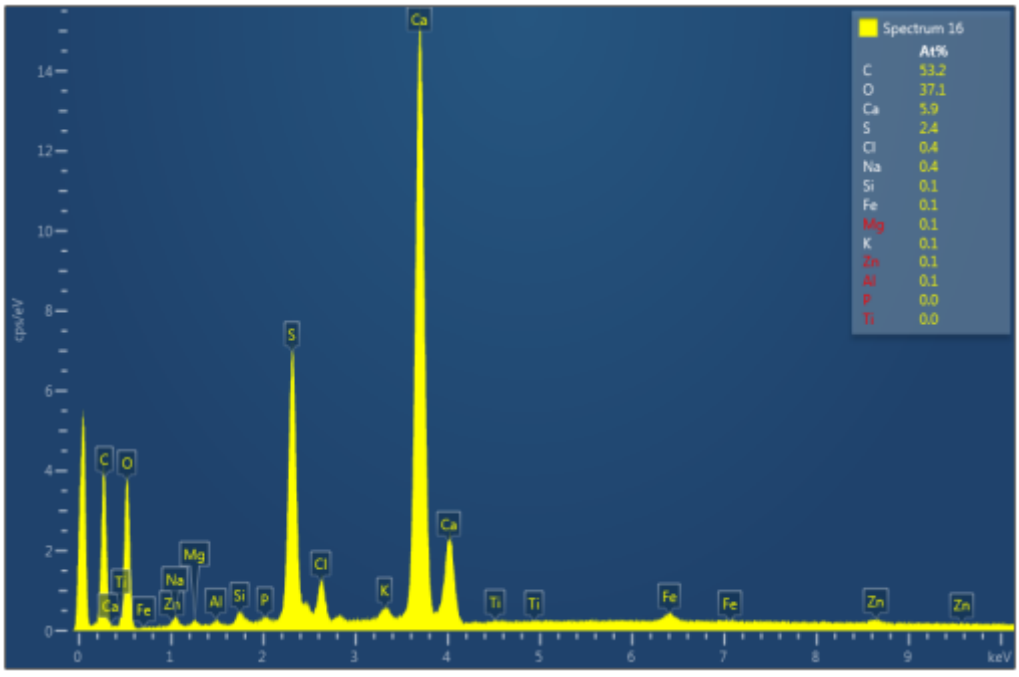

Figure 6.51 Sample 2, Area 1, Spot 16 EDX atomic percentage.

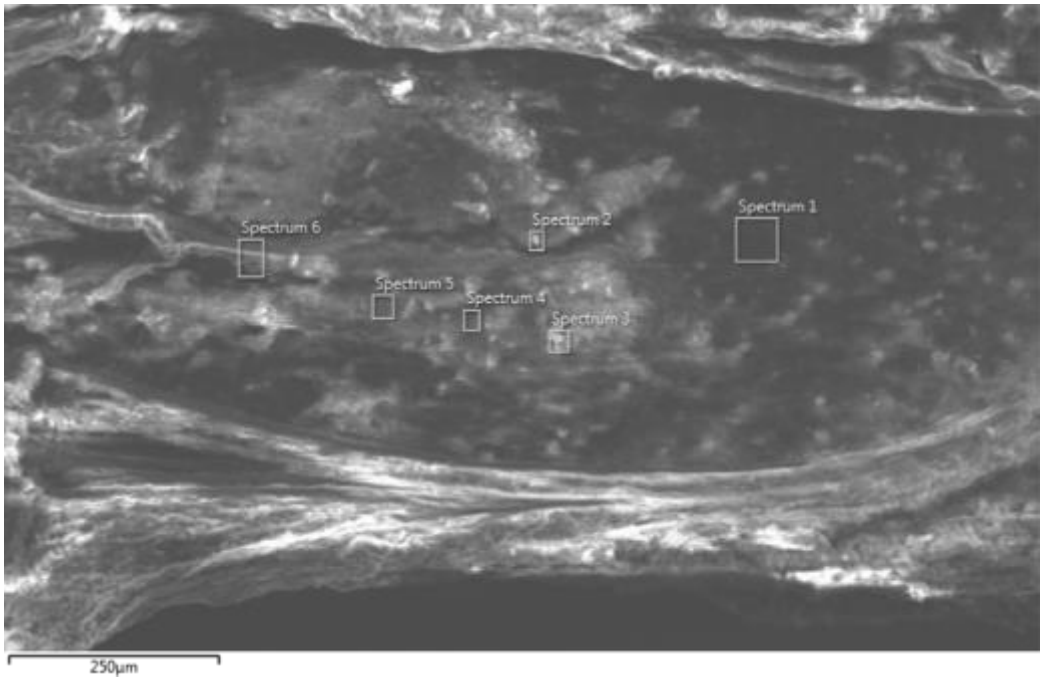

Figure 6.52 Sample 2, Area 2 SEM showing spots analyzed by EDX.

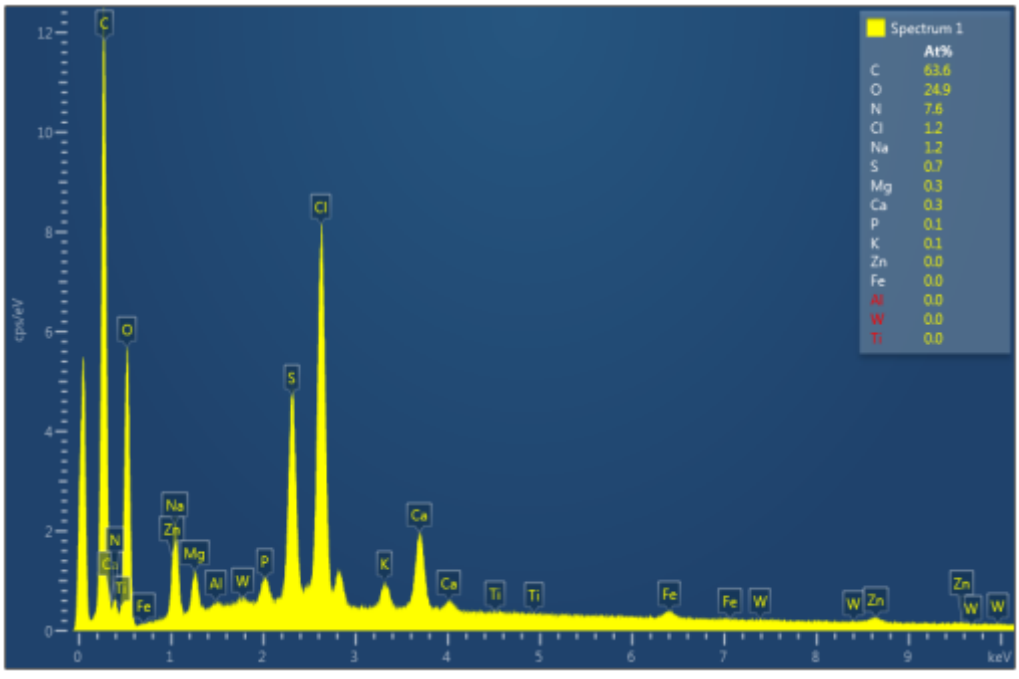

Figure 6.53 Sample 2, Area 2, Spot 1 EDX atomic percentage.

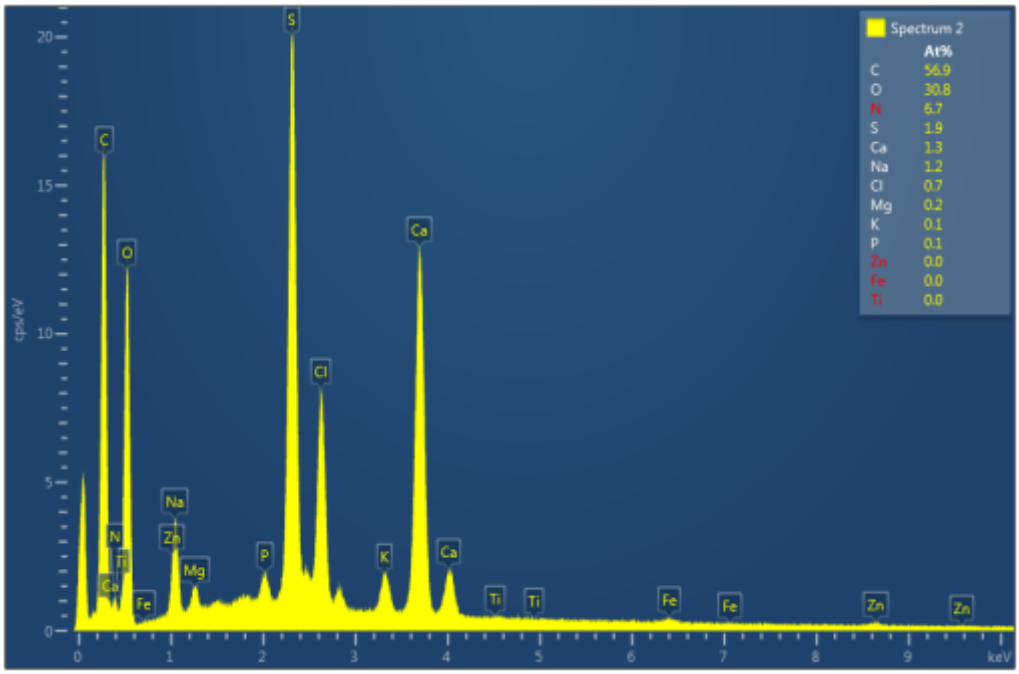

Figure 6.54 Sample 2, Area 2, Spot 2 EDX atomic percentage.

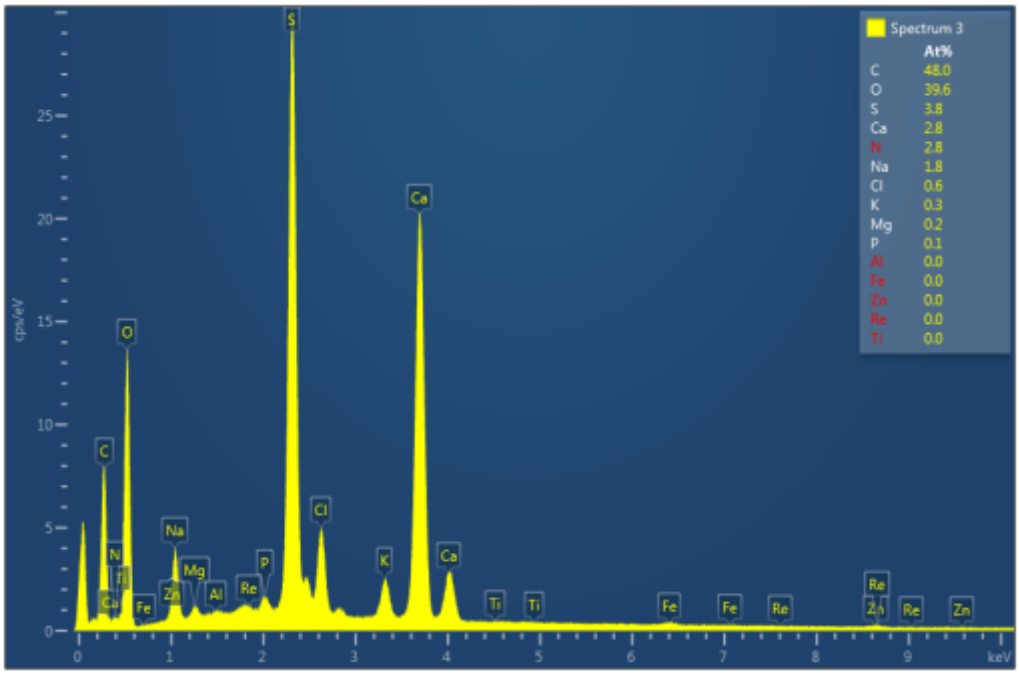

Figure 6.55 Sample 2, Area 2, Spot 3 EDX atomic percentage.

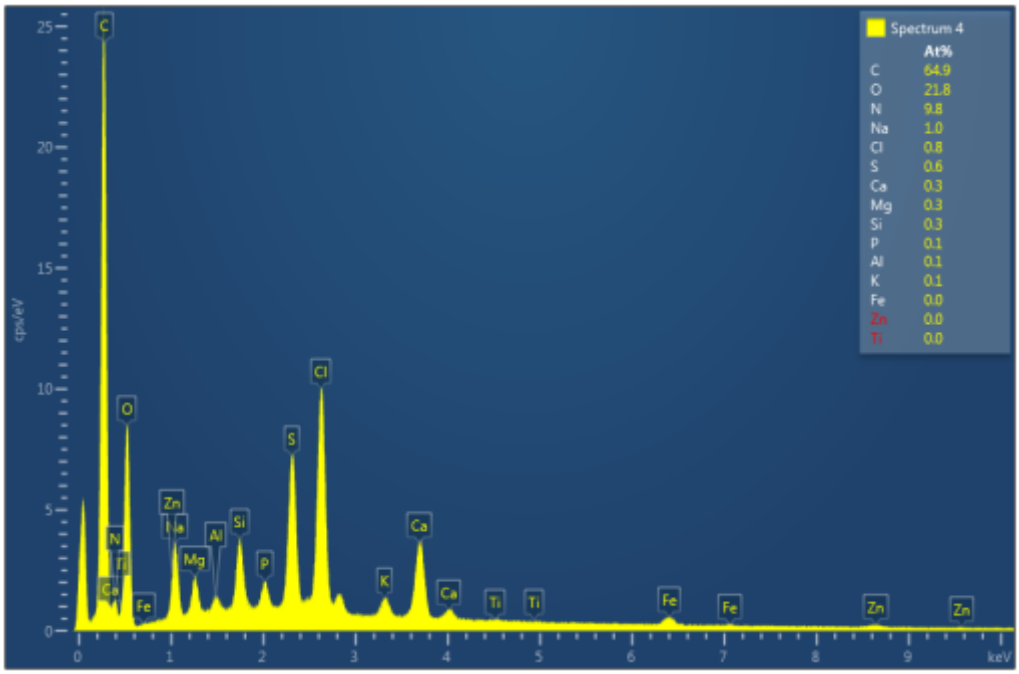

Figure 6.56 Sample 2, Area 2, Spot 4 EDX atomic percentage.

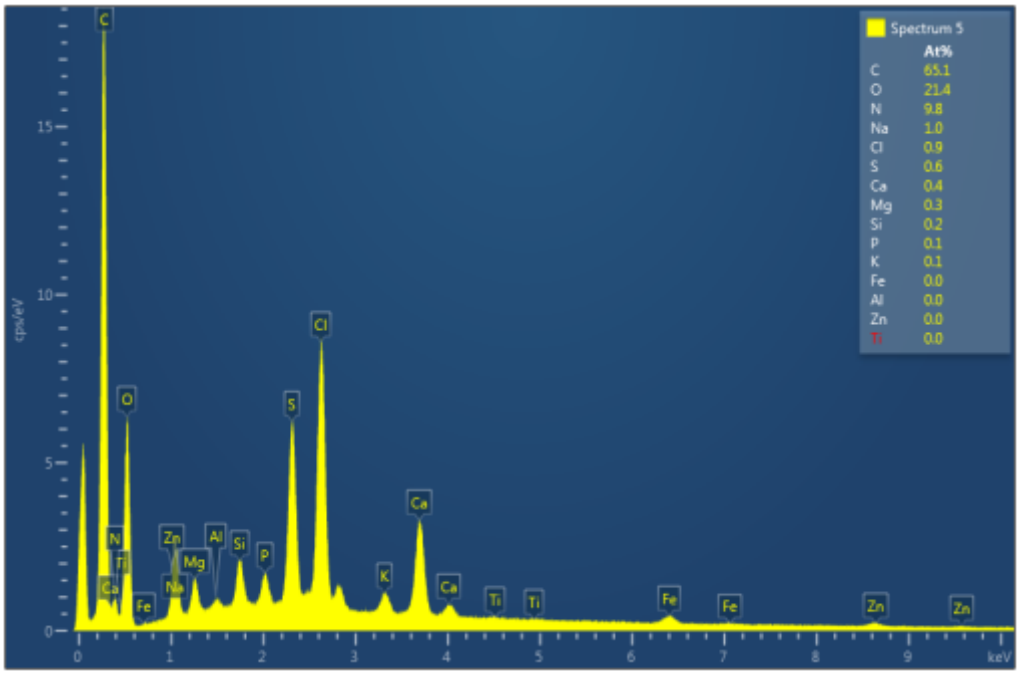

Figure 6.57 Sample 2, Area 2, Spot 5 EDX atomic percentage.

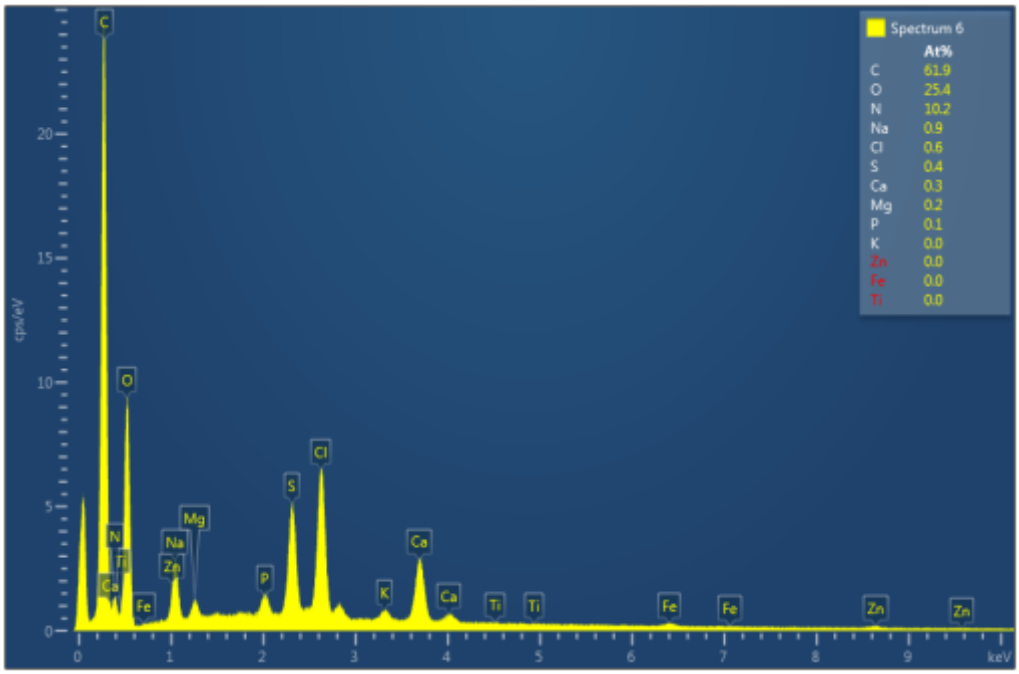

Figure 6.58 Sample 2, Area 2, Spot 6 EDX atomic percentage.

CHAPTER 7. LOCALIZATION OF OLIGOMERIZATION LINKAGE OF FERRITIN

7.1. Introduction

At neutral pH the chemistry of iron can become a problem in aerobic organisms, as ferric ions (Fe^{2+}) oxidize quickly in the presence of dioxygen. This Fenton reaction produces biologically damaging reactive oxygen species, ferric ions (Fe^{3+}), and toxic ferrihydrite (rust). Organisms must resolve the complex problem of iron availability and iron toxicity simultaneously. To solve this, many aerobic organisms have evolved the ferritin family of proteins.[1, 2]

Ferritin proteins are found throughout the animal, plant, and bacterial kingdoms. Most members of the ferritin family assemble into a 24-mer of monomers forming a roughly spherical cage into which the iron is deposited. The 24-mer cage has an outer diameter of ~12 nm, an inner diameter of ~8 nm, and can hold up to 4300 iron atoms. The 24-mer has two-, three-, and fourfold axes with eight pores that act as ion channels (Figure 7.1).[3, 4] When fully loaded, soluble iron concentrations as high as 0.25 M can be achieved in vitro, compared to the solubility of Fe^{3+} at neutral pH (10^{-17} M).

The human ferritin monomer comes in two forms, the L-chain, and the H-chain. These designations are historical and refer the identification of H in heart and L in liver tissues. The L-chain is only found in animals. The L-chain and H-chain monomers self-assemble in different H:L ratios depending on the cell type. 24-mers dissociate into dimers at acidic pH.

Multiple studies have observed oligomers of ferritin 24-mers.[5-10] Oligomers of holoferritin and apoferritin have been found in various species with a concentration in

various tissues between 10 and 15 percent.[8, 11] Alzheimers patients have demonstrated altered iron homeostasis in their brain tissue, including formations of ferritin 24-mer dimers.[12, 13]

Yang *et al.* proposed different types of dimers including one that involves the covalent linkage of two monomers.[9] Disulfide bonds, electrostatic interactions, and interdigitation between ferritin 24-mers were also proposed in most of what they considered the strong ferritin dimer interactions. They recognized that horse L-chain ferritin has only two cysteine residues that are located on the inner surface of the ferritin cage but still observe a strong, likely covalent, ferritin dimer. The cysteine residues facing the inner surface means the covalent linkage cannot be attributed to disulfide bonds. Likewise, human L-chain ferritin has only one cysteine residue near the three-fold axis that faces the inside surface of the cage (Figure 7.2).

Rachel Meserole from our lab previously found dimers of human L-chain ferritin during purification from over expression in *E. coli*. The purification by size exclusion chromatography gave a bifurcated peak. Size exclusion chromatography is counter-intuitive as the larger molecules move faster through the column (Figure 7.3). This is due to the pore size on the separation material which allows the smaller molecules to spend more time traversing the pores while larger molecules spend less time trapped in the pores. Analysis of fractions from the size exclusion column on SDS-PAGE showed two bands. A low molecular weight band at ~21 kDa corresponding to L-chain ferritin monomer and a second band at ~42 kDa which is consistent with a dimer of L-chain ferritin monomers. Identification by SDS-PAGE ensures that the dimer we are seeing is

not due to disulfide bonds, electrostatic interactions, or interdigitation. This work attempts to identify the covalent dimer linkage.

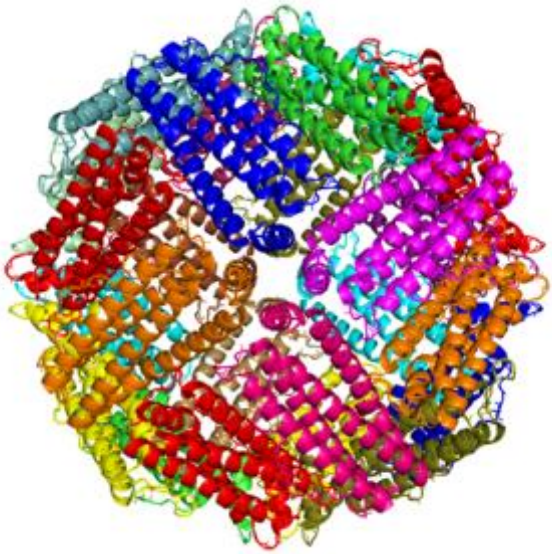

Figure 7.1 Crystal structure of ferritin 24-mer viewed down the 4-fold axis.

Each ferritin monomer has a different color. Prepared using PyMol and the coordinates for PDB 2FG4.[3]

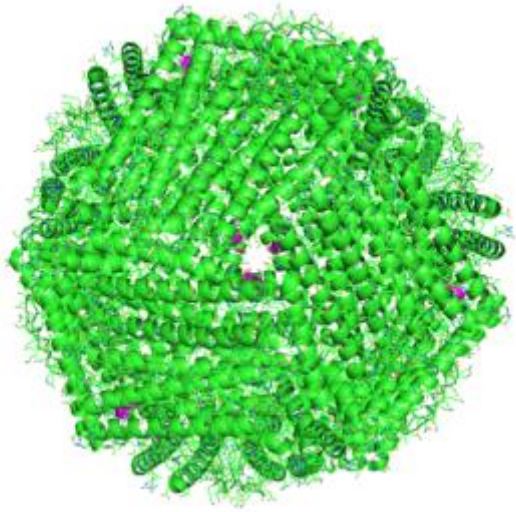

Figure 7.2 Crystal structure of ferritin 24-mer viewed down the 3-fold axis.

Each cysteine residue has been colored magenta. Prepared using PyMol and the coordinates for PDB 2FG4.[3]

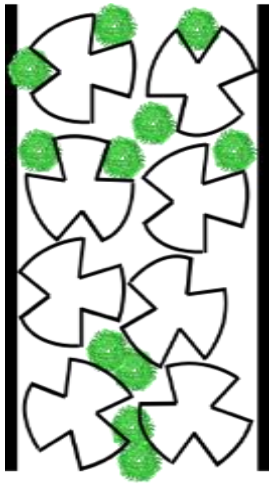

Figure 7.3 Size exclusion chromatography schematic. Ferritin 24-mers at the top of the column spend more time traversing the bead pores, while ferritin 24-mer dimers at the bottom of the column do not get trapped as easily in the pores.

7.2. Materials

All solutions were made using Barnstead NANOpure Diamond (18.2 MΩ-cm) water. HEPES was purchased from American Bioanalytical. Size exclusion chromatography (SEC) was performed using a HiPrep Sephacryl S-300 16/60 column. Protein digests were performed using Trypsin Gold, Mass Spectrometry Grade, and Chymotrypsin, Sequencing Grade from Promega. High performance liquid chromatography was performed using HPLC grade water and acetonitrile, and mass spectrometry grade formic acid on an Agilent 1260 Infinity HPLC. Mass spectrometry was performed using an Agilent 6520 Q-TOF with an electrospray ionization source.

7.3. Methods

Human L-chain ferritin had been previously cloned into and purified from *E. coli* by Rachel Meserole.[14] During purification by SEC, in MOPS buffer, a heavy peak and light peak both consistent with ferritin monomer and ferritin dimer as determined by SDS-PAGE were isolated but not completely resolved (Figure 7.4). The heavy and light fractions were drop frozen in liquid nitrogen and stored at -80 °C on May 11, 2010.

The pooled peaks were run on sodium dodecyl sulfate polyacrylamide gel electrophoresis (SDS-PAGE) to separate the monomer and dimer ferritin (Figure 7.5). The secondary structures of samples for SDS-PAGE are denatured by the addition of SDS and heat, and disulfide linkages are reduced by the addition of 2-mercaptoethanol. SDS is negatively charged and binds to a polypeptide chain or protein in amounts relative to its molecular mass. This gives all proteins the same mass-to-charge ratio. The mass-to-charge ratio being nearly the same for all proteins means that the separation is due to differences in molecular mass. The monomer and presumed dimer bands were cut out of

the gel removing as much of the gel as possible. The excised bands were then used to prepare the ferritin samples for identification by LC-MS/MS by trypsin digestion following the manufacturers protocol.[15] The mass spectral data were identified using MASCOT by Matrix Science.

Size exclusion chromatography of the pooled light fractions and the pooled heavy fractions was performed using the a HiPrep Sephacryl S-300 16/60 column with 50 mM HEPES 0.15 M NaCl pH=7.4. The light and heavy fractions of the original light fraction, LL and HL respectively, were each separately pooled. The light and heavy fractions of the original heavy fraction, LH and HH respectively, were each separately pooled. The LL, HL, LH, and HH samples were precipitated with a 100% (w/v) trichloroacetic acid (TCA) solution to a final concentration of 20% TCA in the sample and centrifuged. Each sample had 0.2 mL of acetone added and was centrifuged. Each sample was resuspended in 70 μL of SDS gel loading buffer and run on SDS-PAGE (Figure 7.8). Bands from the gel were cut out of the gel removing as much of the gel as possible. The excised bands were then used to prepare the ferritin samples for identification by LC-MS/MS by trypsin and chymotrypsin digestion following manufacturer protocol.[15, 16] The mass spectra data were identified using MASCOT by Matrix Science.

7.4. Results

The original SEC performed by Rachel Meserole showed a bifurcated UV peak. Fractions were collected and separated, and labeled the heavy peak and the light peak (Figure 7.4). Pooled heavy and light peak fractions collected from SEC analyzed by SDS-PAGE showed bands consistent with ferritin monomer. The heavy peak has an additional darker band consistent with the mass of a ferritin dimer (Figure 7.5). Both light

and heavy peaks contained bands other than ferritin monomer and dimer. UV-Vis spectroscopy shows consistent absorbance spectra between the heavy and light peaks.

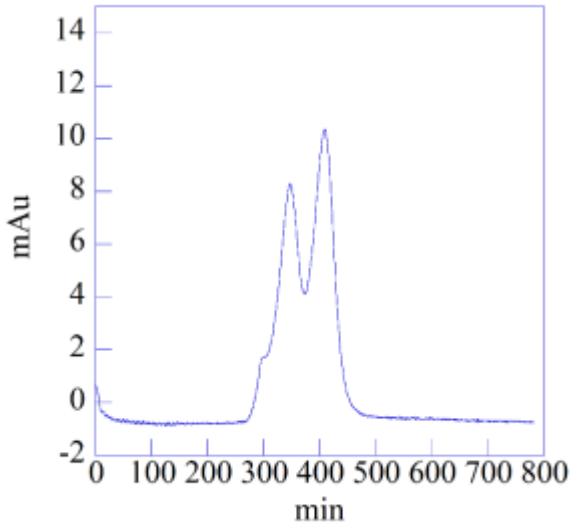

Figure 7.4 SEC FPLC UV-trace of L-chain ferritin run by Rachel Meserole.

The first peak to come off the column is the ferritin dimer, and the second the ferritin monomer.

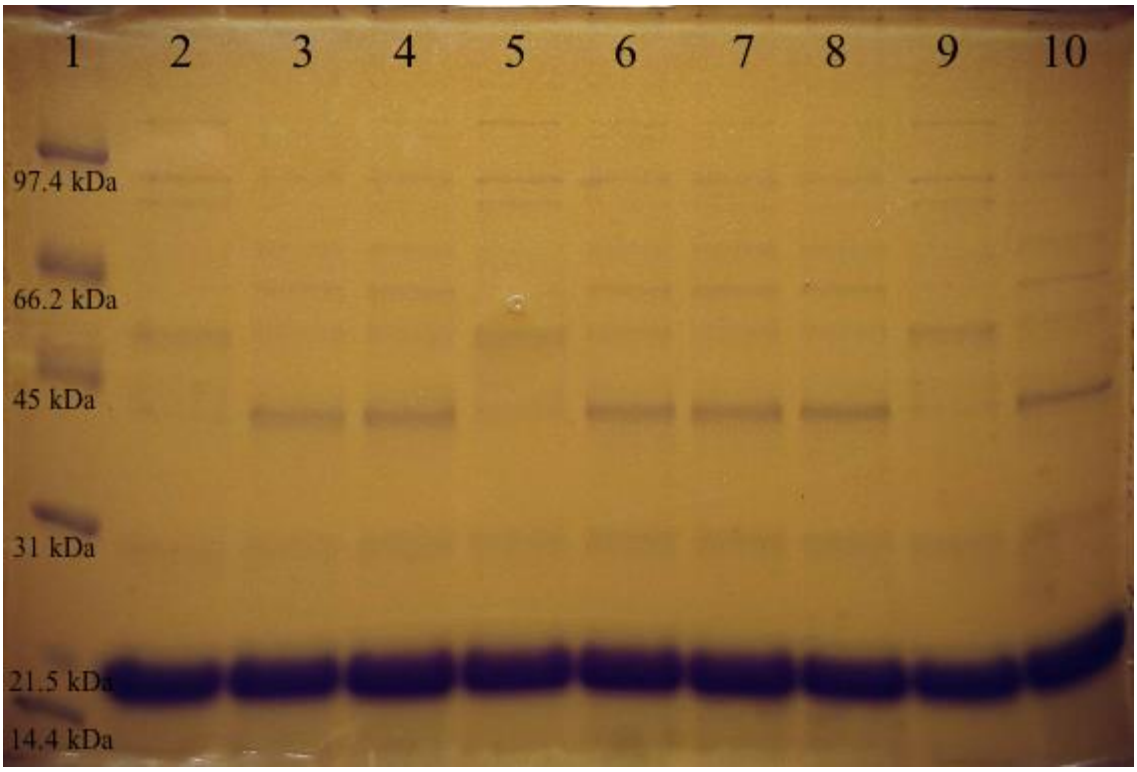

Figure 7.5 SDS-PAGE gel of pooled peaks isolated by Rachel Meserole.

Lane 1 is molecular weight markers. Lanes 2, 5, and 9 are the pooled light peaks. Lanes 3, 4, 6, 7, 8, and 10 are the pooled heavy peaks.

SEC separation of the light and heavy peaks give almost baseline resolved heavy and light peak fractions of their own (Figure 7.6 and Figure 7.7). SDS-PAGE of these peaks show dimer ferritin in the heavy peak of the original pooled heavy peak. Ferritin monomer is abundant in the heavy (HH) and light (LH) peaks of the original heavy peak and in the light peak of the original light peak (LL). The monomer in the LL and LH peaks are from the dissociation of the pure monomer while the monomer in the HH is from the dissociation of the dimers with 46 monomers for every dimer. The heavy peak of the original light peak (HL) shows minimal monomer which is likely due to a smaller amount of protein run on the gel. (Figure 7.8).

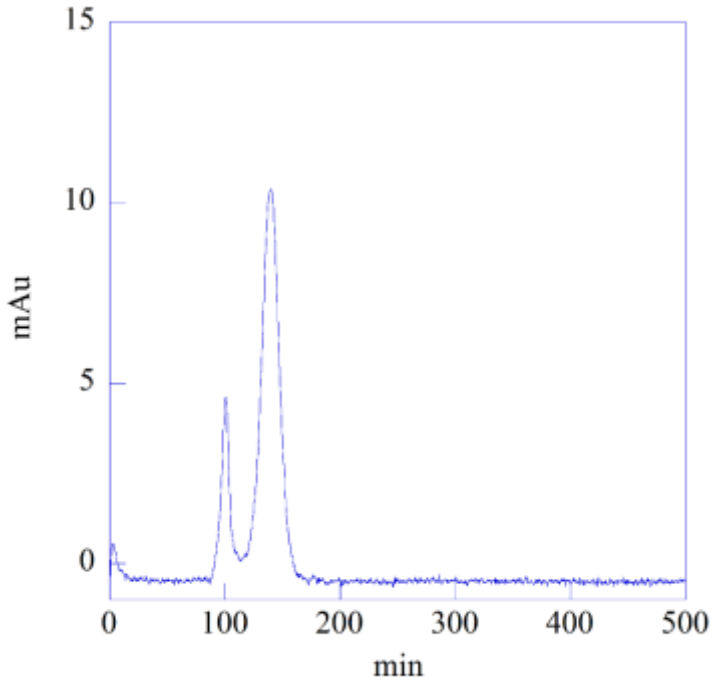

Figure 7.6 FPLC UV-trace of SEC of original pooled light peaks.

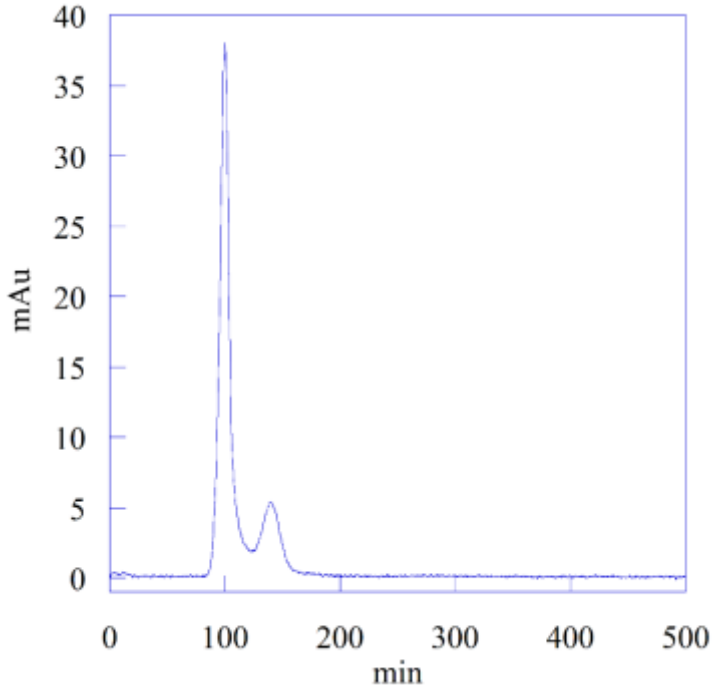

Figure 7.7 FPLC UV-trace of SEC of original pooled heavy peaks.

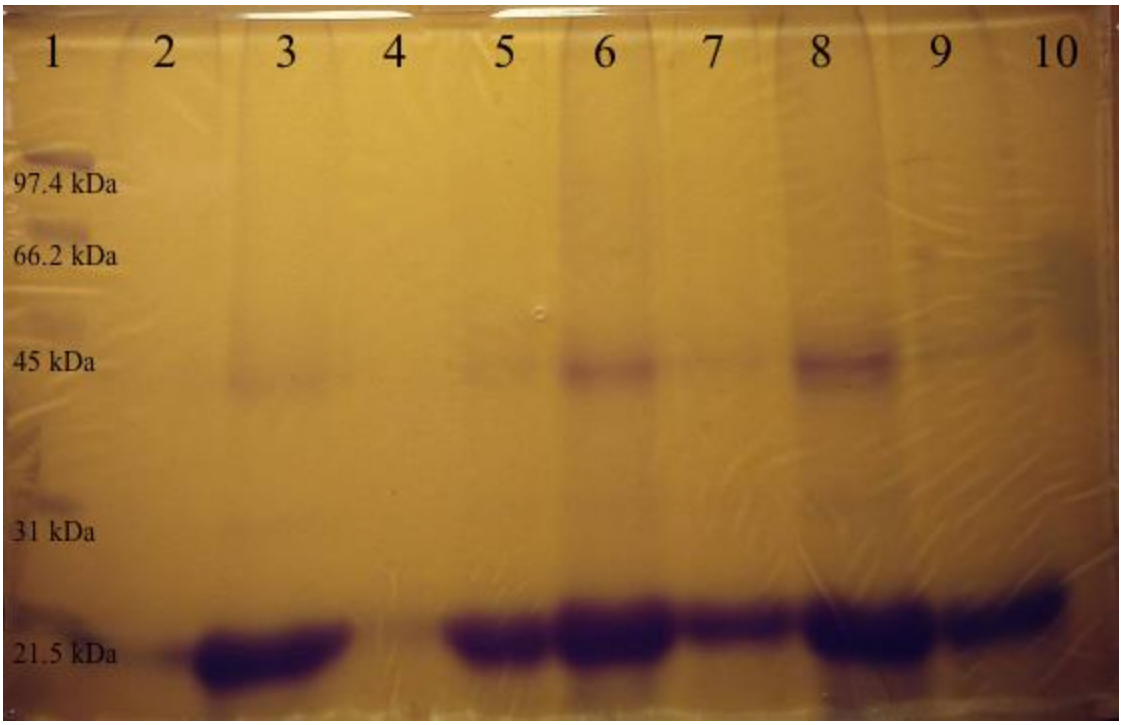

Figure 7.8 SDS-PAGE gel of SEC purified light and heavy pooled fractions.

Lane 1 is molecular weight markers. Lanes 2, and 4 are the heavy pooled fractions from the original light pooled fractions (HL). Lanes 3, and 5 are the light pooled fractions from the original light pooled fractions (LL). Lanes 6, and 8 are the heavy pooled fractions from the original heavy pooled fractions (HH). Lanes 7, and 9 are the light pooled fractions from the original heavy pooled fractions (LH).

Peptide identification by LC-MS/MS using MASCOT has identified similar peptides in both the monomer and dimer bands isolated by SDS-PAGE. Both bands excised from SDS-PAGE are identified as ferritin by MASCOT. Frequently the dimer band is contaminated with *E. coli* porin protein. SEC of the original peaks eliminated the *E. coli* porin protein. The percent coverage of ferritin protein was increased for the dimer with SEC, while the monomer percent coverage remained consistent.

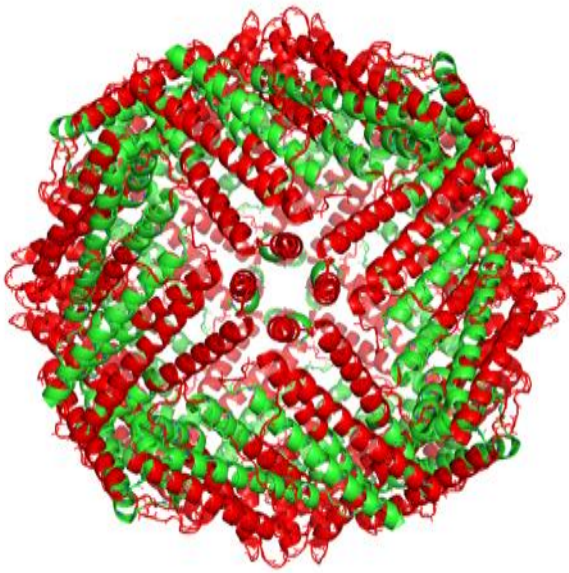

Figure 7.9 Crystal structure of ferritin 24-mer viewed down the 4-fold axis.

Red sequences were identified by MASCOT from LC/MS results of excised dimer band after SEC. Green sequences were not found. Prepared using PyMol and the coordinates for PDB 2FG4.[3]

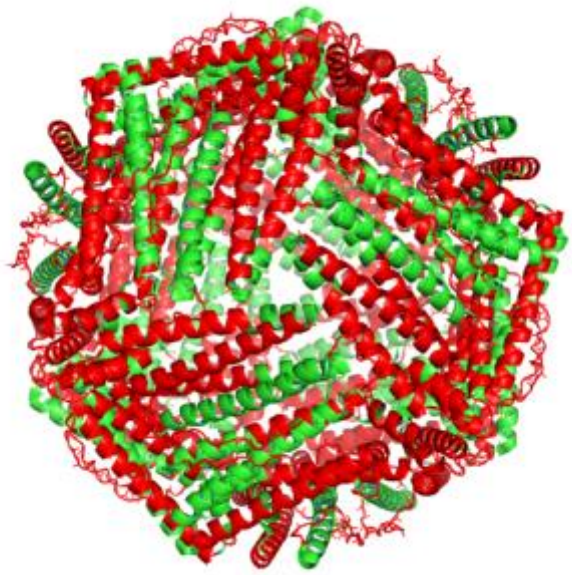

Figure 7.10 Crystal structure of ferritin 24-mer viewed down the 3-fold axis.

Red sequences were identified by MASCOT from LC/MS results of excised dimer band after SEC. Green sequences were not found. Prepared using PyMol and the coordinates for PDB 2FG4.[3]

MSSQIRQNYS TDVEAAVNSL VNLYLQASYT YLSLGFYFDR DDVALEGVSH
FFRELAEEKR EGYERLLKMQ NQRGGRALFQ DIKKPAEDEW GKTPDAMKAA
MALEKKLNQA LLDLHALGSA RTDPHLCDFL ETHFLDEEVK LIKKMGDHLT
NLHRLGGPEA GLGEYLFERL TLKHD

Figure 7.11 FASTA sequence of amino acids identified in monomer sample.

Amino acids highlighted in red were identified by LC-MS/MS and MASCOT.

MSSQIRQNYS TDVEAAVNSL VNLYLQASYT YLSLGFYFDR DDVALEGVSH
FFRELAEEKR EGYERLLKMQ NQRGGRALFQ DIKKPAEDEW GKTPDAMKAA
MALEKKLNQA LLDLHALGSA RTDPHLCDFL ETHFLDEEVK LIKKMGDHLT
NLHRLGGPEA GLGEYLFERL TLKHD

Figure 7.12 FASTA sequence of amino acids identified in dimer sample.

Amino acids highlighted in red were identified by LC-MS/MS and MASCOT.

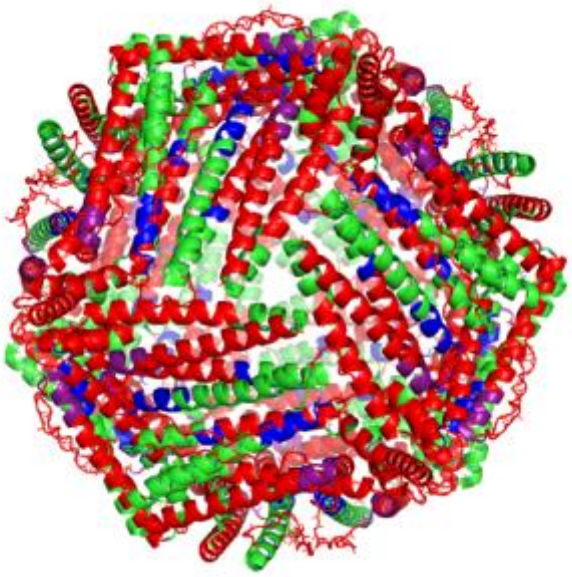

Figure 7.13 Crystal structure of ferritin 24-mer viewed down the 3-fold axis.

Red sequences were identified by MASCOT from LC/MS results of excised dimer band after SEC, blue sequences were identified by MASCOT from LC/MS results of excised monomer band not found in dimer band, and purple sequences were identified by MASCOT from LC/MS results of excised dimer band not found in monomer band. Green sequences were not found. Prepared using PyMol and the coordinates for PDB 2FG4.[3]

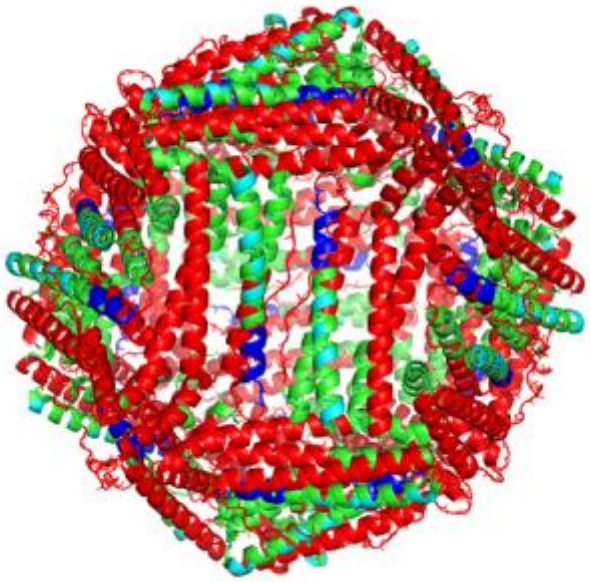

Figure 7.14 Crystal structure of ferritin 24-mer viewed down the 2-fold axis.

Red sequences were identified by MASCOT from LC/MS results of excised dimer band after SEC, and blue sequences were identified by MASCOT from LC/MS results of excised monomer band not found in dimer band. Green sequences were not found, and cyan sequences were not identified in either monomer or dimer and present side chains outward. Prepared using PyMol and the coordinates for PDB 2FG4.[3]

7.5. Discussion

Trypsin digestion of the monomer bands followed by LC-MS/MS, and identification using the MASCOT program identified these samples as human L-chain ferritin and found ~50% of the amino acid sequence. Trypsin digestion of the presumed dimer bands followed by LC-MS/MS, and identification using the MASCOT program frequently the best match for these samples to be *E. coli* porin proteins of approximately the same mass (~40 kDa) as a human L-chain dimer. Human L-chain ferritin was listed as lower score match and ~50% of the amino acid sequence was found. SDS-PAGE treatment of the protein confirms that the dimer is covalently linked. This is due to the

denaturing process of heating and SDS that would eliminate the electrostatic and interdigitation interactions, as well as the addition of β-mercaptethanol that reduces disulfide bonds.

SEC chromatography of the previously prepared ferritin (Figure 7.6 and Figure 7.7) provided for more pure samples as the gel showed two bands close to each other at around 40 kDa (Figure 7.8). The ability to separate the monomer and dimer by SEC means that the monomer of 24-mers and dimer of 24-mers do not equilibrate on the timescale of the experiment, which was on the order of days from SEC separation to SDS-PAGE. The lower mass band was identified as *E. coli* porin protein and the higher mass, darker band was identified as human L-chain ferritin. This allowed for more confident identification of which peptides are found in the dimer sample. The light dimer bands in the LL and LH lanes are likely due to the inability to achieve complete baseline separation of the fractions as those bands are identified as L-chain ferritin by LC-MS/MS and MASCOT. It is probable that there is dimer L-chain ferritin in the HL lane but it is too light as less protein was added. The LC traces for LC-MS/MS analysis show no difference between monomer and dimer samples of the same enzymatic digest.

The MASCOT software also finds and identifies peptides that do not have a protein match. MASCOT scores the individual peptides as well as the proteins. A peptide score of 68 or higher is determined to be significant as it has a less than 1 in 20 chance of being a random match. In the dimer sample, a peptide with a high score but not included in the L-chain ferritin protein sequence may be the covalent linkage. No peptides not included in the L-chain ferritin protein sequence were found to have a score higher than 68.

While a specific peptide or peptides were not identified as the covalent linkage a likely region for the linkage can be narrowed down. Figure 7.14 presents the most likely regions for the dimerization to occur. These are the regions highlighted in blue and cyan. The residues colored cyan are near the surface of the protein and points outward, most noticeable at the top of the figure, and is highly accessible to other ferritin proteins. The residues highlighted in blue were found in the monomer but not the dimer and are buried a bit deeper in the crystal structure but the region blocking it is random coil and could easily move allowing access.

This study did not find the cause of the ferritin oligomerization but we have found a likely region within the ferritin protein that the oligomerization occurs. There is no conclusive evidence that oligomerization is due to a peptide linkage either. Further studies using other proteases of mass spectrometric techniques may elucidate the origin of the linkage.

REFERENCES CITED

1. E. C. Theil, T. Tosha and R. K. Beherat, Solving Biology's Iron Chemistry Problem with Ferritin Protein Nanocages, *Accounts of Chemical Research*, 2016, **49**, 784-791.
2. N. D. Chasteen and P. M. Harrison, Mineralization in ferritin: An efficient means of iron storage, *Journal of Structural Biology*, 1999, **126**, 182-194.
3. Z. M. Wang, C. Li, M. Ellenburg, E. Soistman, J. Ruble, B. Wright, J. X. Ho and D. C. Carter, Structure of human ferritin L chain, *Acta Crystallographica Section D-Biological Crystallography*, 2006, **62**, 800-806.
4. X. F. Liu, W. L. Jin and E. C. Theil, Opening protein pores with chaotropes enhances Fe reduction and chelation of Fe from the ferritin biomineral, *Proceedings of the National Academy of Sciences of the United States of America*, 2003, **100**, 3653-3658.
5. A. A. Suran and H. Tarver, Heterogeneity of Horse Spleen Ferritin and Apoferritin: Comparison of Electrophoretic and Chromatographic Fractions, *Archives of Biochemistry and Biophysics*, 1965, **111**, 399-&.
6. M. A. Williams and P. M. Harrison, Electron-Microscopic and Chemical Studies of Oligomers in Horse Ferritin, *Biochemical Journal*, 1968, **110**, 265-&.
7. Y. Niitsu and I. Listowsky, Mechanisms for the Formation of Ferritin Oligomers, *Biochemistry*, 1973, **12**, 4690-4695.
8. S. S. C. Lee and G. W. Richter, Monomers and Oligomers of Ferritin and Apoferritin: Association and Dissociation, *Biochemistry*, 1976, **15**, 65-70.

9. D. W. Yang, K. Matsubara, M. Yamaki, S. Ebina and K. Nagayama, Heterogeneities in Ferritin Dimers as Characterized by Gel Filtration, Nuclear Magnetic Resonance, Electrophoresis, Transmission Electron Microscopy, and Gene Engineering Techniques, *Biochimica Et Biophysica Acta-Protein Structure and Molecular Enzymology*, 1994, **1206**, 173-179.

10. B. R. Thomas, D. Carter and F. Rosenberger, Effect of microheterogeneity on horse spleen apoferritin crystallization, *Journal of Crystal Growth*, 1998, **187**, 499-510.

11. P. M. Harrison, R. J. Hoare, T. G. Hoy and I. G. Macara, in *Iron in Biochemistry and Medicine*, eds. A. Jacobs and M. Wordwood, Academic Press, London, 1974, p. 73.

12. J. R. Connor, B. S. Snyder, J. L. Beard, R. E. Fine and E. J. Mufson, Regional Distribution of Iron and Iron-Regulatory Proteins in the Brain in Aging and Alzheimers-Disease, *Journal of Neuroscience Research*, 1992, **31**, 327-335.

13. J. R. Connor, S. L. Menzies, S. M. Stmartin and E. J. Mufson, A Histochemical Study of Iron, Transferrin, and Ferritin in Alzheimers Diseased Brains, *Journal of Neuroscience Research*, 1992, **31**, 75-83.

14. F. F. Amos, K. E. Cole, R. L. Meserole, J. P. Gaffney and A. M. Valentine, Titanium mineralization in ferritin: a room temperature nonphotochemical preparation and biophysical characterization, *Journal of Biological Inorganic Chemistry*, 2013, **18**, 145-152.

15. P. Corporation, Trypsin Gold, Mass Spectrometry Grade: Instructions for use V5280, 2015).

16. P. Corporation, Chymotrypsin, Sequencing Grade: Protocol, 2016).